RSC Advances

REVIEW

View Article Online
View Journal | View Issue

Cite this: *RSC Adv.*, 2026, **16**, 292

Nitrone chemistry: a versatile gateway to diverse heterocycles

Suhasini Mohapatra, Kamalika Prusty, Subhashree Bhol, Gopinatha Panigrahi and Sabita Nayak *

Nitrones (azomethine *N*-oxides) are among the most versatile intermediates in organic synthesis, enabling the efficient construction of heterocyclic frameworks that underpin advances in medicinal chemistry, materials science, and chemical biology. Over the past few years, transition-metal-catalyzed strategies have delivered remarkable control over regio- and stereoselectivity, yet their cost and limitations in substrate scope have encouraged the search for alternatives. In this context, transition-metal-free protocols, including [3 + 2], [2 + 2] and [4 + 2] cycloadditions, have emerged as sustainable and economical approaches. Complementing these methods, new developments such as asymmetric click reactions, deoxygenative cyclizations, silylacetate-promoted addition reactions, photoredox catalysis, and self-oxidative cyclizations further broaden the synthetic toolbox, enabling access to structurally complex and biologically relevant scaffolds. By integrating these diverse methodologies, nitrone chemistry continues to evolve as a dynamic platform for heterocycle construction. This review highlights recent synthetic strategies for nitrone-derived heterocycles reported from 2021 to 2025, critically evaluating their advantages and limitations while outlining promising directions toward greener, more versatile, and practically useful methodologies.

Received 10th October 2025
Accepted 17th December 2025

DOI: 10.1039/d5ra07748f

rsc.li/rsc-advances

1 Introduction

Nitrones (azomethine *N*-oxides) are recognized as important molecules in medicinal chemistry, in addition to their applications in agrochemicals, polymers, and material science.[1–3] Various nitrone derivatives have exhibited promising biological activities, including antioxidant, neuroprotective, anticancer, and antiviral effects. Furthermore, nitrones have been extensively explored as 1,3-dipoles in cycloaddition reactions, providing access to diverse biologically active heterocycles.[4,5] Owing to this broad spectrum of utility, significant research efforts have been devoted to the synthesis of diverse nitrone frameworks.[6,7]

Organic Synthesis Laboratory, Department of Chemistry, Ravenshaw University, Cuttack-753003, Odisha, India. E-mail: sabitanayak18@gmail.com

Suhasini Mohapatra

Suhasini Mohapatra was born in Jagatsinghpur, Odisha, India in 1998. She received her M.Sc. in Organic Chemistry from Veer Surendra Sai University & Technology, Burla, India in 2020. She has completed an internship in ISER, Berhampur, India. She completed her M.Phil. in Chemistry from Ravenshaw University, Cuttack, India in 2022. Now, she is continuing her PhD. under the supervision of Dr Sabita Nayak at Ravenshaw University, Cuttack, India. Her research interests focus on the synthesis of biologically active molecules following cycloaddition reaction.

Kamalika Prusty

Kamalika Prusty was born in Bhadrak. Odisha, India, in 2000. She completed her B.Sc. at Utkal University in 2020 and her M.Sc. at Ravenshaw University in 2022. She is currently pursuing her PhD. in organic Chemistry under the supervision of Prof. Sabita Nayak at Ravenshaw University, Cuttack, Odisha. She is a BPRF and MRF fellow, and she has also qualified CSIR- NET and GATE. Her research area focuses on the design and synthesis of bioactive molecules via 1,3-dipolar cycloaddition reactions.

Among them, α-phenyl-*N*-*tert*-butylnitrone (PBN) has emerged as the prototypical spin trap, exhibiting diverse pharmacological activities including neuroprotective, cardioprotective, and anti-teratogenic effects.[8–16] Its water-soluble analog, disodium [(*tert*-butylimino)methyl]benzene-1,3-disulfonate *N*-oxide (NXY-059), advanced to phase III clinical trials as a neuroprotective drug, although its mechanism of action remains incompletely understood.[17] Meanwhile, other nitrones such as 5,5-dimethyl-1-pyrroline *N*-oxide (DMPO) have been less extensively studied for pharmacological activity. To address limitations of poor stability and limited cellular uptake, structurally modified nitrones such as DEPMPO, PPN, 5-ChEPMO, MitoPBN, and LPBNAH (Fig. 1) have been developed with improved spin trapping properties and bioavailability.[18,19] These advances highlight the dual importance of nitrones in both chemical and biomedical research.

From a synthetic perspective, nitrones are easy to prepare and serve as versatile intermediates in cycloaddition chemistry. Their electronic structure allows them to react with alkenes, alkynes, and carbonyl groups, leading to a wide variety of heterocyclic products. Nitrones are best known for their classical [3 + 2] dipolar cycloadditions, which produce isoxazolidines and isoxazolines important five-membered heterocycles often found in natural products and pharmaceuticals.[20–28] However, they can also participate in other reaction modes, including [2 + 2], [3 + 3], [4 + 1], and [4 + 2] cycloadditions, which expand their synthetic scope.[29] The nature of the nitrone framework plays a crucial role in these reactions. Based on these structural classifications, the nitrone derivatives in Fig. 2 (compounds **9–21**) highlight representative examples used widely in contemporary 1,3-dipolar cycloaddition chemistry. Compounds **9–10** represent cyclic nitrones derived from isoxazolidine or pyrroline scaffolds, whose conformational rigidity improves regio- and stereoselectivity in cycloaddition reactions.[30,31] Compound **11** corresponds to an α,β-unsaturated ketonitrone, which exhibits enhanced electrophilicity and reacts efficiently with electron-rich dipolarophiles.[32,33] Compounds **12–13** are *N*-aryl isatin nitrones and ketonitrones that serve as versatile precursors in the synthesis of spirocyclic and fused heterocyclic scaffolds.[34] Compound **14** is a dinitrone derivative capable of undergoing sequential cycloaddition pathways, enabling rapid molecular complexity. Compounds **15–17** include *N*-aryl and *C*-aryl nitrones that allow electronic tuning and participate effectively under metal-free or organocatalytic conditions. Compounds **18–19** represent heteroaryl and carbohydrate-derived chiral nitrones that provide enantioselective access to stereo defined heterocycles. Finally, compounds **20–21** are unsaturated and adamantane-derived nitrones widely utilized in the construction of rigid polycyclic and biologically relevant frameworks.[6,31]

Recent advancements in nitrone chemistry have further broadened their synthetic potential, particularly in the context of metal-free and metal-catalyzed methodologies. Transition-metal catalysts such as Cu, Ag, Yb, and Ni have been

Subhashree Bhol

Shubhashree Bhol was born in 2002 in Khordha district of Odisha, India. She completed her B.Sc. and M.Sc. under Utkal University and is currently pursuing her PhD in Organic Chemistry at Ravenshaw University, Cuttack, under the guidance of Dr Sabita Nayak. Her research area emphasizes Synthesis of spirooxindole-pyrrolidine fused 3-nitro-1,2-dihydroquinoline by 1,3-dipolar cycloaddition reaction.

Gopinatha Panigrahi

Gopinatha Panigrahi was born in Narendrapur, Bhadrak, Odisha, India in 2000. He obtained his M.Sc. in Chemistry from Utkal University, Bhubaneswar, Odisha, India in 2022. He has completed an internship in CSIR-IMMT, Bhubaneswar, India. (May–July 2022). He has qualified GATE in 2023. He joined as DST INSPIRE fellow in 2022 and is continuing his PhD. work in the area of heterocyclic chemistry under the supervision of Dr Sabita Nayak at Ravenshaw University, Cuttack, Odisha, India. His research interests include design and synthesis of small bioactive heterocycles, spirocyclic molecules, 1,3-dipolar cycloaddition reaction, medicinal chemistry and carbohydrate chemistry.

Sabita Nayak

Dr Sabita Nayak was born in Nayagarh, Barabati, Odisha, India in 1975. She completed her PhD. under the supervision of Dr Mukund. K. Gurjar from National Chemical Laboratory, Pune, India in 2008 and after that, she worked as a post-doctoral fellow in the research group of Prof. J. R. Falck at Southwestern medical research center, Dallas, Texas, USA till December 2009. She joined in Ravenshaw University, Cuttack, Odisha, in 2010 and currently continuing as An Associate Professor. She has a special interest in synthesis of hybrid natural product, synthesis of biologically active molecules following 1,3 dipolar cycloaddition and [4 + 2] cycloaddition, medicinal chemistry and carbohydrate chemistry.

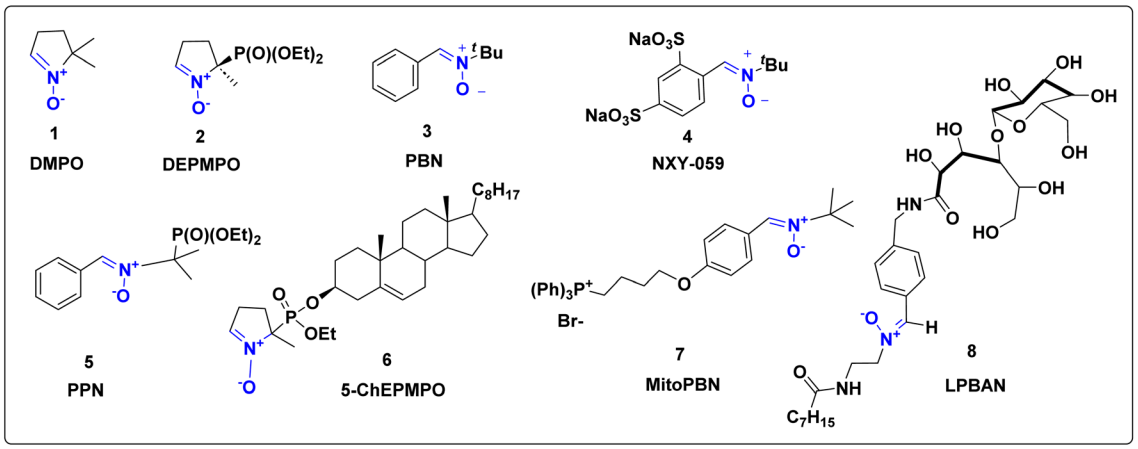

Fig. 1 Nitrone based bioactive molecules.

employed to mediate regio- and stereoselective cycloaddition reactions under mild conditions with improved efficiency.[36–39] In parallel, organocatalytic and Lewis's acid/base-promoted protocols have enabled greener and more sustainable approaches. These innovations facilitate the construction of not only simple five- and six-membered rings, but also complex, highly functionalized heterocycles with pharmaceutical relevance.[40,41]

In this review, we aim to provide a comprehensive overview of recent developments in nitrone-mediated synthesis of heterocyclic compounds. Special emphasis is placed on categorizing these methodologies based on the type of cycloaddition, the nature of catalysis (metal-free *vs.* metal-catalyzed), and the structural complexity of the products formed. Through this exploration, we seek to highlight the strategic value of nitrone chemistry in modern heterocyclic synthesis and its growing impact on the development of bioactive molecules. Herein, we have discussed in detail almost 47 publications from the last four years, *i.e.*, from 2021 to 2025.

1.1 Metal-catalyzed synthesis

Transition-metal catalysis has emerged as one of the most versatile and powerful strategies for nitrone transformations, enabling the construction of complex heterocyclic architectures with high efficiency, selectivity, and functional group tolerance.

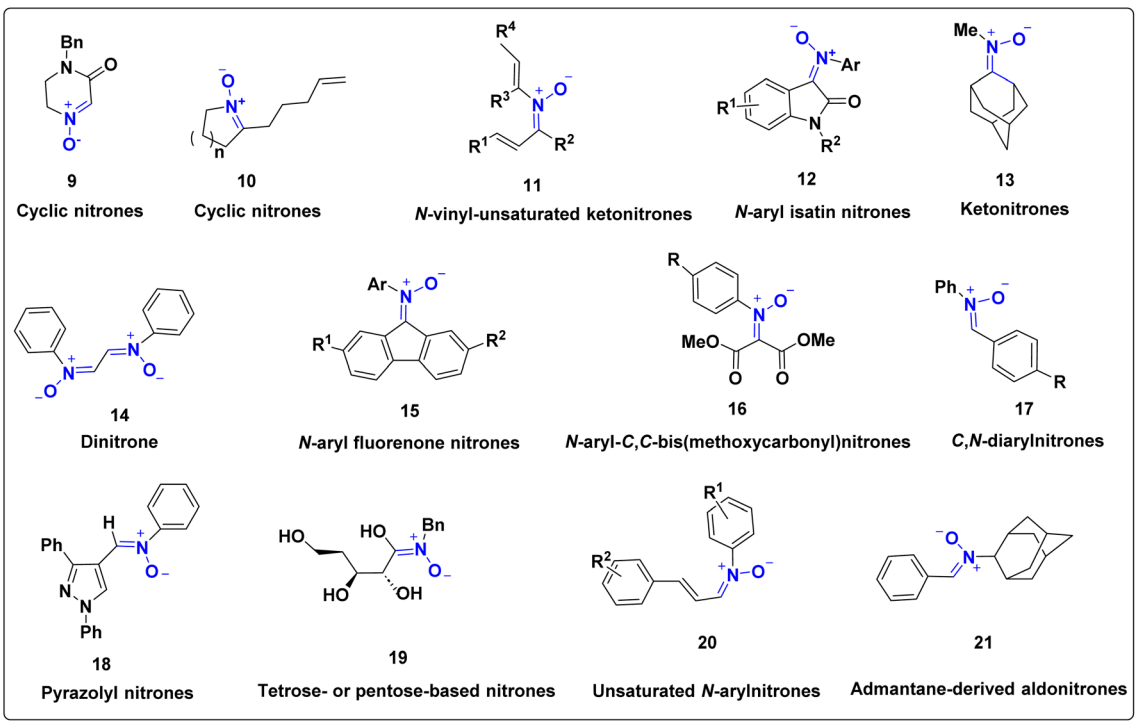

Fig. 2 Various types of nitrones.

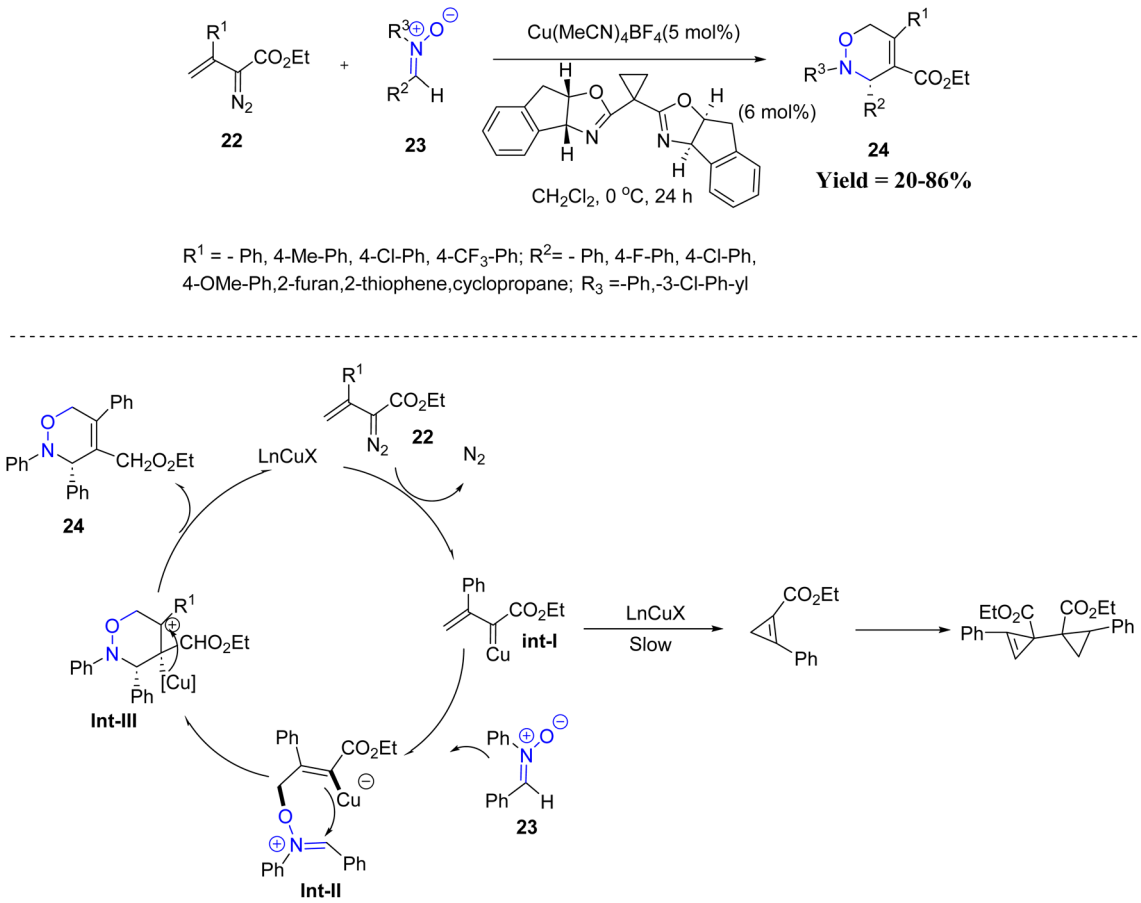

Scheme 1 Cu(I)-Catalyzed [3 + 3] cycloaddition of β-aryl/alkyl vinyl diazoacetates with nitrones.

Transition metals such as Cu, Au, Ir, Ag, Pd, Co, Rh, Ru, Yb, Bi and Fe have been widely employed to mediate a variety of cycloadditions, annulations, and oxidative couplings involving nitrones.[35–39] These catalytic systems often operate under mild conditions and allow access to frameworks that are otherwise difficult to achieve through metal-free or purely thermal processes. Moreover, transition-metal catalysts enable precise control over regio- and stereoselectivity, and in many cases facilitate cascade or multicomponent reactions that enhance step economy.[31] Despite concerns regarding cost, toxicity, and metal residues, transition-metal catalysis continues to expand the synthetic scope of nitrone chemistry and plays a central role in the development of new methodologies for heterocycle synthesis and drug discovery.[42]

1.1.1 Cu-Catalyzed. In this context, Michael P. Doyle and co-workers in 2021 reported that β-phenyl vinyl diazoacetate undergoes $Rh_2(OAc)_4$-catalyzed dimerization, and the resulting dimer was later applied as a ligand in the Cu(I)-catalyzed [3 + 3] cycloaddition of β-aryl and β-alkyl vinyl diazoacetates with nitrones. In this study, a clear reactivity trend was observed, where β-aryl substituted vinyl diazo compounds reacted more efficiently than β-alkyl analogues. Electron-donating groups on the aromatic ring improved both yield and enantioselectivity, while strong electron-withdrawing groups reduced the reactivity. He main limitations of the protocol include low yields for β-alkyl substrates, poor performance with *para*-CF_3 substituted systems, and a lack of compatibility with certain highly electron-rich precursors. Under the optimized copper(I) catalytic system, the reaction furnished 3,6-dihydro-1,2-oxazine derivatives in good yields with excellent enantioselectivity under mild conditions. A plausible mechanism was proposed, wherein the copper(I) complex reacts with vinyl diazoacetate to generate a metallo–vinylcarbene intermediate (Int-**I**), which is trapped by the nitrone to afford intermediate (Int-**II**). Subsequent intramolecular cyclization of Int-**II**, followed by elimination of the copper(I) species, delivers the 3,6-dihydro-1,2-oxazine product (Scheme 1).[43]

Building upon the utility of nitrones in Cu-mediated transformations, Dong-Liang Mo *et al.* in 2023, reported a copper-catalyzed reaction between *N*-aryl nitrones and disubstituted allenoates for the synthesis of [1,3]oxazino[3,2-*a*]indolines and dihydropyrido[1,2-*a*]indolines in good to excellent yields with high diastereoselectivity. In this study, both electron-donating and electron-withdrawing substituents on the nitrone aryl ring reacted smoothly, giving comparable yields, indicating no strong electronic preference. Temperature had a clear influence on product outcome, where lower temperatures favoured formation of oxazinoindoline products, whereas higher temperatures promoted dehydration to give the corresponding dihydro-pyridoindolines. Although the method demonstrates

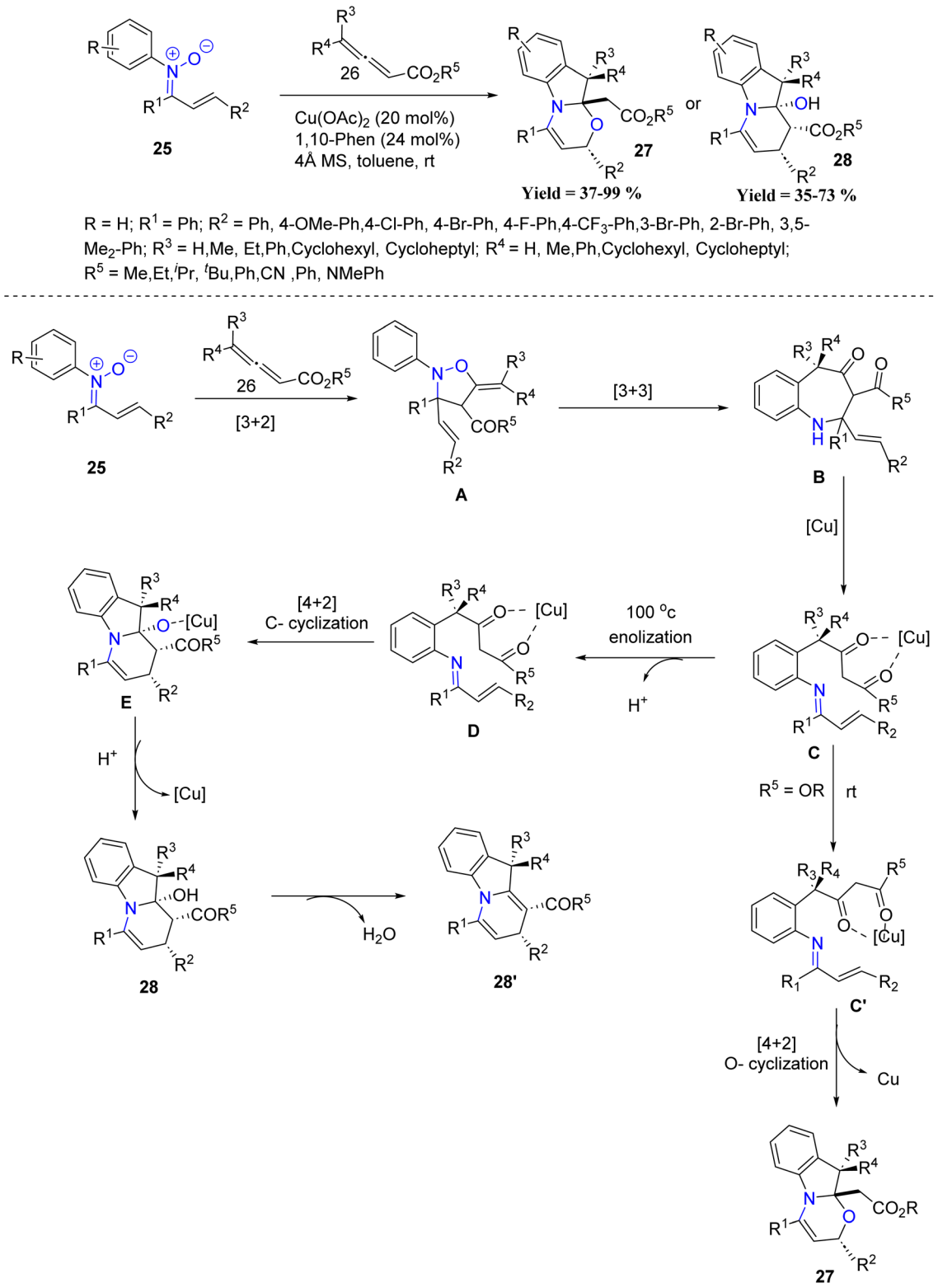

Scheme 2 Copper(II)-catalyzed cascade reactions of *N*-aryl nitrones and disubstituted allenoates.

a broad substrate scope and good functional group tolerance, several limitations were noted, including reduced yields with unsubstituted allenoates, formation of side products with ketone- or amide-substituted allenoates, longer reaction times for some substrates, and modest enantioselective induction. Mechanistically, nitrones first react with allenoates to form isooxazoline intermediate **A**, which undergoes [3,3]-sigmatropic rearrangement to yield azepinone **B**. Copper catalysis then

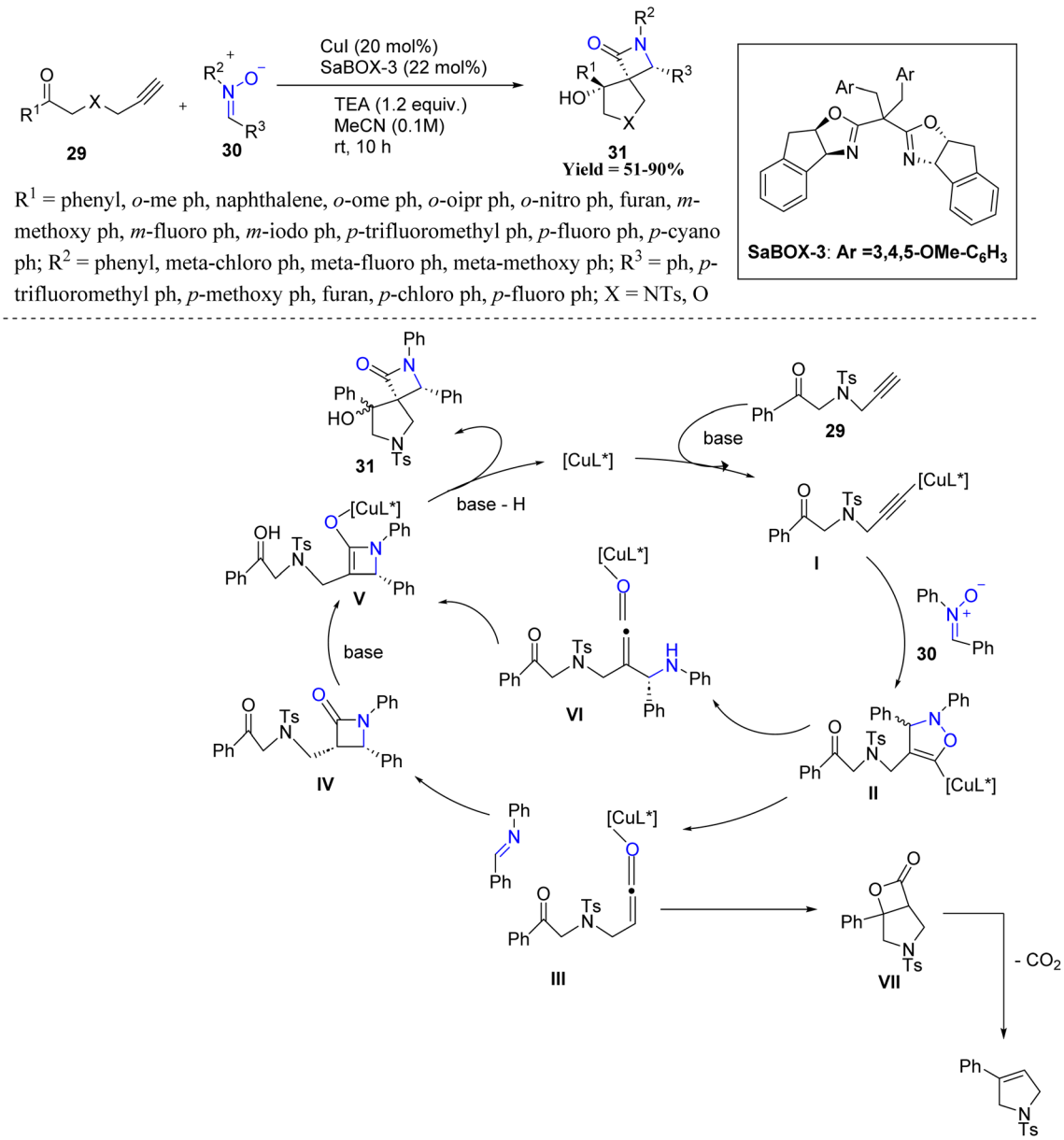

R^1 = phenyl, *o*-me ph, naphthalene, *o*-ome ph, *o*-oipr ph, *o*-nitro ph, furan, *m*-methoxy ph, *m*-fluoro ph, *m*-iodo ph, *p*-trifluoromethyl ph, *p*-fluoro ph, *p*-cyano ph; R^2 = phenyl, meta-chloro ph, meta-fluoro ph, meta-methoxy ph; R^3 = ph, *p*-trifluoromethyl ph, *p*-methoxy ph, furan, *p*-chloro ph, *p*-fluoro ph; X = NTs, O

Scheme 3 Copper-catalyzed Kinugasa/aldol domino reaction of alkyne-tethered ketones and nitrones.

promotes a *retro*-Mannich reaction, generating imine intermediate **C**. At low temperature, **C** adopts conformer **C′**, which proceeds through oxa-[4 + 2] cycloaddition to afford oxazinoindolines **27**. Alternatively, enolization of **C** gives intermediate **D**, which undergoes C-[4 + 2] cycloaddition to form **E**, followed by protonolysis to give compound **28**. Dehydration of **28** subsequently yields dihydropyridoindolines **28′**. The high diastereoselectivity is attributed to copper(II) coordination, which controls the stereochemistry of key intermediates during the cycloaddition steps (Scheme 2).[44]

In a related vein, Mark Lautens and co-workers in 2023 designed an enantioselective copper-catalyzed Kinugasa/aldol domino reaction that provides efficient access to structurally complex spirocyclic β-lactam pyrrolidinones **31**. This innovative approach enables the stereoselective construction of two spirofused ring systems bearing three contiguous stereocenters, all under mild reaction conditions. Reactivity trends reveal that both steric and electronic effects of aryl ketones and nitrones strongly influence diastereo- and enantioselectivity. *Ortho*-methyl and methoxy ketones improved diastereoselectivity, whereas bulkier substituents like ^{i}Pr reduced it. Electron-rich *ortho*- and *meta*-substituents generally enhanced enantioselectivity, while *para*-electron-withdrawing groups (*e.g.*, CF_3) increased diastereoselectivity. Electron-rich or electron-deficient aryl nitrones were well-tolerated, whereas alkyl-substituted nitrones, oxygen-tethered ketones, and alkyl ketones showed poor stereocontrol or indeterminate enantiomeric ratios, highlighting limitations in substrate scope. Mechanistically, the reaction begins with a formal [3 + 2] cycloaddition between a terminal alkyne and a nitrone,

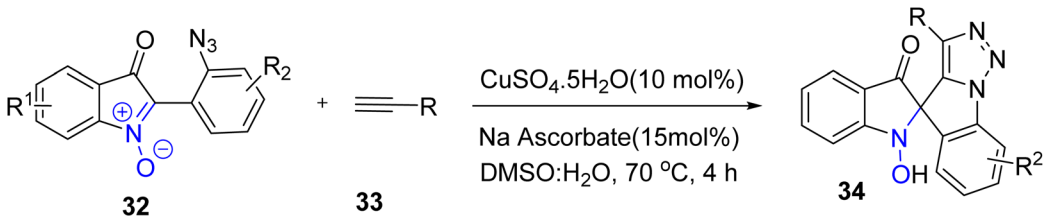

R_1= H, -OCF_3, Me; R_2 = H, -CF_3, -OCF_3; R = Ph, 4-F-Ph, 4-OCF_3-Ph, 4-OMe-ph, 4-CF_3-Ph, 4-CN-Ph, Cyclopropyl propyl, 2-hydroxyethyl, ethoxymethyl benzene, tert butyldimethyl propoxysilane, propoxymethylbenzene, 3aR,4R,6aR)-4-methoxy-2,2-dimethyltetrahydrofuro[3,4-d][1,3]dioxole-yl

Scheme 4 Cu-Catalyzed cycloaddition reaction of azido alkyne and nitrone group.

facilitated by a Cu(I) catalyst and base, yielding an initial cycloadduct. A subsequent retro-[3 + 2] fragmentation generates a ketene and an imine intermediate. These species undergo a copper-mediated asymmetric [2 + 2] cycloaddition to form a β-lactam, which then undergoes a base-promoted, diastereoselective intramolecular aldol cyclization, forming the final spirocyclic product **31** (Scheme 3).[45]

More recently, Chepuri V. Ramana and co-workers developed an efficient strategy for the construction of 1,2,3-triazole-fused spirocyclic frameworks **34**. The methodology is based on a copper-catalyzed azide–alkyne cycloaddition (CuAAC), in

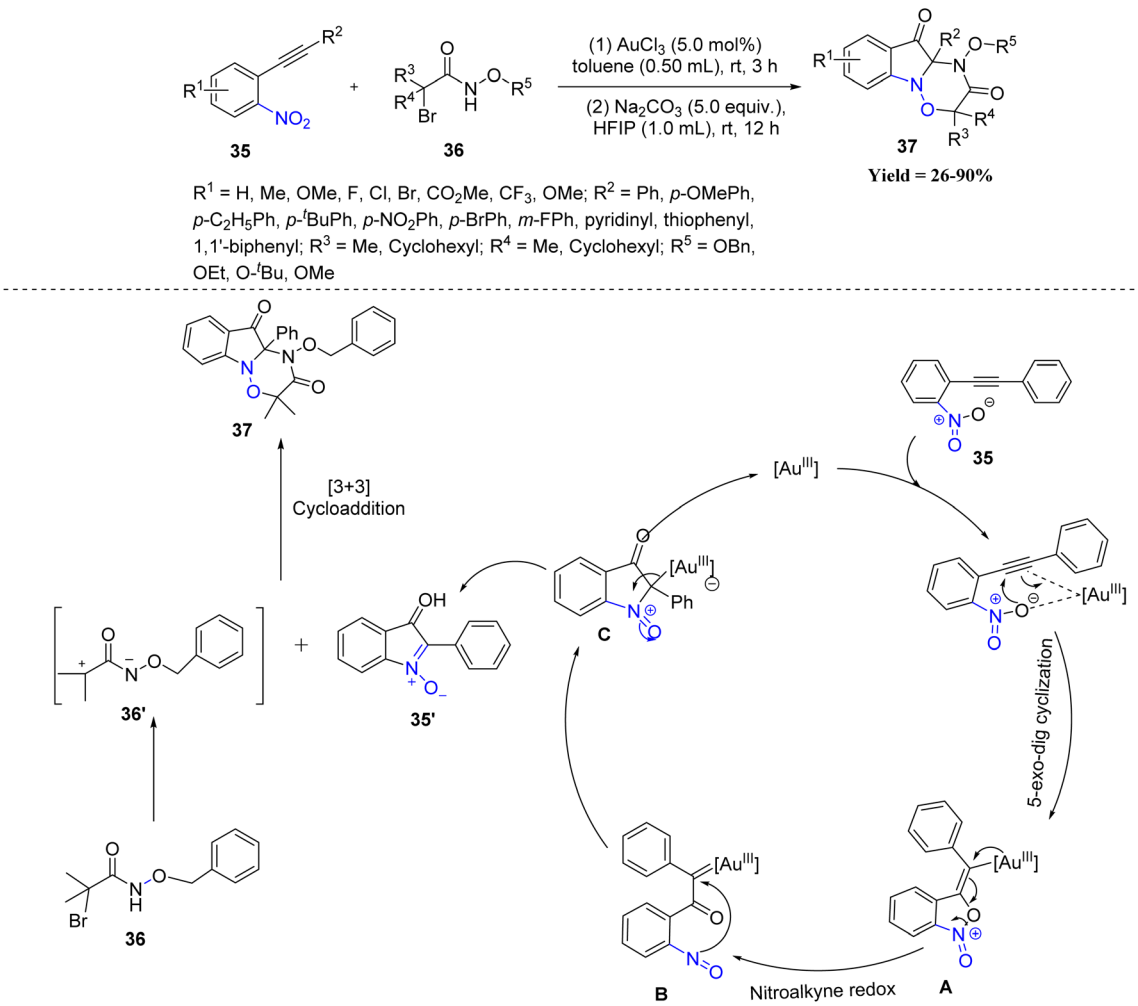

Scheme 5 Au catalyzed [3 + 3] cycloaddition reaction of isatogens with azaoxyallyl cations.

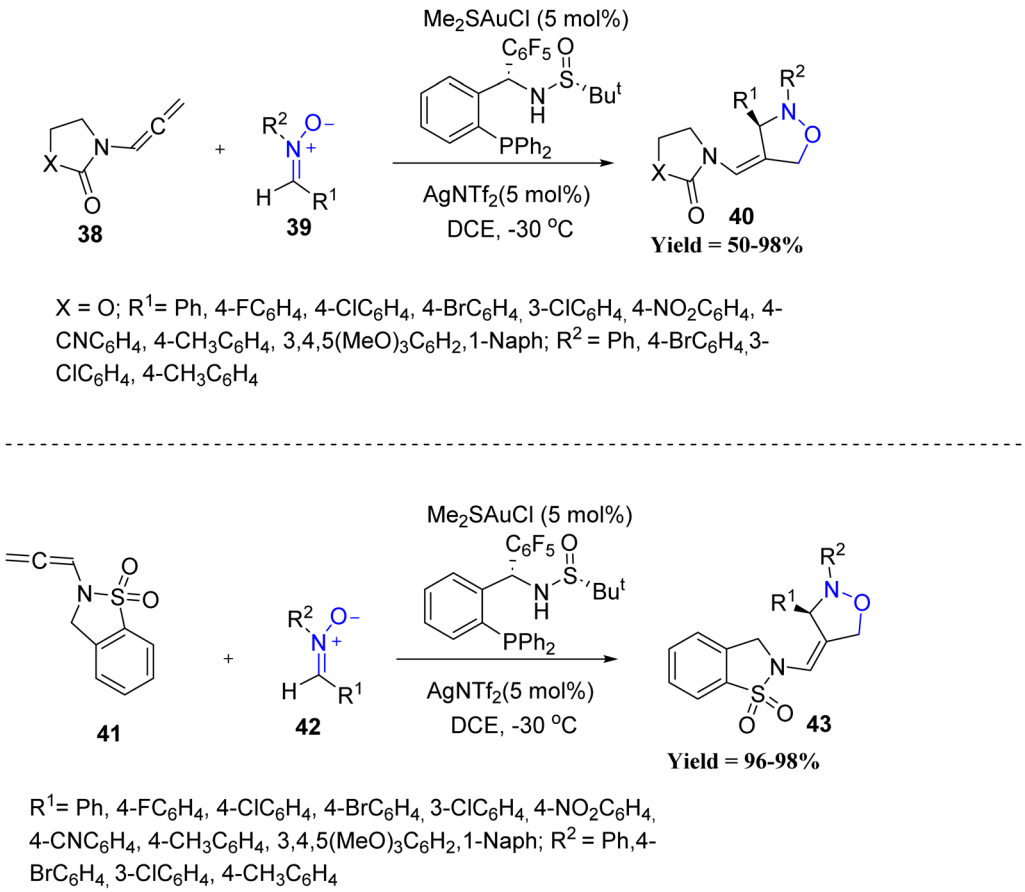

Scheme 6 Gold-catalyzed intermolecular [3 + 2] cycloaddition of *N*-allenamides with nitrones.

which an appropriately positioned nitrone group effectively intercepts the reactive triazolide intermediate. This intramolecular trapping event enables the straightforward assembly of unprecedented spiro-polyheterocyclic scaffolds. The reaction tolerates a wide range of azido–isatogens and terminal alkynes, including aryl, cyclopropyl, and aliphatic substituents, delivering products in moderate to good yields. Protected alcohols and cyclopropyl groups were compatible, and even ribose-derived alkynes furnished products, albeit as diastereomeric mixtures. Mechanistically, the transformation proceeds *via* a Cu-catalyzed [3 + 2] cycloaddition of (2-azidoaryl) isatogen **32** with a terminal alkyne **33**, followed by intramolecular capture of the Cu-triazolide by the isatogen. The reaction sequence results in the formation of one C–C and two C–N bonds, leading to a spiro-annulated heterocyclic framework **34**. Limitations include modest yields with certain functional groups, difficulty in reducing the N–OH bond under mild conditions, and partial diastereoselectivity with more complex alkynes, indicating restricted substrate scope and functional group tolerance (Scheme 4).[46]

1.1.2 Au-Catalyzed. An early advance in this area was reported by Xiuling Cui and co-workers in 2021, who reported a formal [3 + 3] cycloaddition between azaoxyallyl cations and isatogens generated *in situ* from α-halo hydroxamates **36** and *o*-nitroalkynes **35**. The process involved cycloisomerization of *o*-nitroalkynes, base-mediated elimination, and subsequent dipolar cycloaddition, providing access to tricyclic fused indolin-3-ones **37** with excellent functional group tolerance (Scheme 5). Most *o*-nitroalkynes worked well, and the yields did not change much with different groups, even bulky ones, although nitro and some halogen groups gave slightly lower yields. The biggest limitations came from the α-halo hydroxamates, because monoalkyl and trichloro types did not react, and replacing the *N*-alkoxy group completely inhibited product formation, establishing the necessity of the *N*-alkoxy functionality. Importantly, the products exhibited strong DNA-binding fluorescence, highlighting their potential in biological imaging applications.[47]

Junliang Zhang *et al.* in 2022 expanded the synthetic toolbox by developing a highly enantioselective Au-catalyzed [3 + 2] cycloaddition of *N*-allenamides **38** with nitrones **39** using the chiral ligand Ming-Phos M6 (Scheme 6). Careful optimization of the chiral ligand revealed clear structure selectivity relationships. High enantioselectivity was obtained only when the ligand contained both a pentafluorophenyl substituent and a free sulfinamide N–H, demonstrating that these elements are essential for efficient asymmetric induction. In contrast, fluorine-modified or *N*-methylated variants resulted in a pronounced decrease in enantioselectivity, confirming the sensitivity of the system to subtle ligand modifications.

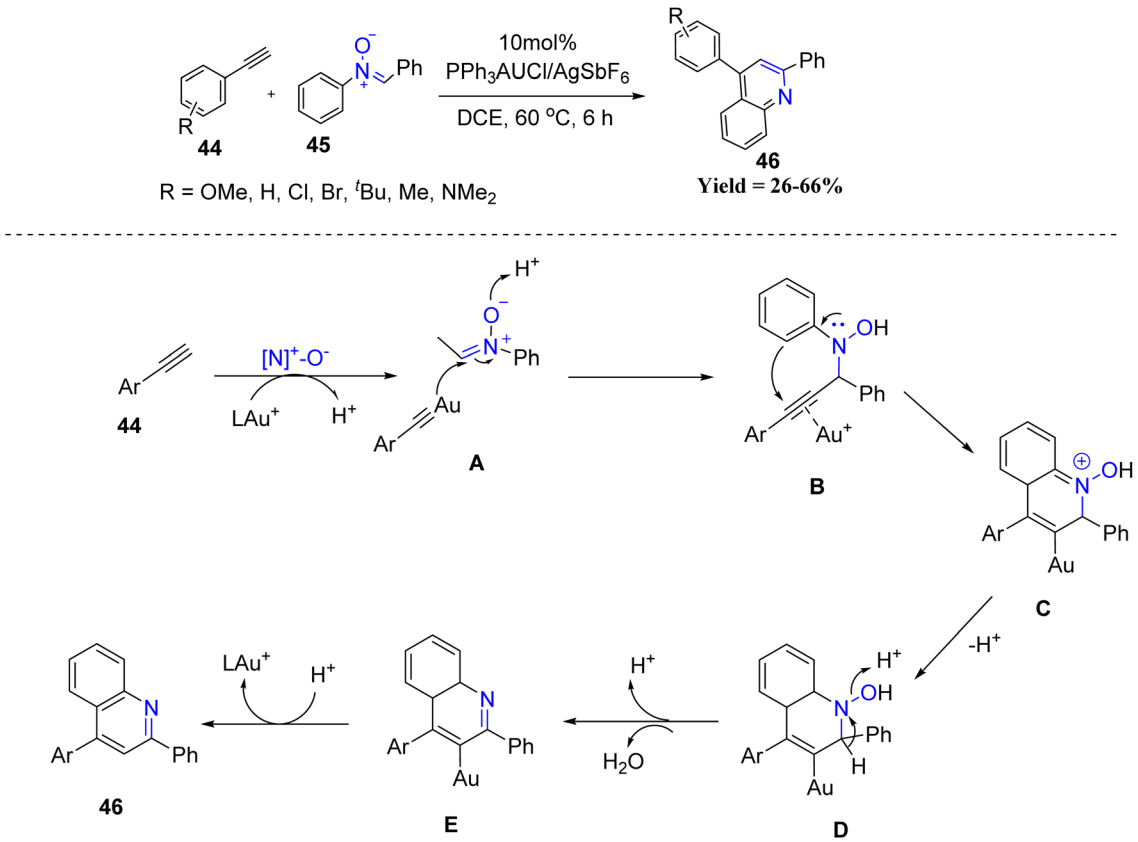

Scheme 7 Gold-catalyzed [4 + 2] annulation between terminal arylynes and nitrones.

However, tosyl-derived allenamides afforded products with lower enantioselectivity, and substrates outside heterocyclic *N*-allenamides were not tolerated, indicating limitations in broader substrate diversity.[48]

In the same year, Rai-Shung Liu *et al.* in 2022 disclosed a gold-catalyzed [4 + 2] annulation of terminal arylalkynes **44** with nitrones **45**, affording quinoline derivatives **46** (Scheme 7). Initially, the terminal alkyne coordinates with a cationic gold(I) catalyst in the presence of an oxidizing additive, such as pyridine *N*-oxide, to generate a reactive alkynyl gold species **A**. This intermediate is known to exhibit enhanced nucleophilicity at the α-position and readily undergoes nucleophilic addition to the electrophilic carbon of the nitrone, forming a propargylic-type intermediate **B**. Subsequent intramolecular cyclization, likely proceeding *via* a 6-*endo*-dig pathway, leads to the construction of a six-membered dihydroquinoline framework **E**. The resulting intermediate then undergoes protodeauration to eliminate the gold catalyst and furnish the dihydroquinoline product **46**. Electron-rich arylalkynes provided higher yields than electron-neutral or electron-withdrawing substrates. The reaction was also compatible with a range of substituted nitrones, although *meta*-substituted nitrones produced mixtures of regioisomers. Despite its broad applicability, the method showed reduced efficiency with electron-deficient alkynes, did not tolerate aliphatic alkynes, and exhibited regioselectivity limitations with sterically or electronically biased nitrones, defining boundaries in substrate scope (Scheme 7).[49]

Further innovation came from the same group in 2023, when they devised a cascade annulation of 1,5-diyn-3-ols **47** with nitrones **48** to furnish carbazole frameworks **49** (Scheme 8). The transformation begins with coordination of the gold catalyst to the alkyne, generating alkenyl–gold species **A**. This intermediate undergoes a 3,3-sigmatropic rearrangement to give species **B**, which upon proton loss produces an iminium cation **C**. Subsequent hydrolysis of **C** yields an aniline bearing a ketone functionality (intermediate **D**), which undergoes intramolecular indole/alkyne cyclization to form species **F**. Finally, dehydration of intermediate **G** delivers the carbazole product **49**. This study demonstrates that gold catalysis can efficiently promote cascade processes for the rapid assembly of complex heterocycles. *Para*-substituted nitrones showed the highest reactivity, whereas *meta*-substituted substrates gave regioisomeric mixtures, and *ortho*-substituted nitrones afforded low yields. A limitation of the protocol is that substrates outside the 1,5-diyn-3-ol framework or lacking the internal alkyne functionality failed to undergo annulation.[50]

In 2024, Liu's group showcased the regioselectivity control achievable in Au catalysis through two oxidative annulation pathways of 1,5-allenynes **50** with nitrones **51**/**53** (Scheme 9). Internal alkynes afforded 3,4-fused nitroxy naphthols **52**, while terminal alkynes gave 2,3-fused analogues **54**. The study revealed that the nature of the alkyne substituent dictates the

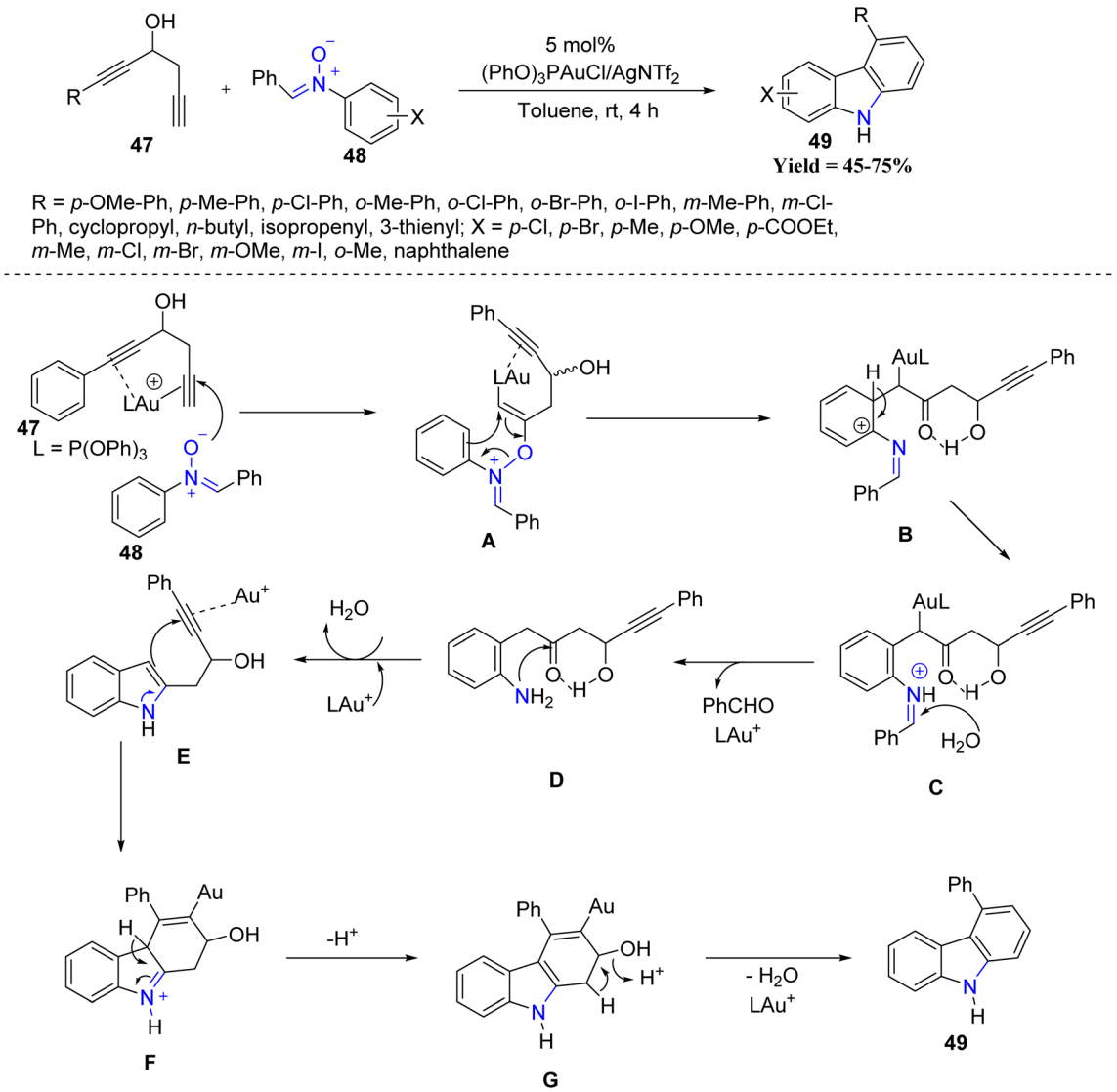

Scheme 8 Au-Catalyzed [3 + 2] annulation cascades between 1,5-diyn-3-ol and nitrone.

annulation outcome, providing a predictable regioselective switch. Despite these productive trends, the methodology exhibited limitations, as substrates outside the 1,5-allenyne framework, non-aromatic nitrone variants, and sterically congested partners failed or gave diminished yields, and regioisomer separation became challenging in several cases.[51]

Wen-Tai Li and co-workers in 2024 introduced a stereoselective spiro-cyclization protocol employing 2-benzyl-3-alkynylchromones **55** and nitrones **56** (Scheme 10). Mechanistically, gold activation of the alkyne forms intermediates **I**, which after deprotonation and 6-*endo*-dig cyclization gives alkenyl–gold species **II**. Subsequent [3 + 2] cycloaddition with the nitrone generates intermediate **III** (isoxazolidine), which undergoes gold-assisted oxirane formation **VI**, followed by ring contraction and opening to produce species **VII**. An intramolecular *N*-attack then completes the formation of the dispiro-benzofuran product **58**. This gold-catalyzed stereoselective spiro-cyclization demonstrated a clear reactivity trend, where variations at the C-6 and C-7 positions of the chromone core were well tolerated, and both electron-donating and electron-withdrawing substituents afforded good yields of spiro-isoxazolidine and dispiro-benzofuran products. *Para-* and *meta*-substituted benzylic aryl groups reacted efficiently, while *ortho*-substituted and sterically encumbered partners delivered comparatively lower conversions. However, the method showed limited applicability, as only suitably substituted 2-benzyl-3-alkynylchromones and aryl nitrones were reactive, while sterically hindered, non-aryl, or structurally deviating substrates failed or gave poor yields (Scheme 10).[52]

1.1.3 Ir-Catalyzed. In this context, Song Sun and co-workers in 2021 developed a redox-neutral iridium-catalyzed dual C–H activation at the C2 and C3 positions of indoles **59** with nitrones **60** (Scheme 11). Under the optimized conditions, a wide range of indoles bearing electron-donating, electron-withdrawing, halogen, and heteroaryl substituents smoothly delivered the desired products in good to excellent yields. Likewise, diverse

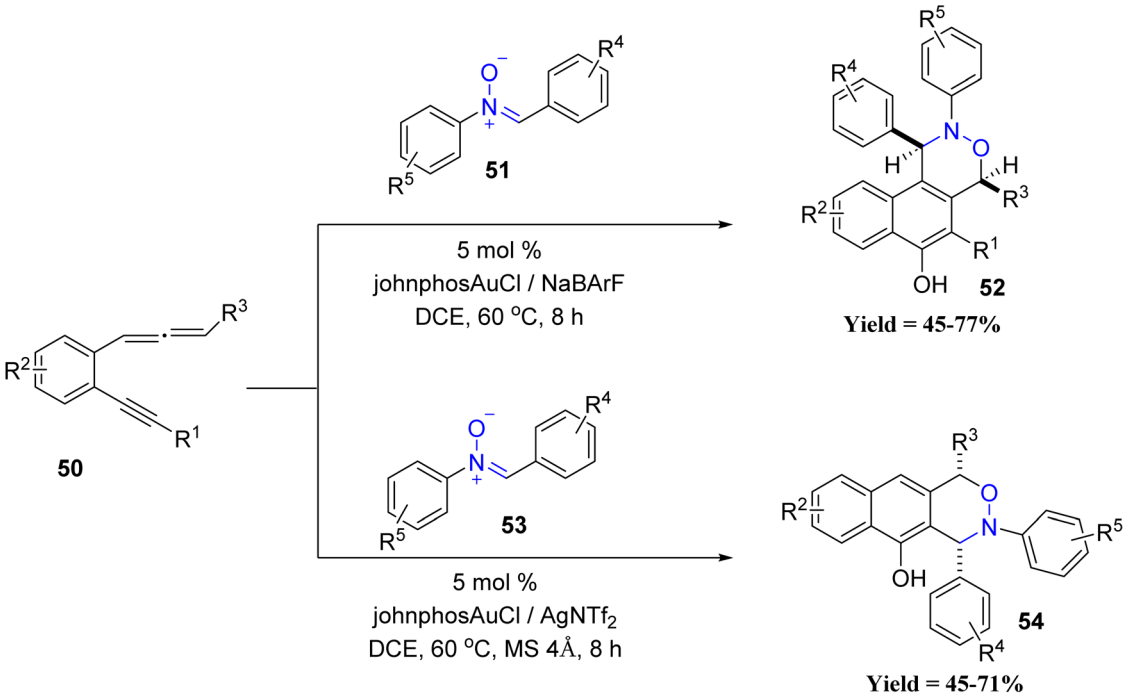

R^1 = Ph, *p*-Cl Ph, *p*-OMe Ph, *p*-Me Ph, *m*-Cl Ph, *m*-Me Ph, *o*-Cl Ph, cyclopropyl, -$(CH_2)_2$OTBS; R^2 = 4-Cl, 4-Me, 4-OMe, 4-COOMe, 5-Cl, 5-Me, 5-OMe, 5-COOMe, 5-CN, 6-OMe, 6-Cl, 3-OMe, Ph; R^3 = Me; R^4 = *p*-Cl Ph, *p*-OMe Ph, *p*-Br Ph, *p*-Me Ph, *m*-Cl Ph, *m*-Me Ph, *o*-Cl Ph, *o*-Me Ph, *o*-Br Ph, Ph, 2- napthayl, 2-thiophenyl; R^5 = *o*-Cl Ph, *o*-Me Ph, *m*-Cl Ph, *p*-Cl Ph, *p*-Me Ph, Ph , *p*-OMe Ph

Scheme 9 Gold-catalyzed oxidative annulations of 1,5-allenynes with nitrones.

nitrones, including sterically hindered, heteroaryl, naphthyl, cinnamyl, and functionally enriched variants, were well tolerated, affording the fused heterocycles efficiently. Mechanistic investigations revealed that nitrones act not only as coupling partners but also as internal oxidants. However, the method displays a key limitation: it strictly requires the 2-pyridyl directing group, as alternative directing groups or imine analogues failed to produce any product.[53]

1.1.4 Ag-Catalyzed. A key contribution to silver catalysis was reported by Dong-Liang Mo and co-workers in 2021, who designed a [3 + 2] cycloaddition/[3,3]-sigmatropic rearrangement cascade between *N*-vinyl α,β-unsaturated nitrones **62** and chiral propioloyloxazolidin-2-ones **63** (Scheme 12). This strategy provided access to chiral nine-membered N-heterocycles **64**/**65** with excellent diastereoselectivity. Systematic evaluation revealed that oxazolidinones bearing Me, ^{i}Pr, ^{t}Bu, Ph, or indenyl substituents afforded the corresponding cycloadducts in good yields and tunable diastereoselectivity, with bulkier substituents enhancing stereocontrol. The reaction exhibited broad nitrone compatibility: aryl, heteroaryl, alkyl-, and ring-substituted *N*-vinyl nitrones efficiently furnished the nine-membered heterocycles in moderate to good yields as single diastereomers under low-temperature conditions. Notably, attempts to perform the reaction at room temperature led to inseparable mixtures of the two diastereomers, highlighting a key limitation, as strict temperature control is essential to obtain single isomers. Mechanistically, coordination of the oxazolidinone substrate to the silver catalyst generates intermediate **A**, which undergoes [3 + 2] cycloaddition with the nitrone to give intermediate **B**. A subsequent [3,3]-sigmatropic rearrangement furnishes the observed products **64** and **65**, with the silver catalyst being regenerated through a reversible equilibrium. This work highlights the ability of silver catalysis to combine pericyclic processes in a highly stereoselective fashion, offering a valuable entry to architecturally complex N-heterocycles (Scheme 12).[54]

1.1.5 Rh-Catalyzed. In recent years, Xuesen Fan *et al.* demonstrated an efficient and mild Rh(III)-catalyzed [4 + 1] spiro-annulation strategy for the synthesis of spirocyclic indole-*N*-oxide derivatives **68**. The reaction involves *N*-aryl nitrones **66** and 2-diazo-1,3-indandiones **67** as C1 synthons, proceeding *via* a C–H activation/spiro-annulation cascade under extremely mild conditions. The method showed excellent functional-group tolerance: *para*-, *meta*-, and even several *ortho*-substituted nitrones bearing alkyl, alkoxy, halogen, CF_3, CN, CO_2Me, heteroaryl, alkenyl, naphthyl, and disubstituted aryl groups reacted smoothly, delivering the products in moderate to excellent yields. The diazo component also displayed wide scope, accommodating alkyl-, halo-, dimethyl-substituted, and naphthalene-fused variants, as well as six-membered diazo

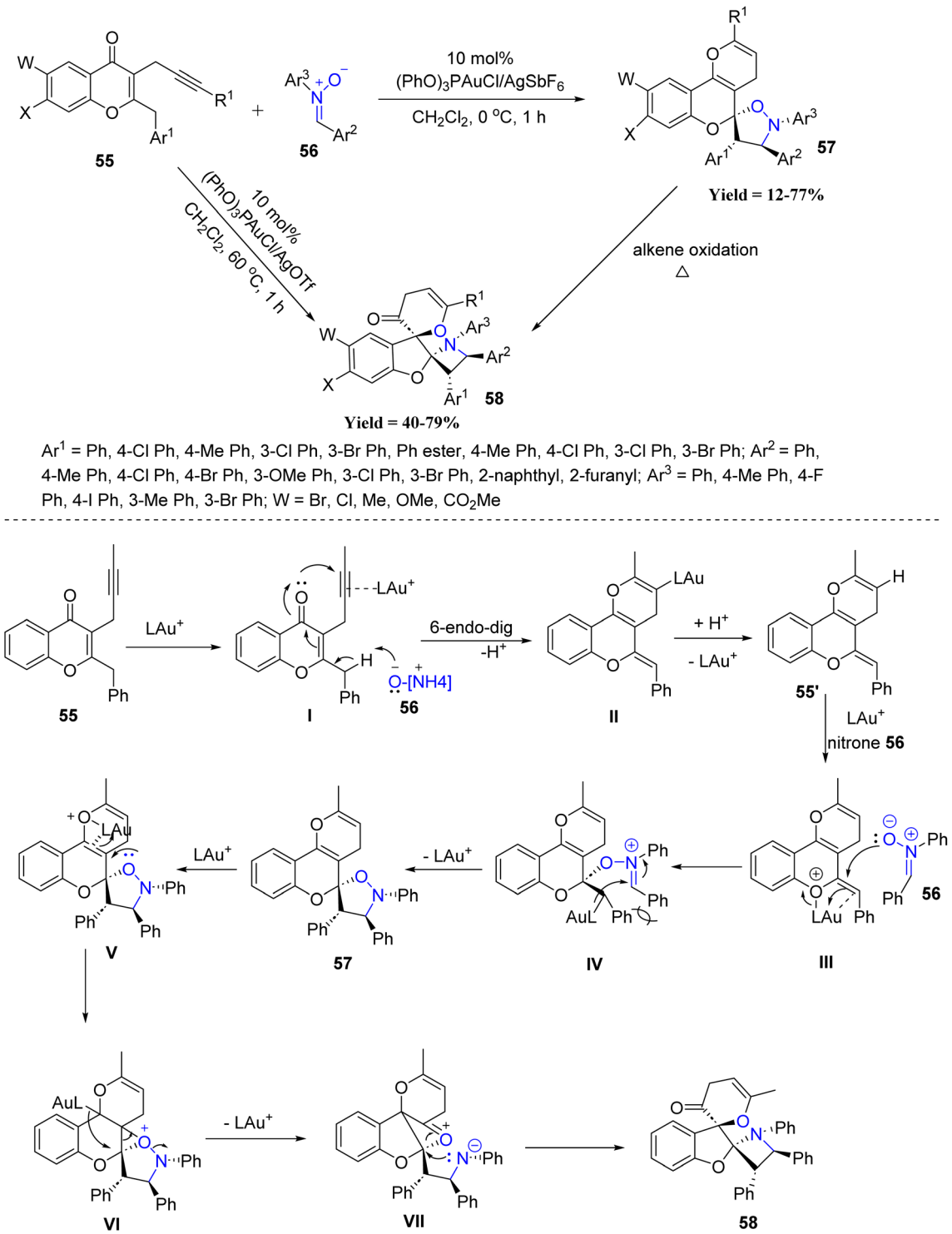

Scheme 10 Gold-catalyzed cascade reactions of 2-benzyl-3-alkynyl chromone and nitrone.

compounds. A notable limitation, however, is that certain *ortho*-substituted nitrones particularly *ortho*-Me failed to undergo spirocyclization due to steric hindrance. Initially, the reaction begins with C–H activation of the *N*-aryl nitrone **66** by the Rh(III) catalyst to form a rhoda-cycle intermediate **A.** Coordination with the diazo compound **67** generates a Rh-carbene **B**, which undergoes migratory insertion followed by intramolecular nucleophilic attack on the C=N bond. Protonation regenerates the catalyst and forms a key intermediate **D**, which is subsequently oxidized by AgOAc to deliver the spirocyclic indole-*N*-oxide **68.** The product **68** is then successfully employed in 1,3-dipolar cycloaddition reactions with maleimides **69**, leading to

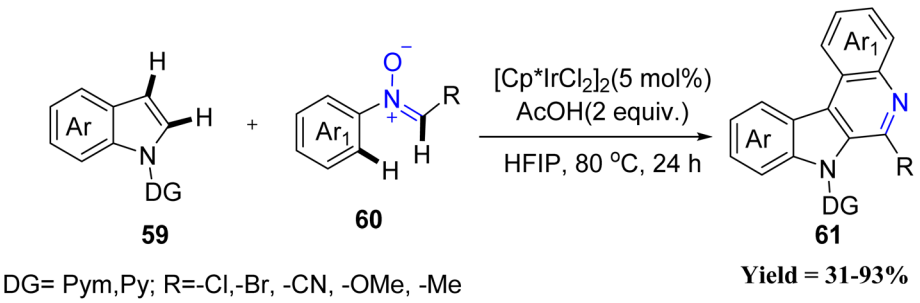

Scheme 11 Iridium-catalyzed C–H functionalization of indoles with nitrones.

the formation of structurally complex maleimide-fused polycyclic scaffolds **70** (Scheme 13).[55]

Following this, Li-Ming Zhao *et al.* in 2023, developed a Rh(III)-catalyzed cascade reaction of nitrones **71** and cyclic 2-diazo-1,3-diones **72** for the efficient synthesis of angular chromendiones. The nitrone serves as a traceless directing group, enabling C–H activation and annulation. Electron-donating nitrones showed the highest reactivity, while electron-withdrawing or strongly electron-deficient nitrones failed. Substitution pattern had minimal effect, though *ortho*-substituted nitrones gave lower yields due to steric hindrance. A range of cyclic diazo compounds was tolerated, but unsubstituted or indantrione-based diazos reacted poorly. Overall, the method is efficient but limited by electron-poor nitrones and specific less-reactive diazo partners. Mechanistically, the reaction starts with coordination of a cationic Rh(III) catalyst to nitrone, followed by C–H activation to form a six-membered rhodacycle **A**. Then **A** reacts with a diazo compound, releasing

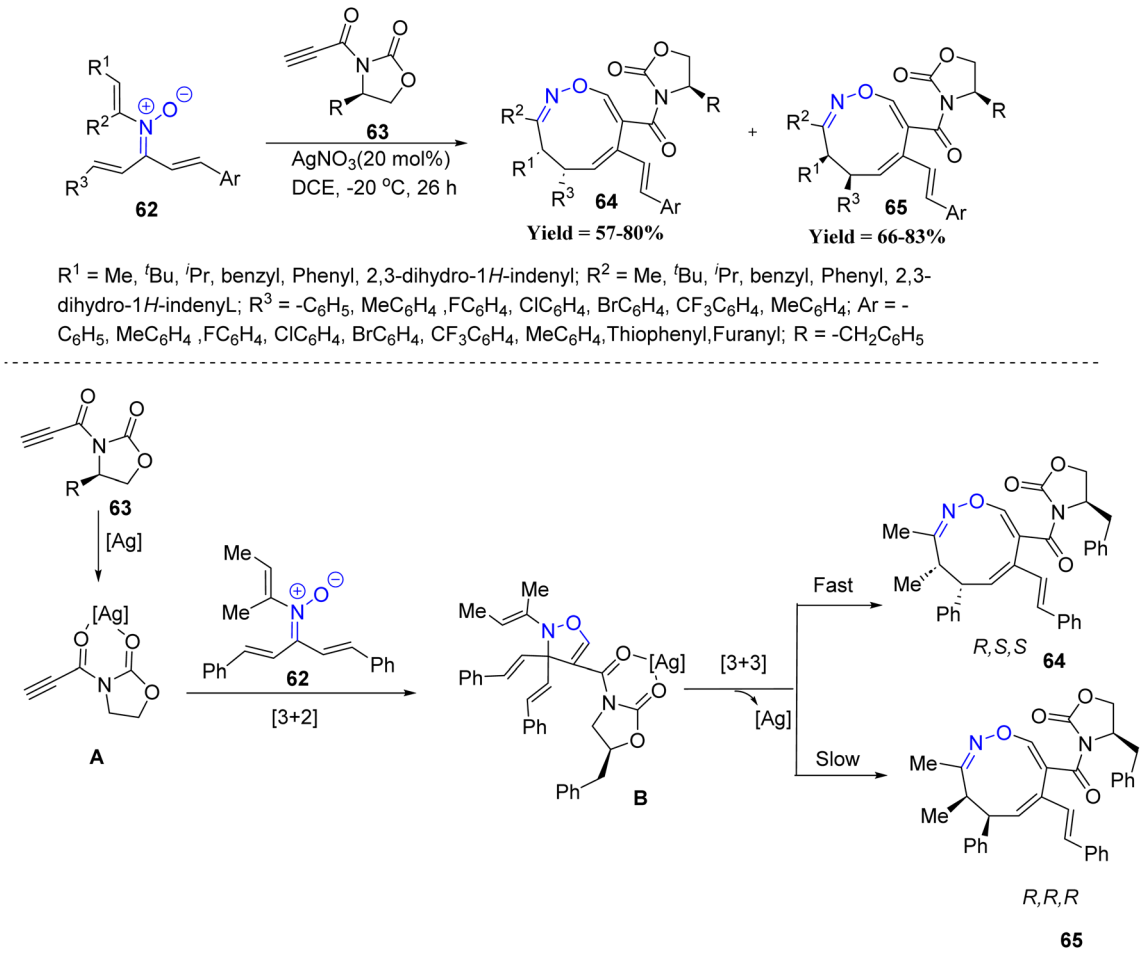

Scheme 12 Silver(I)-promoted cycloaddition and rearrangement from *N*-vinyl-α,β-unsaturated nitrones with chiral 3-propioloyloxazolidin-2-ones.

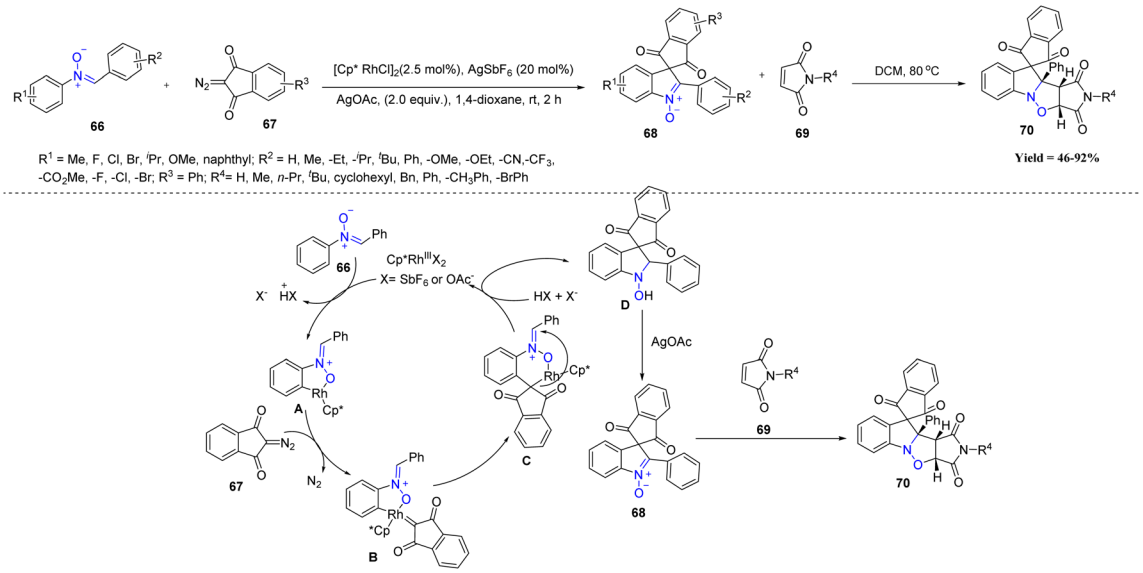

Scheme 13 Rh(III)-Catalyzed spiroannulation reaction of *N*-aryl nitrones with 2-diazo-1,3-indandiones.

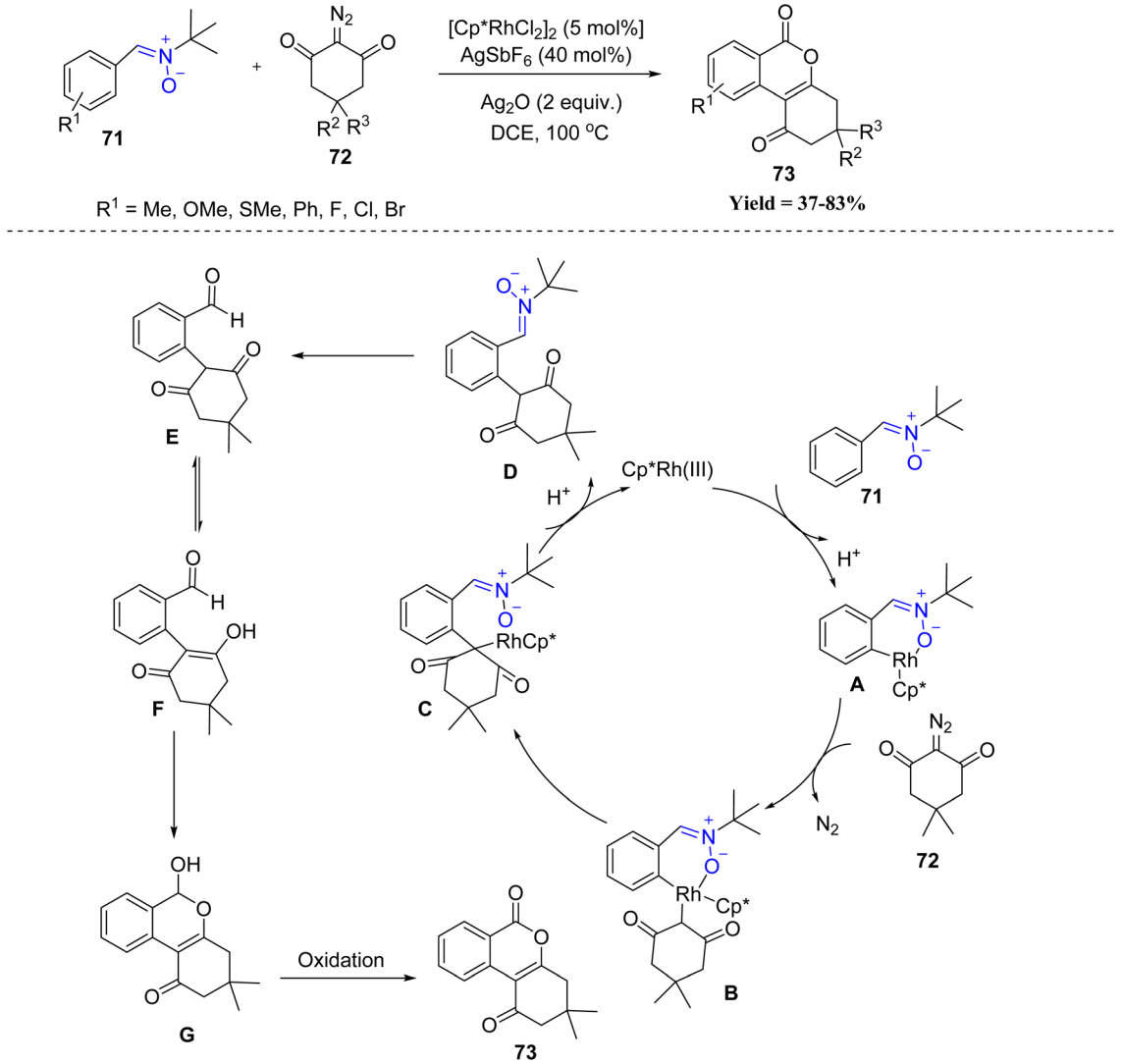

Scheme 14 Rh(III) catalyzed C–H annulation of nitrones with cyclic 2-diazo-1,3 diones.

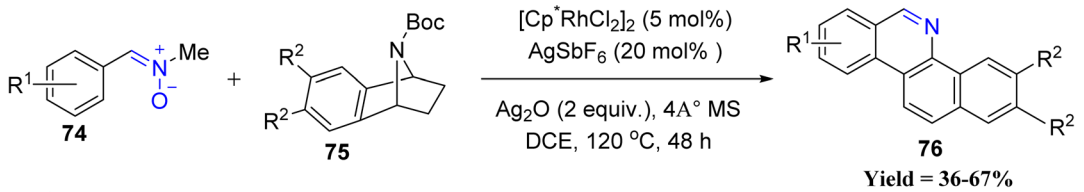

R^1 = H, 4-Me, 4-OMe, 4- F, 4-Cl, 4-Br, 4-I, 4-NO_2, 3-OMe, 3-Me, 3-Br, 3-F, 2-OMe, 2-Me, 2-Br, 2-Cl, 2-F, Thiophenyl, 1,2-dimethoxy, 2,3-dioxolanyl , 3-OH, 2-OMe, 4,5-dimethoxy, 4,5-dioxolanyl, 3,4-dimethyl, 2,3-napthayl
R^2 = 1,3-dioxolene, 3,4-dimethoxy

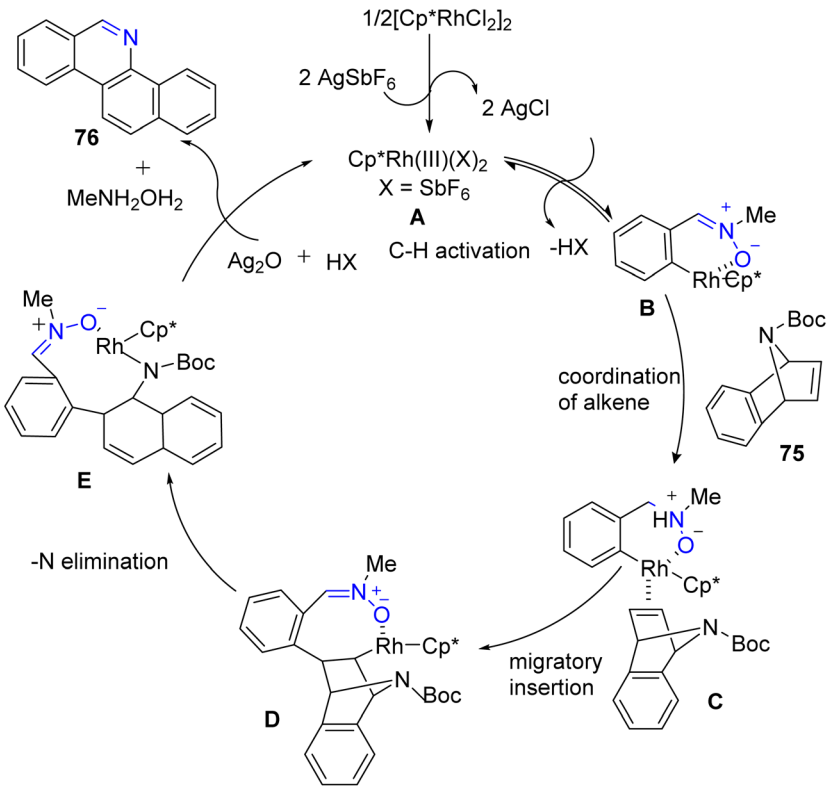

Scheme 15 Rh(III) catalyzed 7-azabenzonorbornadienes and aryl nitrones.

N_2 to generate a Rh-carbene intermediate **B**. Migratory insertion of the Rh–aryl bond forms a seven-membered rhodacycle **C**, which undergoes protonolysis and ligand dissociation to produce intermediate **D**, regenerating the Rh(III) catalyst. The nitrone in **D** rapidly decomposes into an aldehyde, yielding intermediate **E**, an aryl-substituted 1,3-diketone. Tautomerization to the enol form **F** is followed by intramolecular nucleophilic attack on the carbonyl, forming cyclic hemiacetal **G**. Final oxidation of **G** produced the angular chromendione **73** (Scheme 14).[56]

Masilamani Jeganmohan *et al.* applied Rh(III) catalysis to a one-pot synthesis of benzo[*c*]phenanthridine alkaloids **76** through a cascade involving C–C bond formation and cycloaromatization. In this method, aryl nitrones **74** react with 7-azabenzonorbornadienes **75** to afford various biologically important benzo[*c*]phenanthridine derivatives **76** in moderate to good yields. A wide range of nitrones including electron-neutral, electron-rich, halogenated, unsymmetrical, disubstituted, dimethyl, and naphthyl variants reacted efficiently, with electron-donating nitrones showing superior reactivity. The method also tolerated diverse azabenzonorbornadiene partners and enabled the rapid synthesis of bioactive alkaloids such as norchelerythrine, norsanguinarine, and decarine. However, the reaction failed with 2-thiophenyl nitrones due to catalyst chelation, and electron-deficient nitrones delivered comparatively lower yields, marking the main limitations of the protocol. Mechanistically, the active cationic Rh(III) species **A** is generated *via* ligand exchange between a rhodium dimer and $AgSbF_6$. The aryl nitrone coordinates to this Rh(III) center through its oxygen atom, forming a six-membered rhodacycle intermediate **B** *via* a deprotonation process. Subsequent coordination and migratory insertion of the azabenzonorbornadiene lead to an eight-

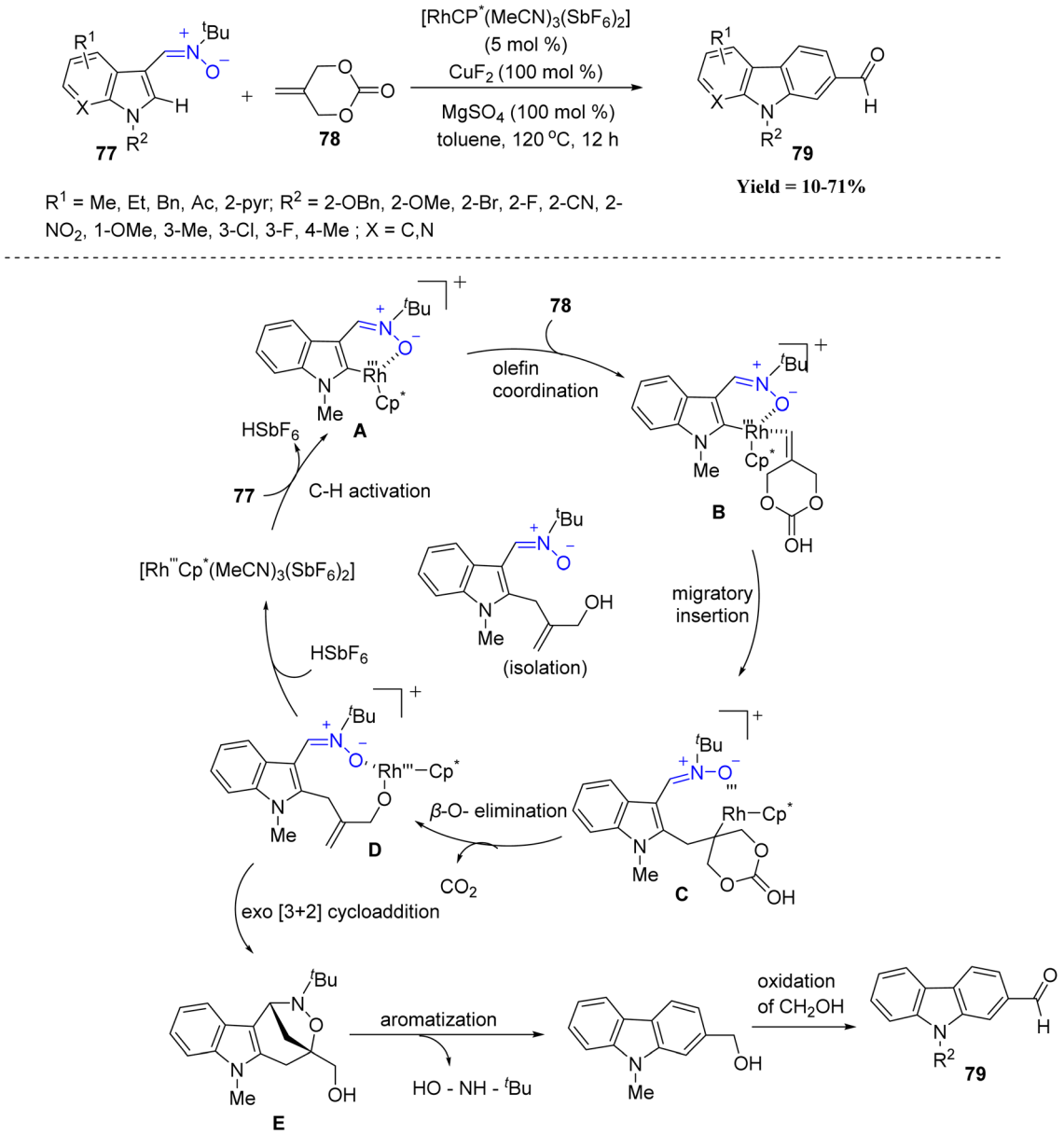

Scheme 16 Rhodium(III)-catalyzed cross-coupling reaction between indolyl nitrones and 2-methylidene cyclic carbonate.

membered rhodacycle **D**, which undergoes β-nitrogen elimination to yield an intermediate **E** bearing a reactive imine motif. A final intramolecular cyclization and aromatization step, assisted by silver oxide, completes the transformation and regenerates the rhodium catalyst (Scheme 15).[57]

Similarly, Su Kim *et al.* in 2023 disclosed a novel Rh(III)-catalyzed cross-coupling between indolyl nitrones **77** and 2-methylidene cyclic carbonates **78**, enabling the synthesis of C2-formylated carbazoles derivatives **79**. Various N-protected and C4–C7 substituted indoles, as well as heteroaryl nitrones, reacted smoothly, delivering the products in good yields. Mechanistically, a cationic rhodium(III) catalyst promotes selective C2–H activation of the indolyl nitrone to form a rhodacycle intermediate **A**. Subsequent coordination and migratory insertion of the cyclic carbonate yields an O–Rh–C complex **C**, which undergoes β-*O*-elimination followed by an *exo*-type [3 + 2] cycloaddition to form a bridged heterocycle **E**. Aromatization and aerobic oxidation of the resulting benzylic alcohol complete the transformation, furnishing the C2-formylated carbazole scaffold **79**. However, the method showed clear limitations: sterically bulkier carbonates (*e.g.*, benzylidene carbonate) completely inhibited the reaction, and altered vinyl carbonate structures diverted the pathway to undesired C3-formylation (Scheme 16).[58]

Further extending Rh(I) catalysis, Weidong Rao *et al.* reported an efficient rhodium(I)-catalyzed strategy for constructing fully substituted furans featuring a 3,4-fused 5–8-membered carbocycle, heterocycle, or spirocycle in 2024. The transformation involves a cascade annulation of 1,*n*-diynyl nitrones, facilitated by 1,1,1,3,3,3-hexafluoroisopropanol (HFIP) as

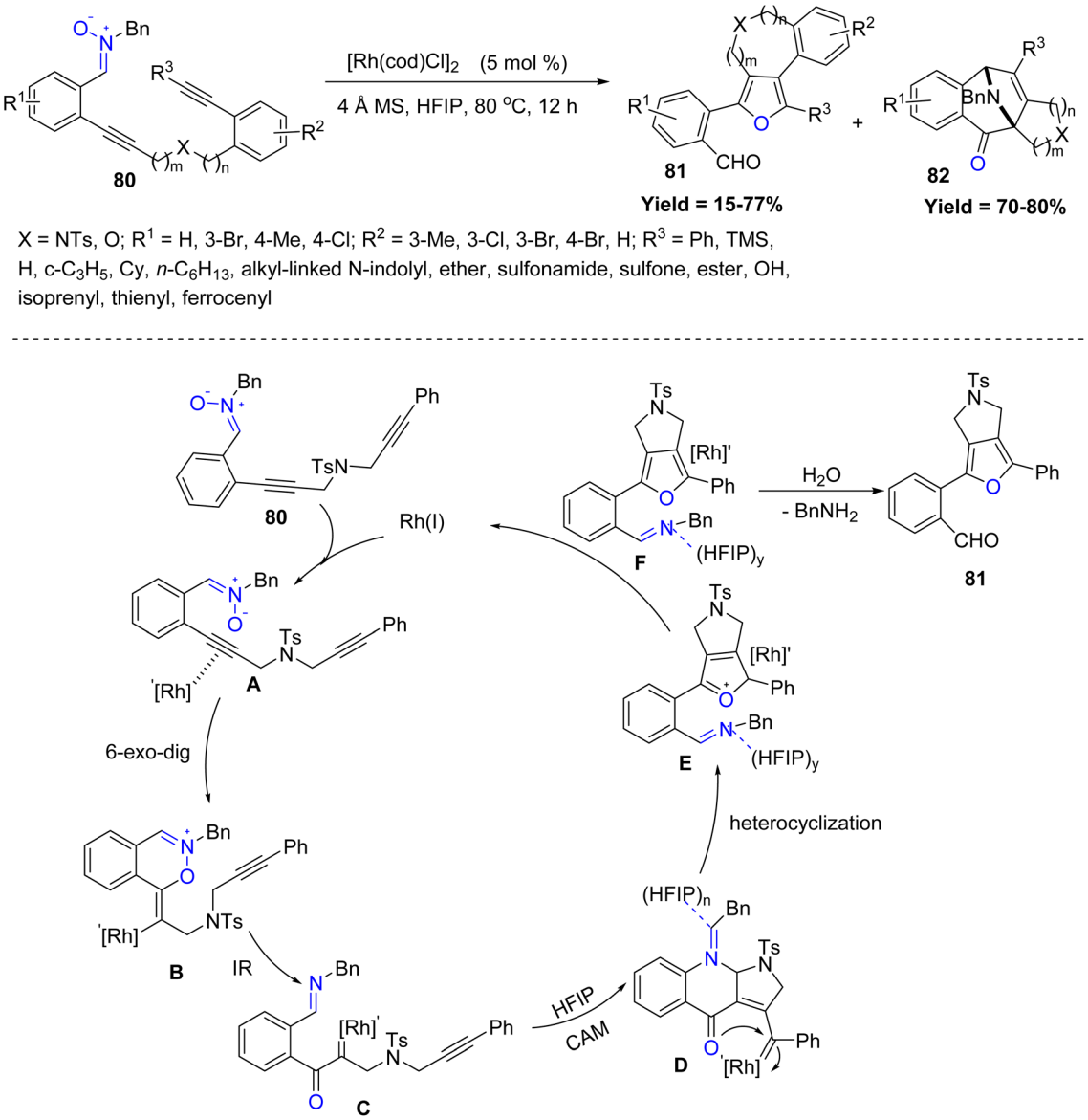

Scheme 17 Rhodium(I)-catalyzed cascade annulation of 1,*n*-diynyl nitrones.

a critical additive. 1,7- and 1,8-diynyl nitrones showed the highest reactivity, O-tethered variants also worked well, while sterically congested or terminal-alkyne substrates and longer tethers (*e.g.*, 1,9-diynyl) displayed markedly reduced reactivity. Mechanistic investigations using 1,6-diynyl nitrone as a model substrate revealed that the Rh(I) catalyst selectively coordinates with the *ortho*-alkynylphenyl moiety to form a Rh-bound intermediate **A**. This species undergoes a 6-*exo*-dig oxycyclization, generating a vinyl-rhodium intermediate **B**. A subsequent N–O bond cleavage driven by an internal redox process leads to the formation of an α-oxo rhodium carbene **C**. Interestingly, instead of following the conventional azomethine ylide pathway, the imino nitrogen of the intermediate interacts *via* hydrogen bonding with the HFIP solvent, altering the course of reactivity. This unique interaction enables the carbene intermediate to undergo a cascade cyclization *via* a carbene-assisted mechanism (CAM), yielding a γ-oxo rhodium carbene complex **D**. Further intramolecular nucleophilic attack by the oxygen atom on the carbene center leads to heterocyclization, forming an oxonium intermediate **E**. Demetalation and subsequent hydrolysis during work-up yield the final 3,4-fused fully substituted furan product **81** along with benzylamine **82** as a byproduct. However, limitations included decomposition of terminal-alkyne substrates and poor yields from 1,6- and especially 1,9-diynyl nitrones due to unfavourable transannular and entropic effects (Scheme 17).[59]

1.1.6 Co-Catalyzed. Xiaoming Feng *et al.* in 2022, developed an efficient *N*,*N*-dioxide/Co(II) catalytic system for the cascade reaction of α,β-unsaturated *N*-aryl nitrones **83** with allenes **84**, yielding dihydro pyridoindoles **85** in good yields with excellent diastereo- and enantioselectivity under mild conditions. The reaction proceeds *via* an initial [3 + 2] cycloaddition, followed by

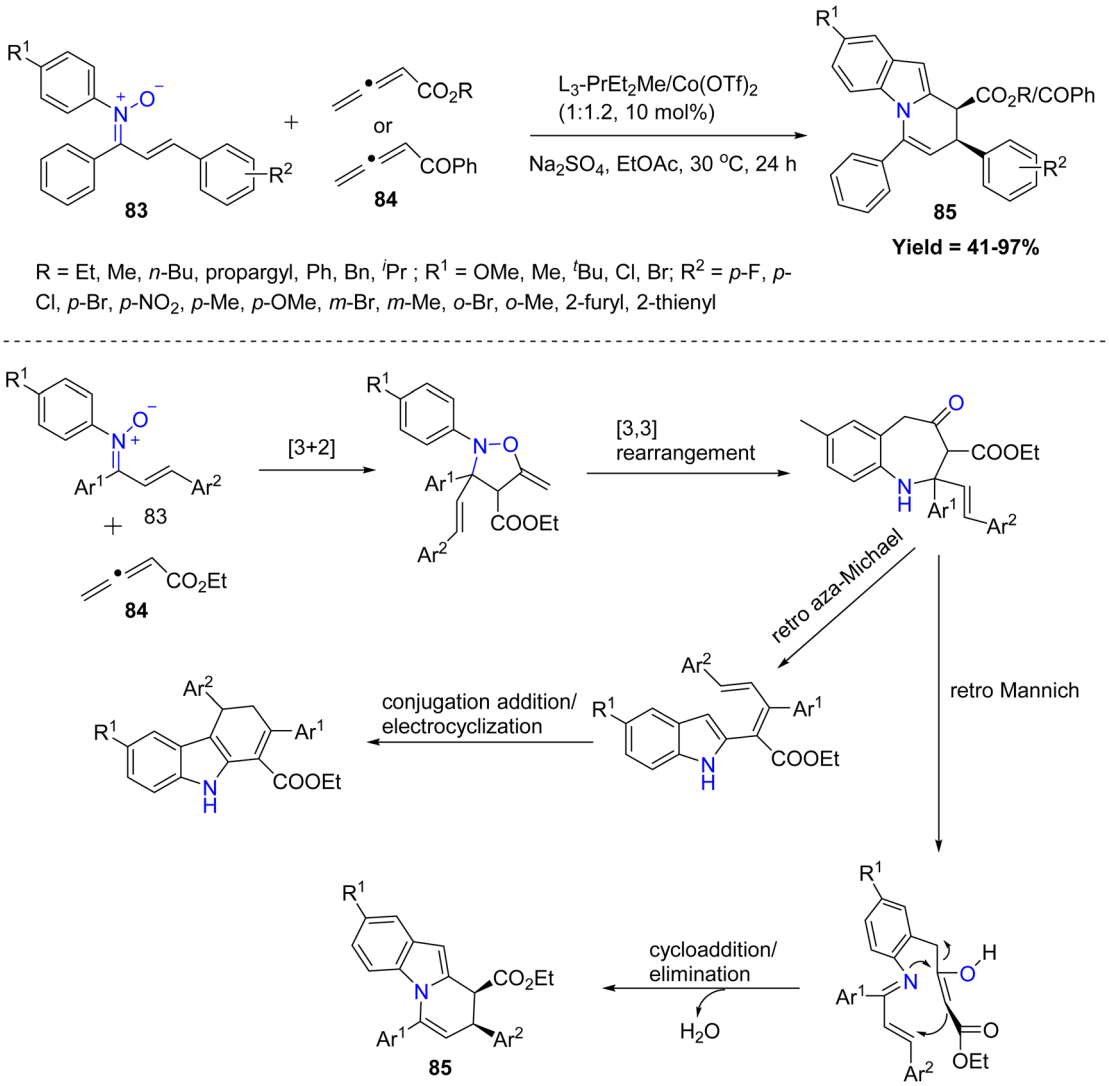

Scheme 18 Cobalt(II) complex catalytic multistep cascade reaction of α,β-unsaturated-*N*-aryl nitroneswithallenes.

a [3,3]-sigmatropic rearrangement to form a benzazepine intermediate, which selectively undergoes a retro-Mannich pathway under cobalt catalysis to give the desired products **85**. Diverse allenoate esters (Me, *n*-Bu, propargyl, Ph, Bn) and a wide range of α,β-unsaturated *N*-aryl nitrones including electron-rich, electron-poor, *ortho*/*meta*/*para*-substituted, heteroaryl, and ring-fused systems gave the dihydropyridoindoles in good yields with excellent diastereo- and enantioselectivity. The main limitations were decreased stereocontrol with sterically bulky allene esters and modest yields for some highly substituted or heteroaryl nitrones, indicating steric and electronic sensitivity at the nitrone component (Scheme 18).[60]

More recently, Rafał Loska *et al.* in 2023, developed a tandem strategy has been developed for the construction of complex spirocyclic isoindolines **88** and pyrrolidines **89**, involving Co(III)-catalyzed dienylation of cyclic *C*-aryl nitrones **86** with 2,3-butadien-1-ol carbonates **87**, followed by intramolecular 1,3-dipolar cycloaddition. In this process, the nitrone moiety functions dually as the directing group for C(aryl)–H activation and as the dipole in the cycloaddition step. Notably, the regioselectivity between fused **88** and bridged products **89** can be tuned by varying the reaction temperature. The proposed catalytic cycle begins with nitrone-directed C–H activation by a carboxylate–Co(III) complex, followed by nucleophilic attack on the central carbon of cumulene **87**. Subsequent elimination furnishes a diene intermediate **E**, which undergoes a rapid intramolecular 1,3-dipolar cycloaddition to form spirocyclic isoindolines **88**. Electron-rich nitrones generally provided better regioselectivity, and both EDG- and EWG-substituted substrates were well tolerated. Moderately substituted allenes reacted efficiently, while bulky *N*-substituents enhanced diastereoselectivity. Key limitations include the failure of heteroaryl nitrones, sterically congested aryl groups (*e.g.*, 2,4-dimethoxyphenyl) that impede C–H activation, reduced yields with cyano-containing nitrones, and poor reactivity of heavily substituted allenes or sterically hindered diene intermediates (Scheme 19).[61]

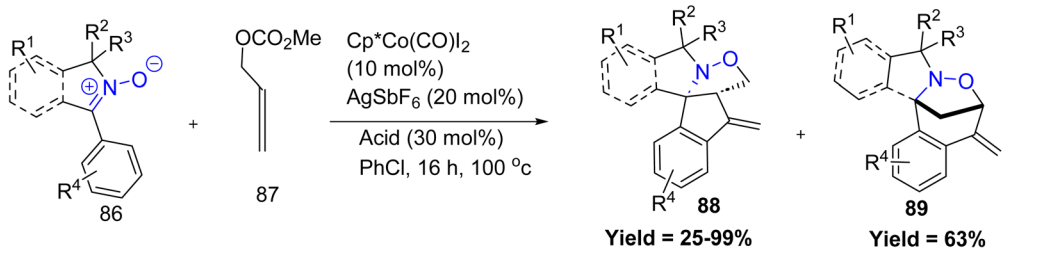

R^1 = H,1,3-dioxolane,F,NO2; R^2 = CH_3,Bn,Cyclopentyl; R^3 = CH_3,Cyclopentyl; R^4 = H,-OMe, -NO_2, -CN, di-OMe,1-tosyl-2,3-dihydro-1H-pyrrole

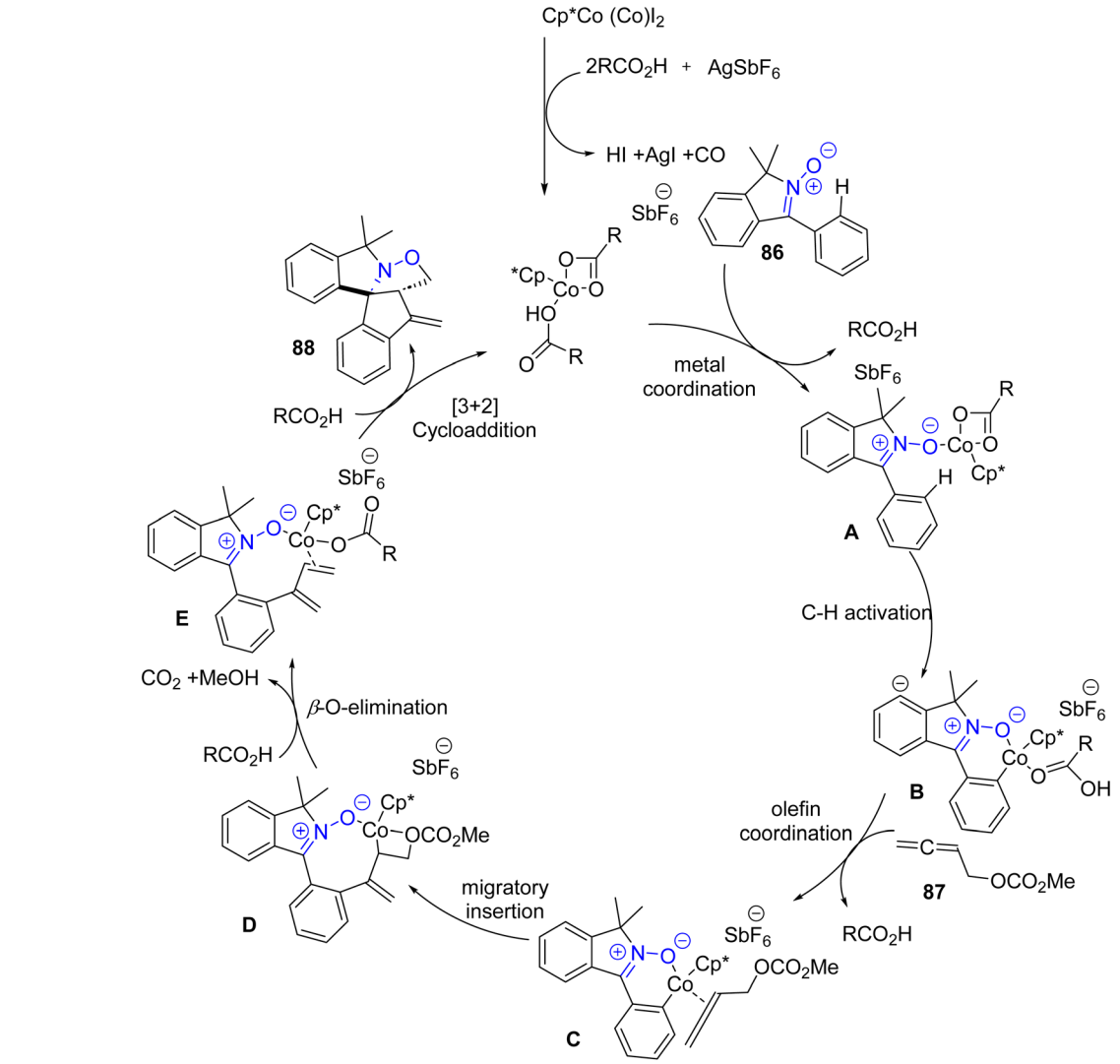

Scheme 19 Co(III) catalyzed dipolar cycloaddition reaction of cyclic *C*-aryl nitrones with 2,3-butadien-1-ol carbonates.

1.1.7 Yb-Catalyzed. Dong-Liang Mo *et al.* in 2025, developed a three-component asymmetric [3 + 3] cycloaddition reaction between *N*-vinyl cinnamaldehyde nitrones **90** and activated cyclopropanes **91** for the efficient synthesis of diverse functionalized 1,2-oxazines **92** in presence of $Yb(OTf)_3$, as catalyst. This reaction offers wide substrate scope, good functional group tolerance, and efficient asymmetric [3 + 3] cycloaddition in a domino sequence. *Para*-substituted aryl nitrones showed the highest reactivity, whereas *ortho*-substituted or aliphatic ester nitrones were significantly less effective. Simple ester-substituted cyclopropanes performed well, but bulky ^{t}Bu or aromatic groups consistently lowered yields and selectivity. Mechanistically, the $Yb(OTf)_3$/L7 catalytic system promotes the ring-opening of cyclopropane **91**, which then undergoes [3 + 3] cycloaddition with nitrone **90** to form intermediate **A**. This species quickly isomerizes to a zwitterionic intermediate **B**

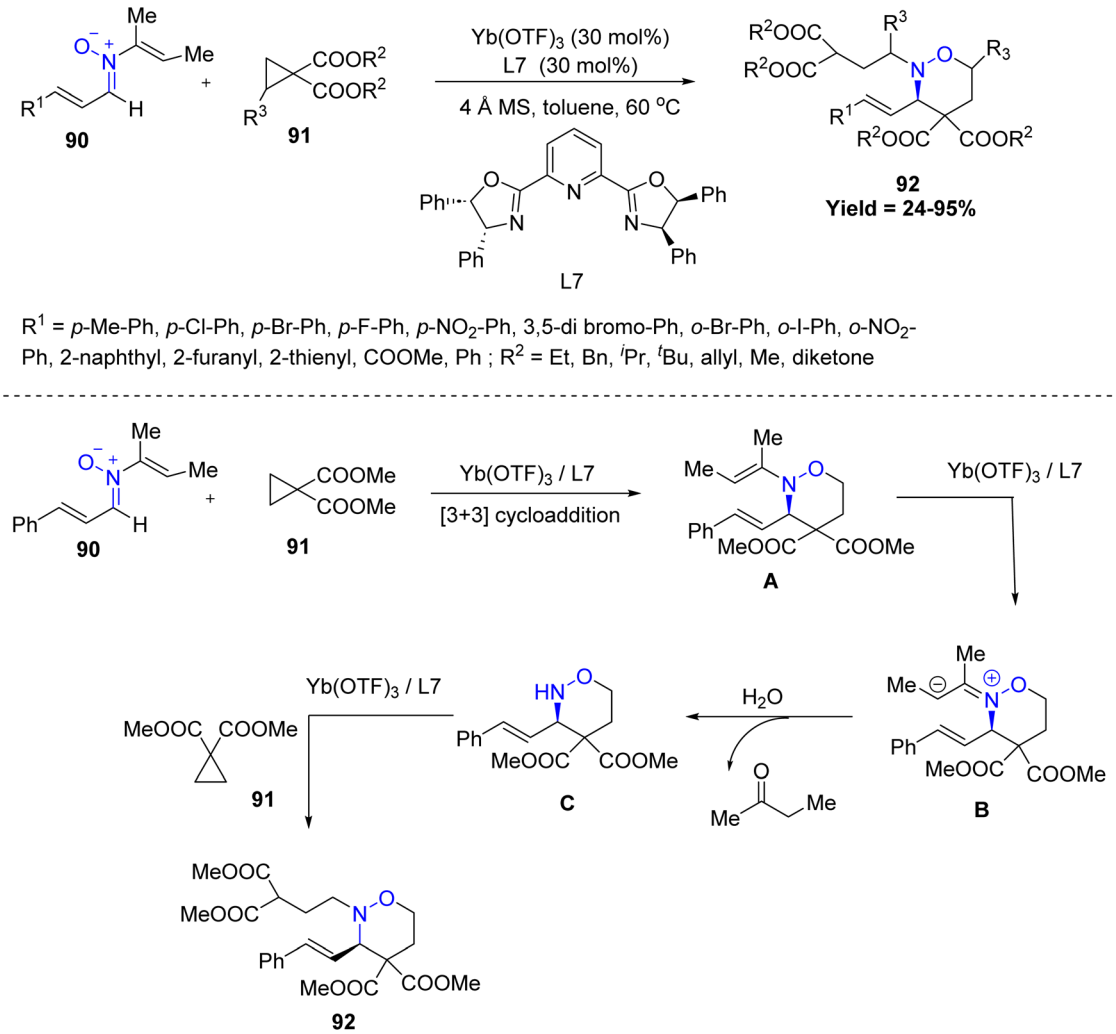

Scheme 20 Yb(Otf)$_3$-Catalyzed asymmetric [3 + 3] cycloaddition of *N*-vinyl nitrones with activated cyclopropanes.

under the influence of the strong Lewis acid catalyst. Hydrolysis of **B** yields 2-butanone as a byproduct and produces intermediate **C**. Finally, **C** undergoes nucleophilic attack on another molecule of cyclopropane **91** in the presence of the Lewis acid to afford the final product **92**. Thus, despite broad applicability, the reaction is limited by steric congestion, strong EWGs, and heavily substituted cyclopropanes (Scheme 20).[62]

1.1.8 Bi-Catalyzed. A significant contribution in this field was made by Charnsak Thongsornkleeb and co-workers in 2024, who reported a novel Bi(OTf)$_3$-catalyzed transformation of 2-arylisatogens **93** with vinyl arenes to synthesize 2,4-diarylquinolines **94**. This unprecedented reaction proceeds efficiently across a broad substrate scope, affording the desired quinoline derivatives **94** in excellent yields. Mechanistically, the Bi(III) catalyst first coordinates with the nitrone oxygen of the isatogen to generate an electrophilic complex **A**. Subsequent nucleophilic attack by the vinyl arene occurs in a stepwise manner, forming a benzylic cationic intermediate **B** that is stabilized by resonance with the adjacent aryl ring. This leads to the formation of a strained tricyclic species **C**, which undergoes rapid carbon monoxide extrusion to generate an intermediate **D** that aromatizes to yield the final quinoline product **94**, completing the catalytic cycle. The reaction showed good tolerance for electronically neutral substrates, while strong electron-donating or withdrawing substituents and steric hindrance markedly reduced yields or diverted the reaction to anthranils. Styrenes bearing *para*-substituents reacted well, whereas *ortho*-substituted and heteroaryl alkenes were ineffective. Non-styrenyl alkenes generally failed, highlighting limitations related to electronic effects, steric congestion, and catalyst deactivation (Scheme 21).[63]

1.1.9 Ru-Catalyzed. In this context, in 2022, Li-Ming Zhao *et al.* demonstrated, a Ru-catalyzed C–H activation strategy allowing for the effective alkenylation of nitrones **95** to give 2-arylethenesulfonyl fluorides **97** and isoindolinones **98** in good yields. Here, directing group concomitantly converts to useful amide moieties (Scheme 22). Electron-rich and moderately substituted aryl nitrones show the highest reactivity, while steric congestion and heteroaryl or strongly withdrawing groups significantly reduce efficiency. *N*-Substituent size strongly influences the pathway, with small groups causing side reactions and limiting overall substrate scope.[64]

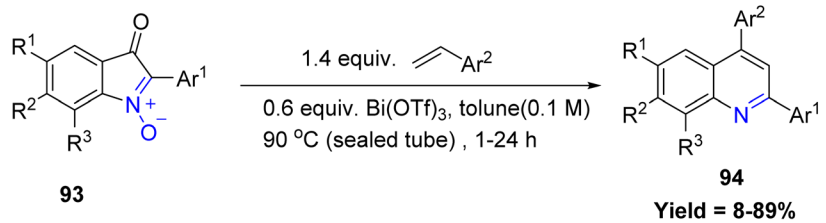

R^1 = H, Me, OMe, F, Cl, CF_3, NO_2; R^2 = H, Me, OMe, F, Cl, CF_3, NO_2; R^3 = H, Me, Cl; Ar^1 = Ph, 2-Me-Ph, 3-Me-Ph, 4-Me-Ph, 4-OMe-Ph, 4-F-Ph, 4-CF_3-Ph, 4-NO_2-Ph, 2-napthyl ; Ar^2 = Ph, 2-Me-Ph, 3-Me-Ph, 4-Me-Ph, 4-OMe-Ph, 4-F-Ph, 4-CF_3-PH, 4 NO_2-Ph, 2-napthyl, 2-pyridyl

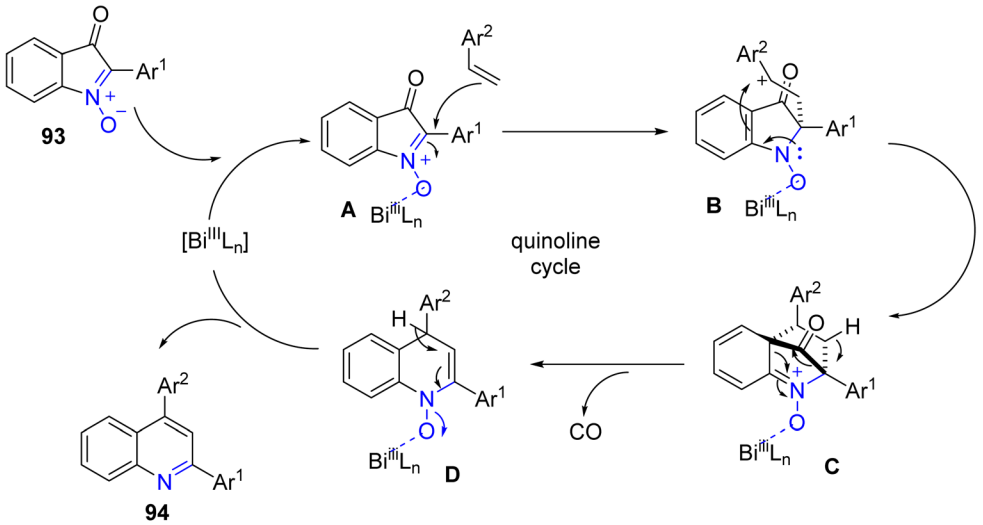

Scheme 21 $Bi(OTf)_3$-Catalyzed cascade cycloaddition–decarbonylation–*N*-deoxygenative aromatization between 2-arylisatogens and styrenes.

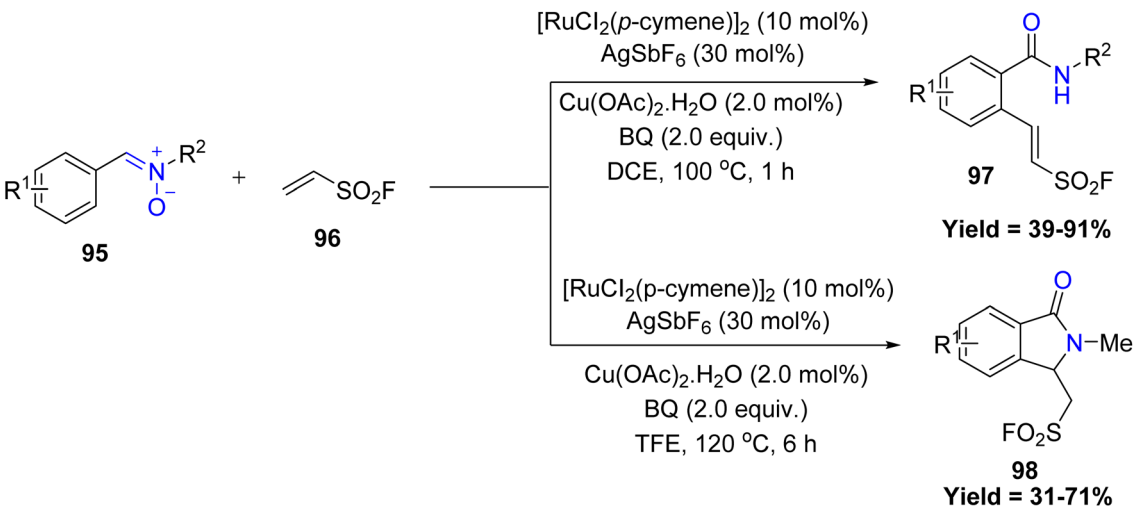

R^1 = *p*-OMe, *p*-SMe, *p*-Ph, *p*-F, *p*-Cl, *p*-Br, *p*-$COOCH_3$, *p*-OH, *m*-Me, *m*-Cl, *m*-Br, *o*-Me, *o*-Cl, 2,3-OMe, 2,3-Cl, 2-naphthyl, 3-pyridyl; R^2 = ^{t}Bu, *n*-Bn

Scheme 22 Ru-Catalyzed C–H activation of nitrones with ethenesulfonyl fluoride.

1.1.10 Pd-Catalyzed. A recent study by Dong-Liang Mo and co-workers showcased this potential through a Pd(II)-catalyzed diastereoselective synthesis of benzazepines featuring three contiguous carbon stereocenters. The transformation begins with a [3 + 2] cycloaddition between *N*-aryl nitrones **99** and allenoates **100**, generating an isooxazoline intermediate **A** that undergoes N–O bond cleavage and a [3,3]-sigmatropic rearrangement, followed by aromatization to deliver a benzazepinone scaffold. Further treatment with $NaBH_4$ delivers the reduced benzazepine product **101**. Alternatively, the benzazepinone can undergo a *retro*-Mannich reaction to generate an imine intermediate, which either proceeds through an intramolecular *O*-[4 + 2] cycloaddition to form a bridged heterocycle **101″** or is reduced to another product **101′** while regenerating the active Pd catalyst. In another pathway, isomerization of the imine yields an enolate–azadiene intermediate, which undergoes an intramolecular [4 + 2] cycloaddition to furnish a distinct polycyclic compound **101‴**, again completing the catalytic cycle. The reaction works best with electron-rich or moderately substituted *N*-aryl nitrones and various allenoates, giving good yields. However, sterically hindered nitrones, heteroaryl nitrones, and bulky or ketone-derived allenes give lower yields, limiting the substrate scope (Scheme 23).[65]

1.1.11 Fe-Catalyzed. In 2024, Yi-Yong Huang *et al.*, reported a Fe-catalyzed asymmetric [3 + 2] cycloaddition between nonterminal alkynyl imides **102** and α-aliphatic nitrones **103**, efficiently generating chiral 4-isoxazolines **104** bearing 3-alkyl-substituted stereogenic centers. A key advantage of this protocol is its scalability to gram-scale synthesis and its compatibility with facile downstream derivatization, highlighting the synthetic utility of the chiral 4-isoxazoline scaffold and the embedded imide functionality. However, the protocol is limited by sterically bulky nitrones, *ortho*-substituted alkynes, and sensitive or strained alkynes, which exhibit reduced yields or undergo decomposition under the reaction conditions (Scheme 24).[66]

2 Metal-free synthesis

Metal-free synthesis has gained significant importance over transition-metal-catalyzed strategies due to its sustainability, cost-effectiveness, and operational simplicity. Unlike transition-metal catalysts, which are often expensive, toxic, and sensitive to air or moisture, metal-free approaches typically rely on cycloaddition reaction, organ catalysts, Lewis's acids, or photochemical activation, making them more environmentally benign and broadly accessible. At the same time, metal-free methods often provide excellent regio- and stereo control, enabling efficient construction of heterocycles from nitrones while maintaining high atom economy and functional group tolerance.[67–71]

2.1 Cycloaddition-based

2.1.1 [3 + 2] dipolar cycloaddition. The scope of [3 + 2] cycloadditions has been continuously broadened with new substrate classes. For instance, in 2023, Jean-François Poisson and co-workers reported a pioneering 1,3-dipolar cycloaddition between *N*-alkyl nitrones **105** and phosphine oxide-substituted allenes **106**, offering a novel and efficient strategy for the synthesis of 4-phosphinylpyrrolidin-3-ones **107**. The reaction proceeds with good yields and excellent 4,5-*trans* diastereoselectivity. Remarkably, under the reaction conditions, the initially formed cycloadducts undergo an *in situ* rearrangement to selectively generate the corresponding pyrrolidin-3-one derivatives. Sterically bulky nitrones, highly substituted allenes, and unstable or sensitive substrates show lower reactivity, decomposition, or reduced selectivity, limiting the overall substrate scope (Scheme 25).[72]

Expanding into carbohydrate chemistry, Jean-Bernard Behr *et al.*, in 2024 described an efficient heat promoted cycloaddition of unprotected carbohydrate-based nitrones **108** with strain-promoted alkyne to give isoxazolidines **110** in good yields. This is a new tool for bioconjugation. The reaction also studied in aqueous media and gives good yield of product. However, the method is limited by the slow reactivity of certain carbohydrate-based nitrones and the instability of electron-rich or *N*-aryl nitrones under the reaction conditions (Scheme 26).[73]

In the same year, Shouchu Tang *et al.*, in 2024 reported a regioselective [3 + 2] cycloaddition and umpolung strategy of 1,3-dithianyl alkynes **111** with nitrones **112**, in presence of KO-^{t}Bu, yielding rearranged 2,3-dihydrooxazole derivatives with moderate to high yields. A broad range of aryl- and *N*-substituted nitrones was tolerated, while alkyl nitrones and certain alkyl-dithiane derivatives failed, indicating substrate limitations. Gram-scale reactions confirmed practicality, and the products could be further transformed into esters, amides, and α-amino carbonyl derivatives, demonstrating synthetic versatility. A plausible mechanism study reveals that, initially, alkynyl-1,3-dithiane undergoes rapid deprotonation in the presence of KO-^{t}Bu, transforming in to an allene anionic intermediate. Subsequently, nucleophilic addition occurs between the allene anion **B** and the electrophilic nitrone **112**, forming allene intermediate **C** and dihydroisoxazole anion **D** through an anion relay process. Cleavage of the N–O bond in anion **D** leads to the formation of aziridine **E**. Finally, the aziridine ring opens, and the capture of the dithianyl anion with H_2O yields the desired 2,3-dihydrooxazole product **113** (Scheme 27).[74]

Longjia Yan *et al.*, in 2024 reported a mild and efficient method for the synthesis of quinolinonyl **115** and coumarinyl-nitrone **117** derivatives. The reaction was carried out between *N*-(2-formylphenyl) propiolamide/2-formylphenyl propiolate and *N*-methylhydroxylamine hydrochloride under an argon atmosphere at room temperature. The resulting quinolinonyl nitrone underwent a [3 + 2] cycloaddition with maleimide, affording tetrahydro-4*H*-pyrrolo[3,4-*c*]isoxazole-dione derivatives **115**. Meanwhile, the coumarinyl nitrone reacted with PhOTfTMS in the presence of TBAF, undergoing a similar [3 + 2] cycloaddition to form 3-(2-isopropyl-2,3-dihydrobenzo[*d*]isoxazol-3-yl)-2*H*-chromen-4-one derivatives **117** in excellent yield. However, the method is limited by sterically hindered or strongly electron-withdrawing substituents, which significantly

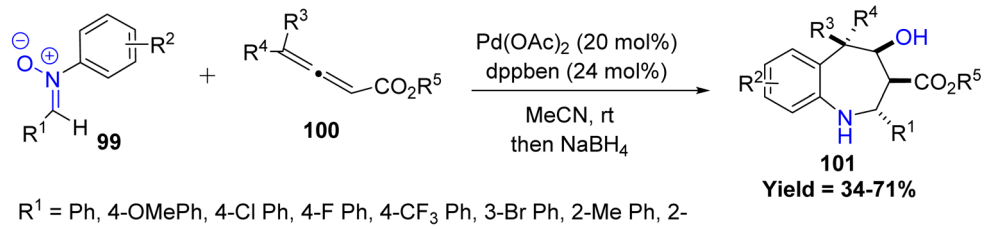

R^1 = Ph, 4-OMePh, 4-Cl Ph, 4-F Ph, 4-CF_3 Ph, 3-Br Ph, 2-Me Ph, 2-thienlyPh ; R^2 = 4-OMe, 4-Me, 4-Br, 4-Cl, 4-F, 4-CF_3, 3-Br, 3-Me, 2-Me; R^3 = H, Me, Ph; R^4 = H, Me, Et; R^5 = Et, *n*-Bu, Bn, ^{i}Pr, ^{t}Bu, Ph, Me

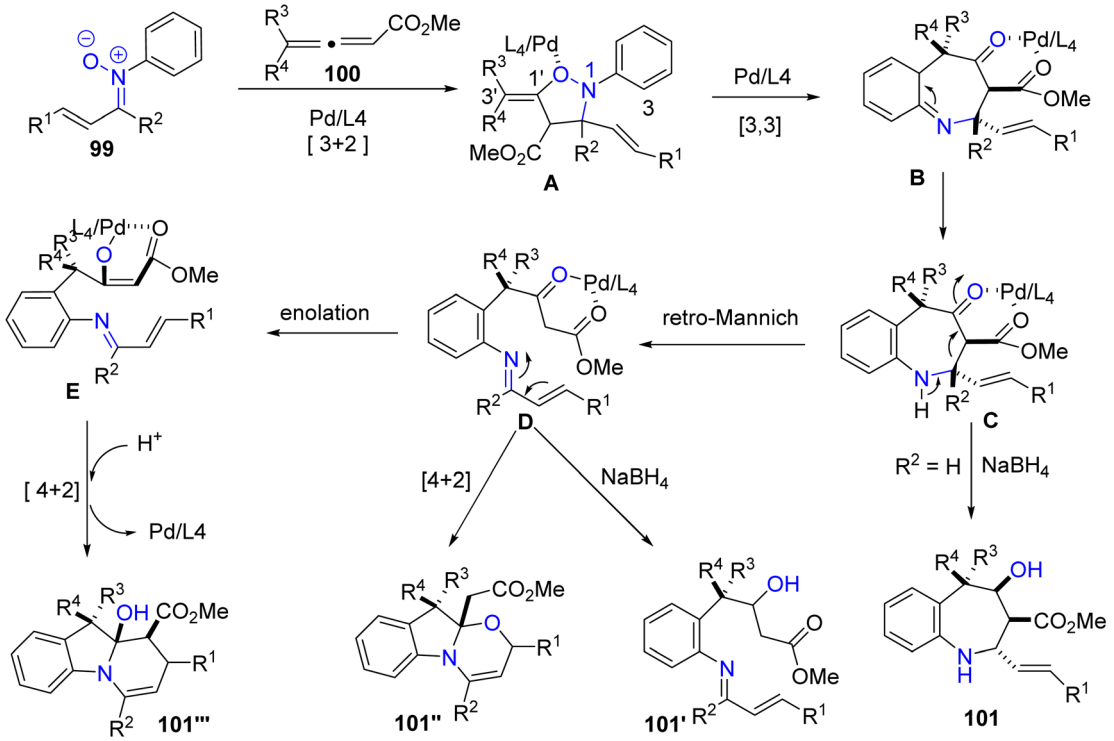

Scheme 23 Pd(II)-Catalyzed [3 + 2] cycloaddition of *N*-aryl nitrones with allenoates.

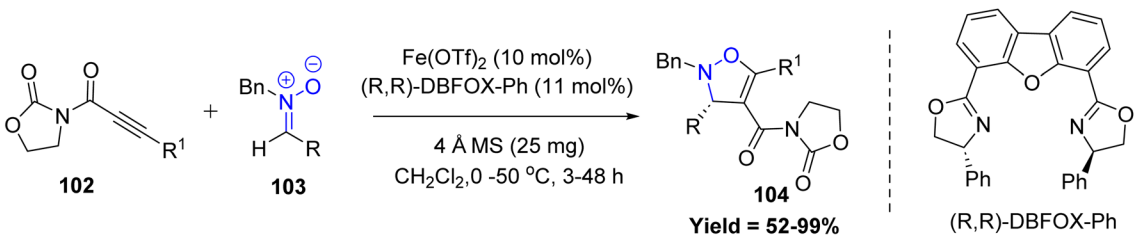

R = Me, Et, Propyl, Butyl, Pentyl,dodecanyl, ethylbenzene, isobutyl, neopentyl, cyclopropyl, cyclobutyl, cyclopentyl, cyclohexyl, tetrahydro-2*H*-pyran, *tert*-butyl piperidine-1-carboxylate, isopropyl,Pentan-3-yl, tert-butyl, tert-pentyl, 3-methylpentan-3-yl, 3-ethylpentan-3-yl, 2,3-dimethylbutan-2-yl, 2-phenylpropan-2-yl, 2-(4-methoxyphenyl)propan-2-yl, 2-(3-(trifluoromethyl)phenyl)propan-2-yl, 2-methyl-1-phenylpropan-2-yl, 2-methyl-1-(p-tolyl)propan-2-yl, 2-methyl-1-(4-(trifluoromethyl)phenyl)propan-2-yl, 2-benzyl-3-(1-(3,5-dimethylphenyl)-2-methylpropan-2-yl, 2-benzyl-3-(1-(3,5-bis(trifluoromethyl)phenyl)-2-methylpropan-2-yl, 2-benzyl-3-(1-(2,3-dimethylphenyl)-2-methylpropan-2-yl, 2-benzyl-3-(2-methyl-1-(naphthalen-1-yl)propan-2-yl, 2-benzyl-3-(2-methyl-1-(naphthalen-2-yl)propan-2-yl; R^1 = 4-OMe-Ph, 4-Me-Ph, 4-CF_3-Ph, 4-Cl-Ph, 4-Br-Ph, 3-Me-Ph, 3-CF_3-Ph, 3-F-Ph, 2-Me-Ph, 2-CF_3-Ph, 2-Cl-Ph, Naphthyl, thiophenyl, Me, Et, Propyl, Butyl, Pentyl, cyclopropyl, cyclohexyl, cyclohex-1-en-1-yl

Scheme 24 Iron catalyzed asymmetric clicking of alkynyl dipolarophiles and nitrones.

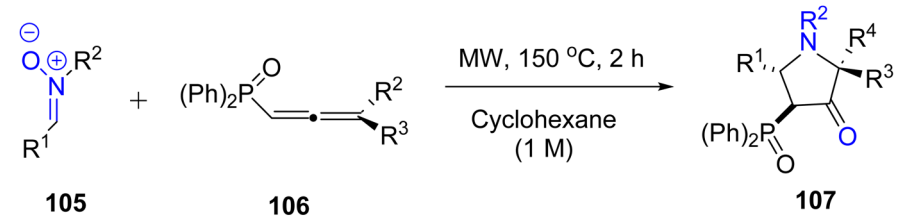

R^1 = Ph, 4-MeC_6H_4, 4-PhC_6H_4, 4-$OMeC_6H_4$, 4-ClC_6H_4, 4-$NO_2C_6H_4$, 1,1-dichloro C_6H_4, Thiophenyl, Furanyl; R^2 = Me, Bn, ^{t}Bu; R^3 = Me; R^4 = Me, Et, Bn

Scheme 25 [3 + 2] cycloaddition of nitrones with phosphinylallenes.

lower the yields, and certain benzyl/alkyl hydroxylamines or terminal alkynes fail to give the desired nitrones (Scheme 28).[75]

Similarly, Shigeru Arai *et al.* in 2024 disclosed a regio- and stereoselective [3 + 2] cycloaddition strategy for the construction of fully substituted indoline frameworks **120** and **122**, demonstrating the synthetic utility of isatogenol **118** as a key building block. This method enables the rapid formation of densely functionalized, multiring-fused heterocycles bearing contiguous tetra-substituted carbon centers in a single step. Electron-rich aryl groups on isatogenol show higher reactivity, while electron-withdrawing or sterically hindered substituents give lower yields. A key limitation is the reduced selectivity or lower reactivity with sterically hindered or α-substituted alkenes. DFT studies further elucidated that the observed regio- and stereoselectivity is predominantly governed by specific hydrogen-bonding interactions during the cycloaddition with acrylate partners. This work highlights a powerful and elegant approach toward structurally complex indoline derivatives (Scheme 29).[76]

Highlighting the advantages of transition-metal-free strategies, Nayak *et al.* reported a transition metal- and base-free [3 + 2] cycloaddition of isatin ketonitrones **123** with β-nitrostyrene **124** to efficiently construct 4′-nitro-2′,5′-diphenyl spiro[indoline-3,3′-isoxazolidin]-2-one derivatives **125**. The reaction proceeds smoothly with a variety of substituted β-nitrostyrenes, and both electron-donating and electron-withdrawing groups on the aromatic ring show minimal influence on product yield. Reactivity trends revealed that *N*-alkyl-substituted nitrones, particularly *N*-methyl, *N*-ethyl, *N*-butyl, and *N*-benzyl variants, significantly enhance the reaction efficiency, providing higher yields relative to unsubstituted nitrones. However, the methodology shows limitations with sterically congested or strongly electron-rich/electron-poor styrenes, as di- and tri-methoxy as well as nitro-substituted styrenes failed to undergo cycloaddition. The antimicrobial activity of all synthesized compounds was evaluated against a panel of Gram-positive and Gram-negative pathogens (Scheme 30).[77]

Dearomative cycloaddition of heteroarenes has appeared as one of the simple and powerful strategies to access polyheterocyclic skeletons. In this connection Zheng Duan *et al.* assembles simple β-chloroethyl-phosphane **126**, alkynyl imines **128** (or alkynyl ketones), and nitrones **130** into structurally complex isoxazolidine fused phospholene scaffolds **131** *via*

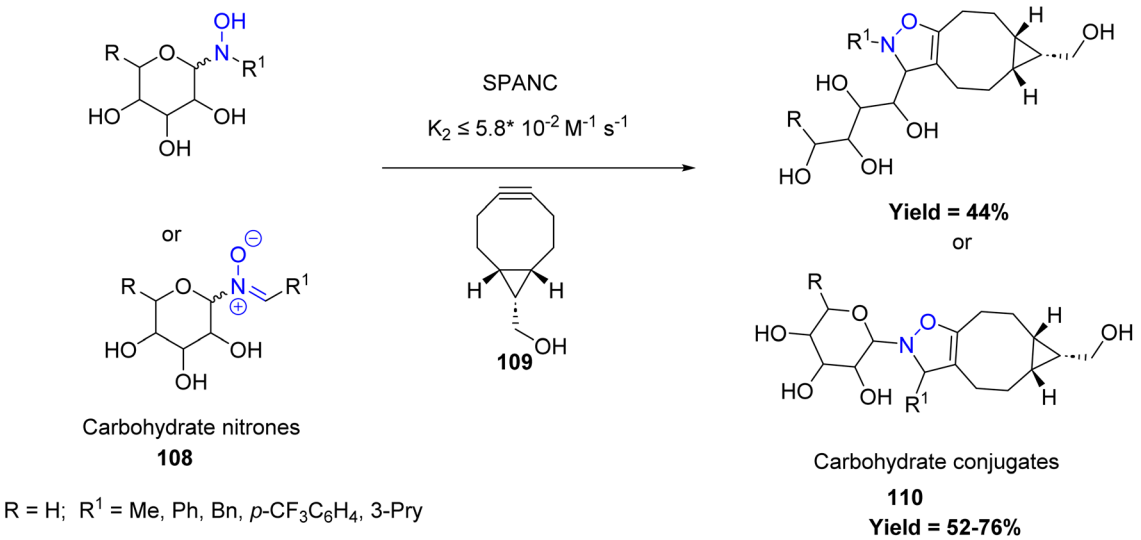

R = H; R^1 = Me, Ph, Bn, *p*-$CF_3C_6H_4$, 3-Pry

Scheme 26 [3 + 2] cycloaddition of unprotected carbohydrate-based nitrones with strain-promoted alkyne.

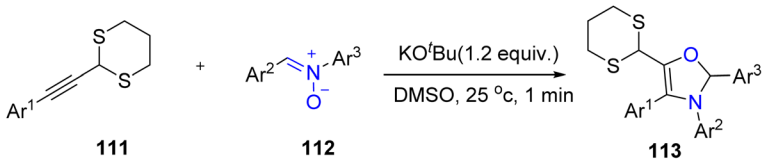

111 112 113

Yield = 43-75%

Ar_1= Ph, Ar_2= Ph; Ar_3= 4-Et-ph, 4-^{i}pr, 4-^{t}Bu, 4-Cl, 4-Br, 4-CH_3SO_2, 4-CF_3, 4-OCF_3,3-OMe-ph, 3-Br-ph, 2-Br-ph, 2-Cl-ph,3,5-di Me-ph, 3,5-Br-ph ,3-OMe-4-Cl-ph,3-Me-4-F-ph, 3,4,5-tri-OMe-ph,Pyridine,quinoline,4-Cl-1,3-dimethyl-1H-pyrazole,3,5-dimethylisoxazolyl

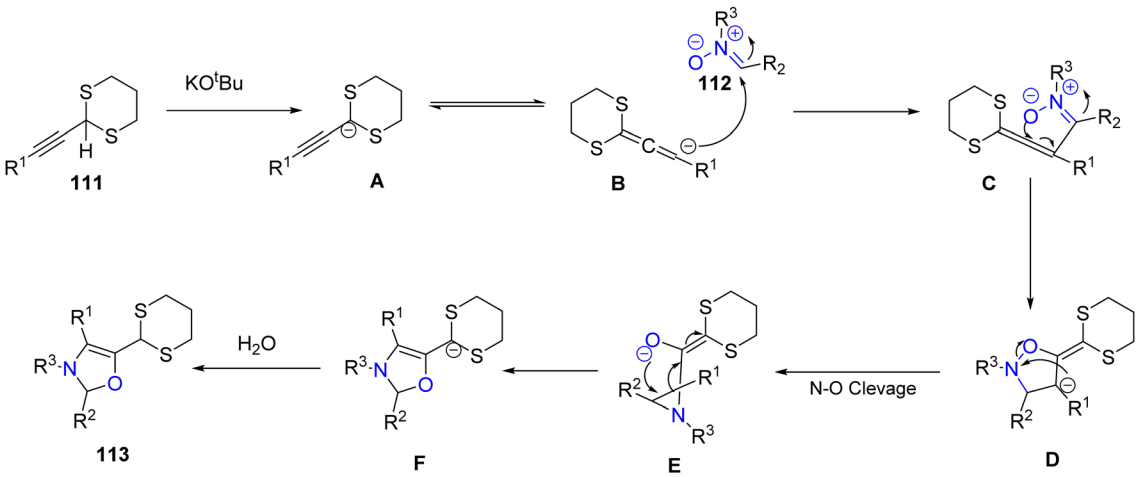

111 A B 112 C D E F 113

Scheme 27 [3 + 2] cycloadditions of alkynyl-1,3-dithianes and nitrones.

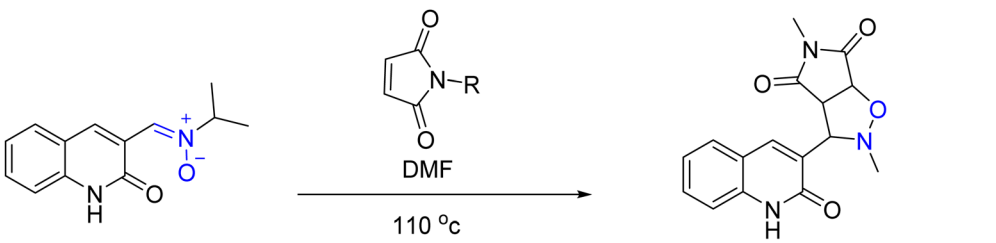

R= Me, Ph

114

tetrahydro-4*H*-pyrrolo isoxazole-dione

115

Yield = 67-75%

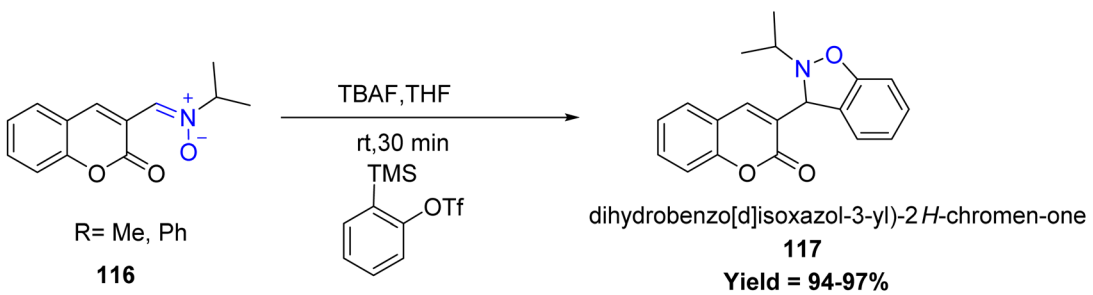

R= Me, Ph

116

dihydrobenzo[d]isoxazol-3-yl)-2*H*-chromen-one

117

Yield = 94-97%

Scheme 28 [3 + 2] reaction of quinolinoneyl nitrones and coumarinyl nitrones with maleimide and PhOTfTMS.

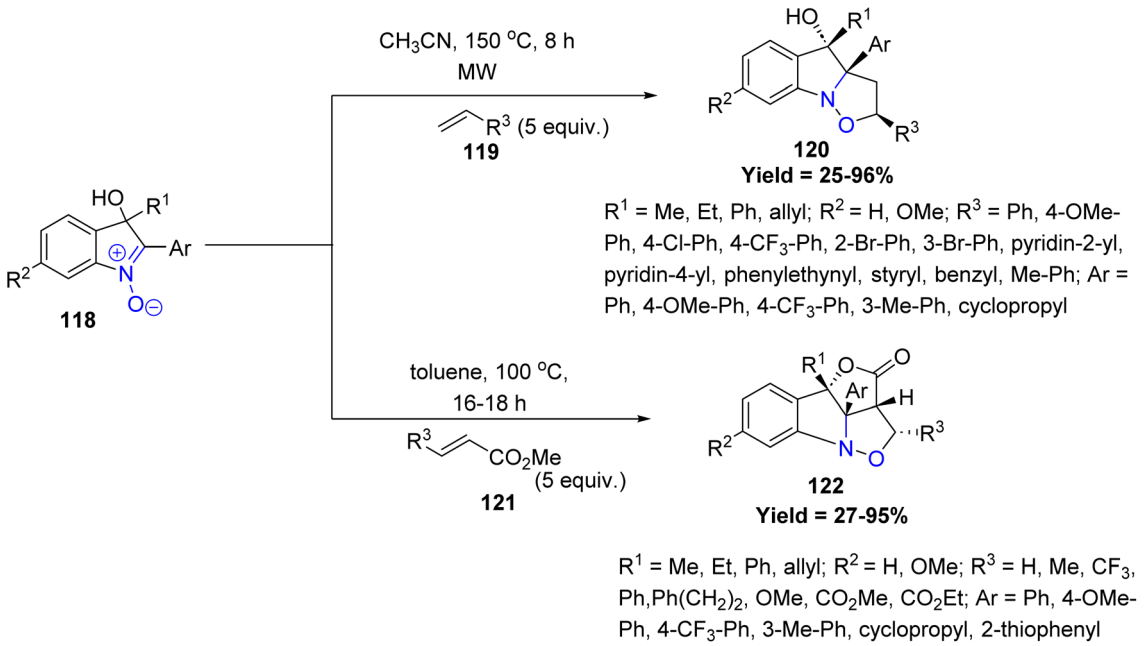

Scheme 29 Regio- and stereoselective [3 + 2] cycloaddition using isatogenol.

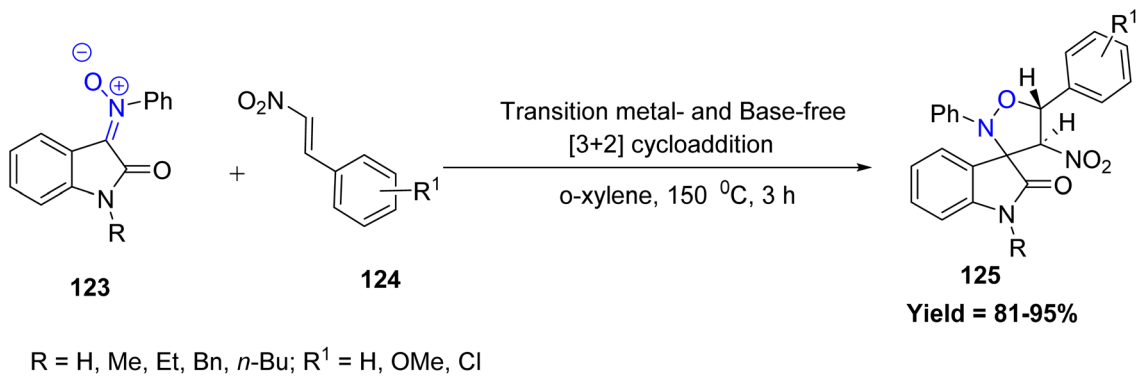

Scheme 30 [3 + 2] cycloaddition reaction of isatin ketonitrone derivatives with β-nitrostyrene.

a sequential process involving phospha-Michael addition, intramolecular cyclization, and dearomatizing [3 + 2] cycloaddition reactions. The method tolerates both electron-rich and electron-poor aryl substituents, whereas sterically hindered or strongly electron-donating groups lead to reduced yields. Electron-donating nitrones display higher reactivity, while *N*-aryl nitrones remain unreactive. This strategy also extends to ynones, enabling access to oxaphospholene analogues and potential P-stereogenic ligand frameworks. Unlike pyrroles and furans, aromatic 2-phosphapyrroles and 2-phosphafurans serve as excellent 2π-components in dearomative [3 + 2] cycloadditions due to the poor 2p–3p orbital overlap within the C=P unit (Scheme 31).[78]

Yogesh P. Bharitkar *et al.* utilized nitrone cycloaddition to synthesize novel spiroisoxazolidino hybrids **134**/**136** of alantolactone **133** and isoalantolactone **135**. Which are two isomeric sesquiterpene lactones of innula recemosa. This study includes the synthesis of dinitrone with glyoxal and terephthalaldehyde. Both nitrone cycloaddition and di-nitrone cycloaddition proceed with high regio- and di-astereoselectivity, resulting in the formation of only one isomer. Notably, the reactions proceeded under mild conditions without the need for chromatographic purification, highlighting the synthetic efficiency of this approach. The antimicrobial activity of all synthesized compounds was evaluated against a panel of Gram-positive and Gram-negative pathogens. Few compounds show potent activity (Scheme 32).[79]

Recently, Dong-Liang Mo *et al.* in 2025 developed an efficient, transition metal-free protocol for the synthesis of a diverse array of spirooxindole-benzo[*d*]oxazoles **139** and dihydrobenzofurans **139′**. This transformation proceeds *via* a [3 + 2] cycloaddition between *N*-vinyl oxindole-derived nitrones **137** and arynes **138**, followed by a selective rearrangement. The nature of the substituent on the *N*-vinyl group of the nitrone

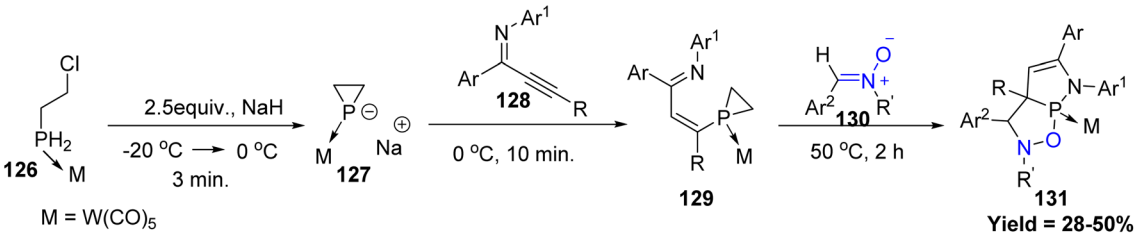

Ar = Ph, *p*-BrPh, *p*-OMePh, thiophnyl ; Ar^1 = Ph, *o*-BrPh, *p*-OMePh; Ar^2 = Ph, *p*-MePh, *p*-OMePh, *p*-ClPh, *p*-CNPh, thiophnyl, $(CH_2)_2$-Ph; R = Ph, *p*-OMePh, *p*-MePh, *o*-MePh, *p*-^{t}BuPh, *p*-ClPh, *p*-CNPh, *n*-Bu, pyridinyl; R' = Me, Ph

Scheme 31 [3 + 2] cycloaddition of P-heteroarenes and nitrones.

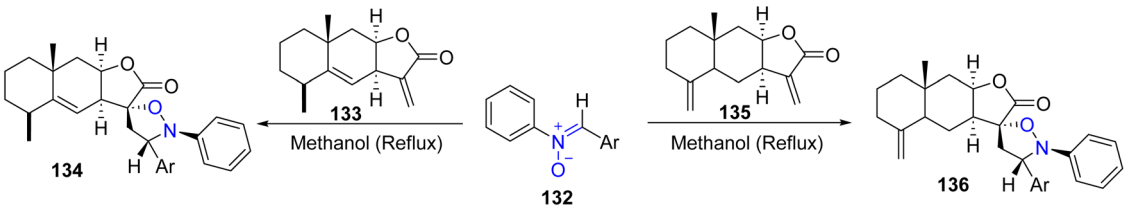

Ar = Ph, Cl-Ph, F-Ph, NO_2-Ph, OMe-Ph, CN-Ph, pyridinyl

Yield = 70-80%

Ar = Ph, Cl-Ph, F-Ph, NO_2-Ph, OMe-Ph, CN-Ph, pyridinyl

Yield = 72-83%

Scheme 32 Cycloaddition reactions of nitrone and alantolactone or iso alantolactone.

plays a critical role, directing either a [1,3]- or [3,3]-sigmatropic rearrangement, primarily influenced by steric effects. The monosubstituted linear *N*-vinyl nitrones gave high yields regardless of chain length, whereas sterically bulky or disubstituted nitrones led to lower yields or favoured formation of dihydrobenzofurans over spirooxindoles. Substituents on the indole ring, whether electron-donating or electron-withdrawing, were generally tolerated, and sensitive functional groups such as chloro and ester were compatible. However, limitations were observed with highly hindered *N*-vinyl nitrones or naphthyl-derived arynes, which either decomposed or gave reduced yields, indicating that steric hindrance can significantly affect reaction efficiency and selectivity (Scheme 33).[80]

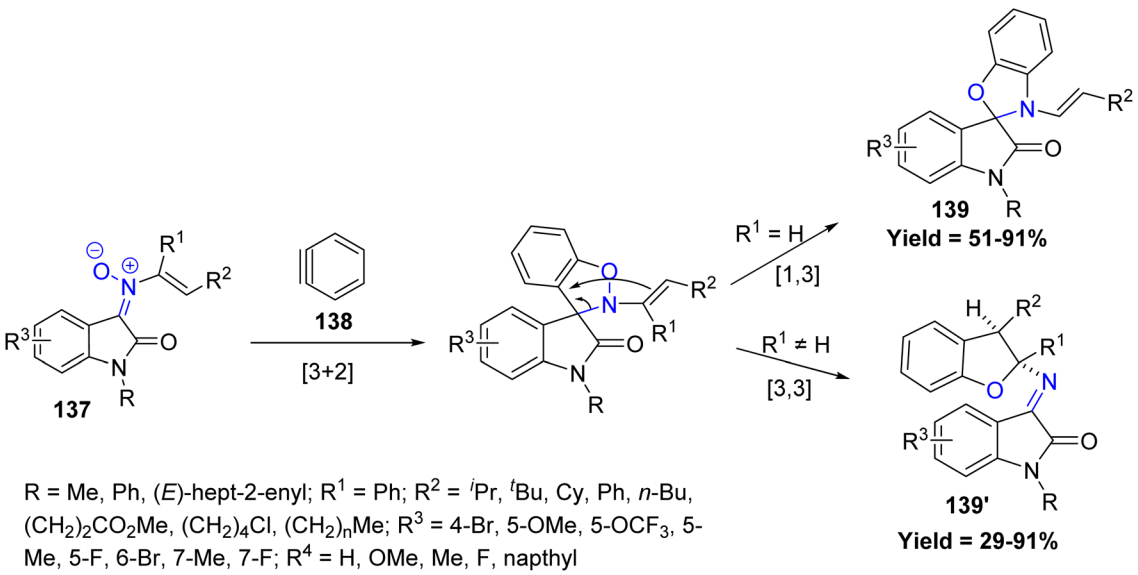

R = Me, Ph, (*E*)-hept-2-enyl; R^1 = Ph; R^2 = ^{i}Pr, ^{t}Bu, Cy, Ph, *n*-Bu, $(CH_2)_2CO_2Me$, $(CH_2)_4Cl$, $(CH_2)_nMe$; R^3 = 4-Br, 5-OMe, 5-OCF_3, 5-Me, 5-F, 6-Br, 7-Me, 7-F; R^4 = H, OMe, Me, F, napthyl

Scheme 33 [3 + 2] cycloaddition and selective rearrangement of *N*-vinyl oxindole nitrones and arynes.

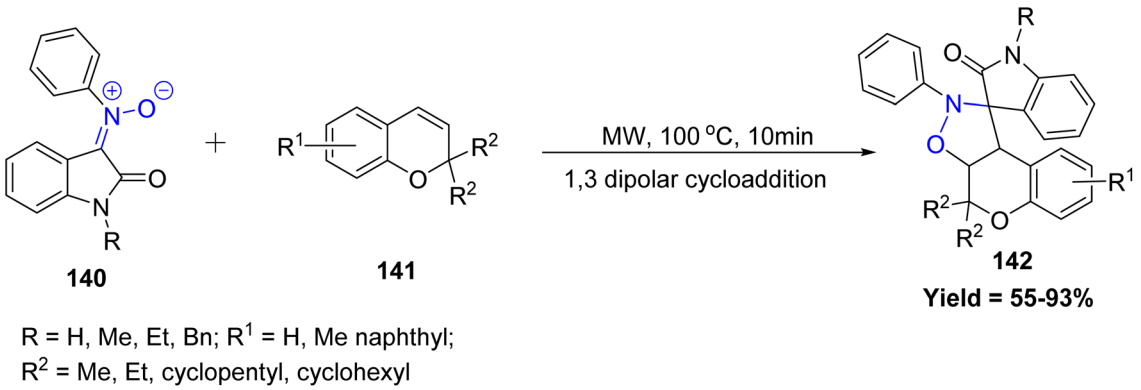

Scheme 34 [3 + 2] cycloaddition of 2*H*-chromene and *N*-arylisatin nitrones.

In a significant contribution to green synthetic methodologies, Nayak *et al.* developed an efficient aqueous-mediated approach for the synthesis of chromene-fused spiro-isoxazolidine derivatives **142** *via* a [3 + 2] cycloaddition reaction. Utilizing 2*H*-chromenes **141** and *N*-arylisatin-derived nitrones **140**, the reaction proceeds under microwave irradiation, offering notable advantages such as reduced reaction times, minimized by-product formation, and excellent yields. Reactivity trends indicated that substitution at the 2-position of the chromene core significantly influenced yields, with cyclopentyl and cyclohexyl substituents giving higher yields compared to 2,2-dimethyl or 2,2-diethyl groups. Similarly, larger substituents on the nitrone (methyl < ethyl < benzyl) slightly improved reaction efficiency. However, limitations were observed with certain C3- and C4-substituted chromenes, such as 4-bromo, 4-styryl, or carbonyl/nitro-substituted derivatives, which either gave complex mixtures or failed to react, highlighting the sensitivity of this cycloaddition to steric and electronic effects (Scheme 34).[81]

2.1.2 [4 + 2] hetero-Diels–Alder reactions. In 2023, Osamu Tamura *et al.*, reported an elegant strategy for constructing *N*-alkoxycarbonylated polycyclic compounds **144** through an intramolecular nitrone cycloaddition. This method involves the thermal treatment of δ,ε-unsaturated oximes bearing a alkene groups with *O*-alkyl *S*-(pyridin-2-yl) carbonothioates ($PySCO_2R$), resulting in the *in situ* formation of *N*-alkoxycarbonyl nitrones. These intermediates then undergo intramolecular [3 + 2] cycloaddition to furnish multi-cyclic frameworks. Reactivity

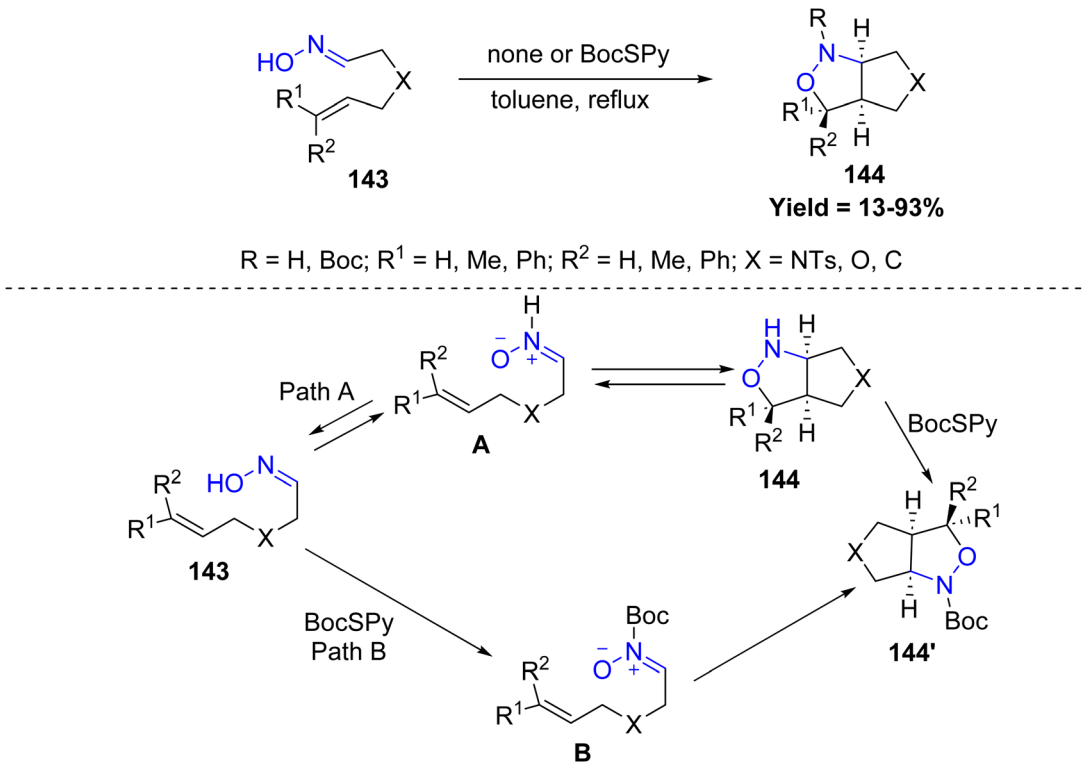

Scheme 35 [4 + 2] intramolecular cycloaddition of *N*-alkoxycarbonyl nitrones.

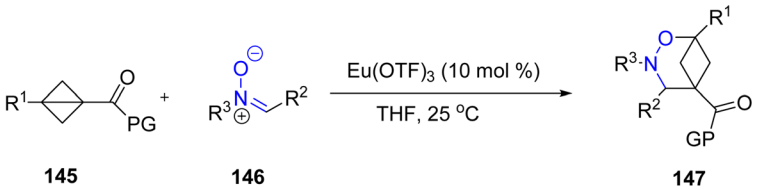

R^1 = Ph, *m*-OMe-Ph, *m*-F-Ph, *p*-Me-Ph, *p*-Cl-Ph, *p*-F-Ph, *p*-CF_3-Ph, Me, H; R^2 = Ph, *o*-OMe-Ph, *o*-Me-Ph, *m*-OMe-Ph, *m*-Me-Ph, *m*-Br-Ph, *m*-Cl-Ph, *m*-F-pH, *m*-NO_2-Ph, *p*-OMe-Ph, *p*-O^{t}Bu-Ph, *p*-OH-Ph, *p*-Me-Ph, *p*-^{t}Bu-Ph, *p*-I-Ph, *p*-Br-Ph, *p*-F-Ph, *p*-ethynyl-Ph, *p*-Ph-Ph, 3,4-diOMe-Ph, 3,5-diMe-Ph, 3,4-diCl-Ph, alfa-naphthyl, beta-naphthyl, 2-furyl, 3-furyl, 3-thienyl, 2-indolyl, PMP; R^3 = Ph, *p*-Me-Ph, *p*-Br-Ph, *p*-Cl-Ph, Me, Bn; PG = Pyr, Ph

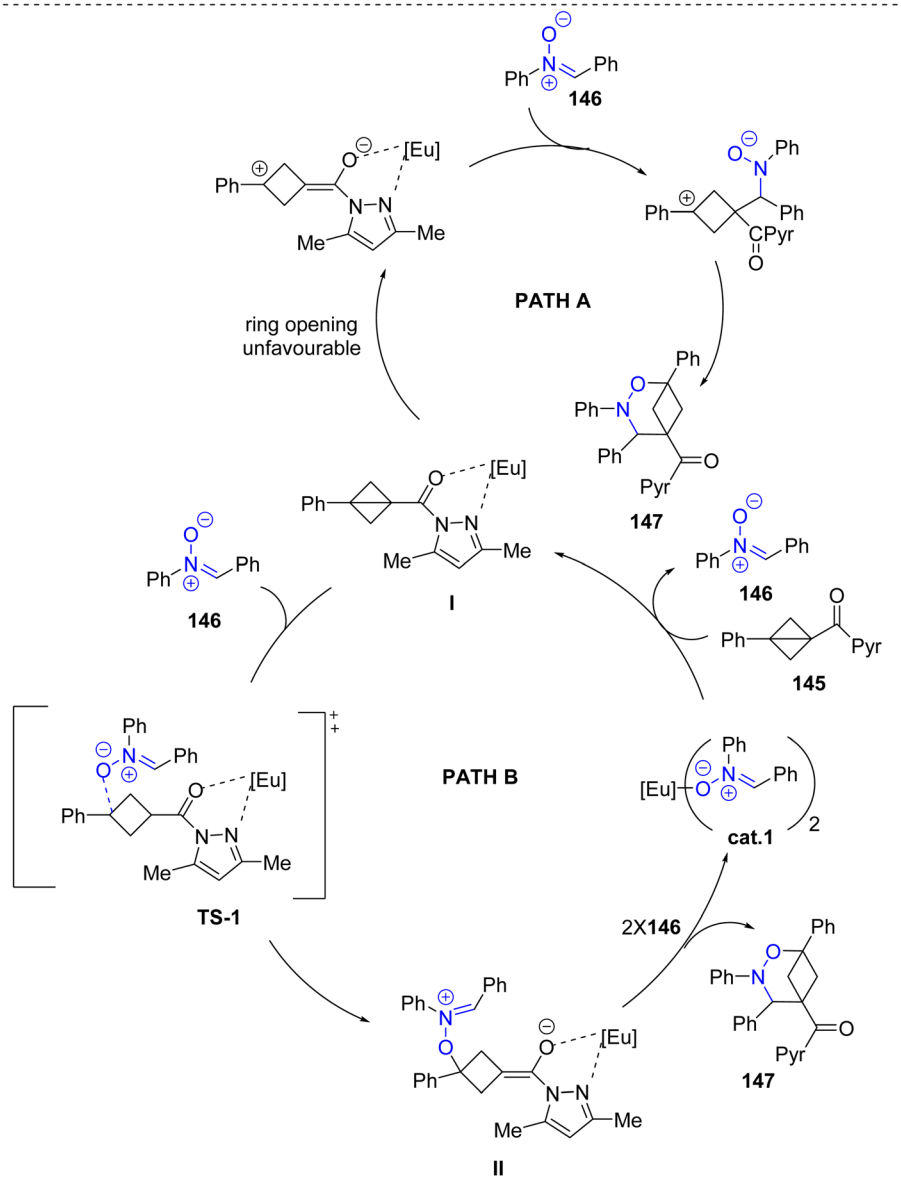

Scheme 36 Formal dipolar [4 + 2] cycloaddition of bicyclo-[1.1.0]butanes with nitrones.

trends revealed that substrates bearing quaternary centers or dimethyl-substituted alkenes delivered higher yields compared to less substituted analogues, while simple heating in the absence of BocSPy often led to poor conversion or recovery of starting materials. Two mechanistic pathways were proposed: in Path **A**, the oxime **143** first equilibrates with a transient NH-

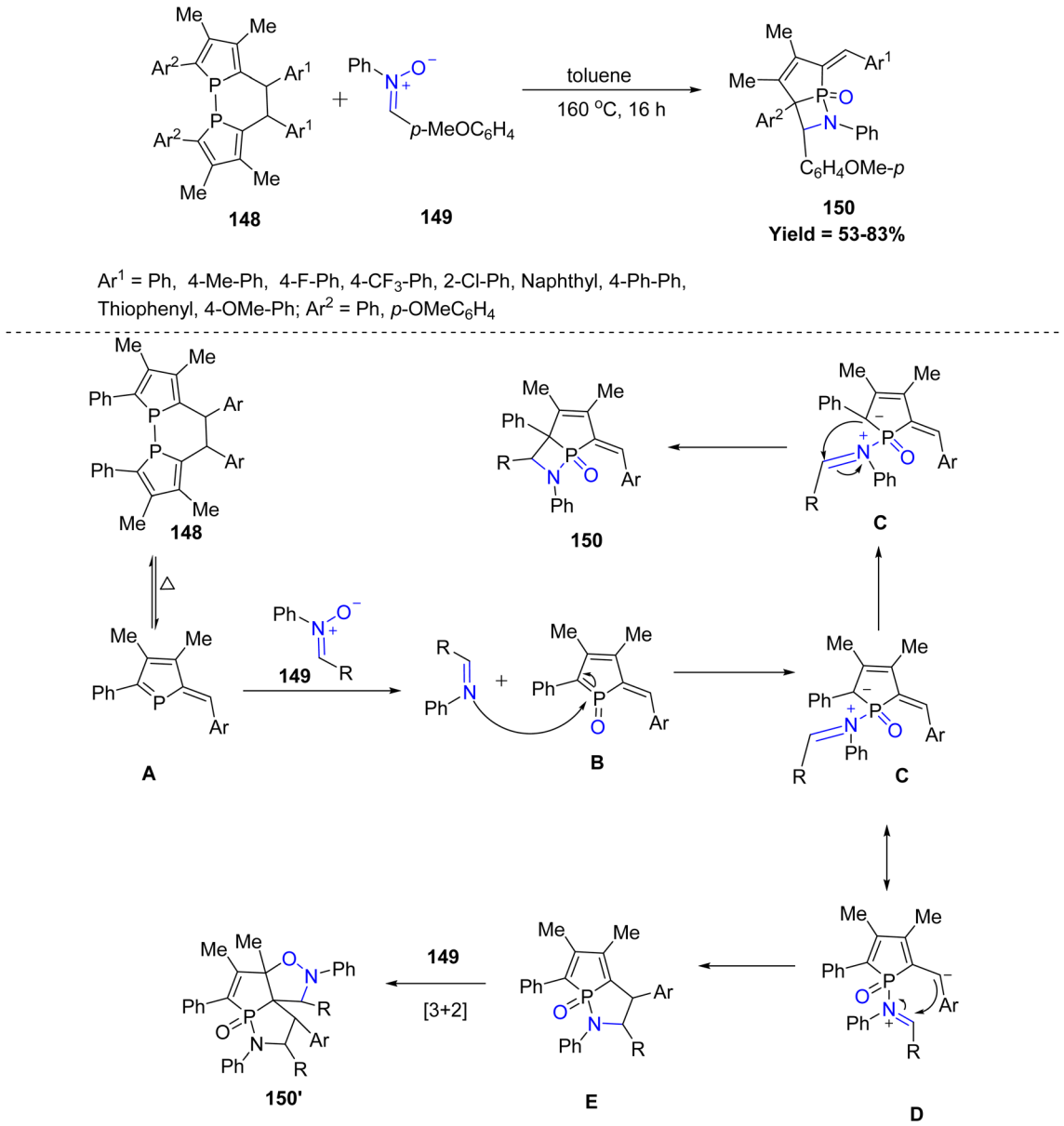

Scheme 37 [4 + 2] cycloaddition reaction of α-C2-bridged biphospholes and nitrones.

nitrone **A**, which cyclizes to form **144**, this **144** is then acylated by the $PySCO_2R$ to form **144′**. In Path **B**, direct acylation of the oxime **143** leads to the formation of an N-Boc nitrone **B**, which subsequently undergoes cycloaddition **144′**. Both pathways effectively demonstrate the utility of *in situ* nitrone generation for rapid construction of complex heterocyclic compounds (Scheme 35).[82]

Similarly, Wei-Ping Deng *et al.* in 2024 reported a strategy for synthesizing valuable hetero-BCHeps **147** *via* dipolar cycloadditions of bicyclo[1.1.0] butanes **145** (BCBs) with hetero-1,3-dipoles **146** under mild conditions, showcasing broad functional group tolerance. The method displays broad substrate tolerance: BCBs bearing electron-rich, electron-poor, or sterically varied aryl substituents reacted smoothly to deliver the corresponding products in moderate to excellent yields. Similarly, nitrones with diverse electronic and steric properties including mono- and disubstituted aryl, heteroaryl, and naphthyl groups were well accommodated, whereas strongly aliphatic nitrones showed reduced reactivity. Mechanistically, the transformation proceeds *via* a formal [4π + 2σ] cycloaddition reaction and proceeds through two pathway. In pathway-1, the nitrone first activates the BCB, followed by ring closure to afford the final product **147**. Alternatively, in the second pathway, intermediate **I** reacts with compound **146** to form transition state TS-1, which leads to intermediate **II**. This intermediate then eliminates the catalyst to produce the final compound **147**. Then the catalyst reacts with compound **145** to reform compound **146** (Scheme 36).[83]

2.1.3 [2 + 2] cycloaddition. An unprecedented reaction of nitrone-based [2 + 2] cycloaddition was reported in 2024 by

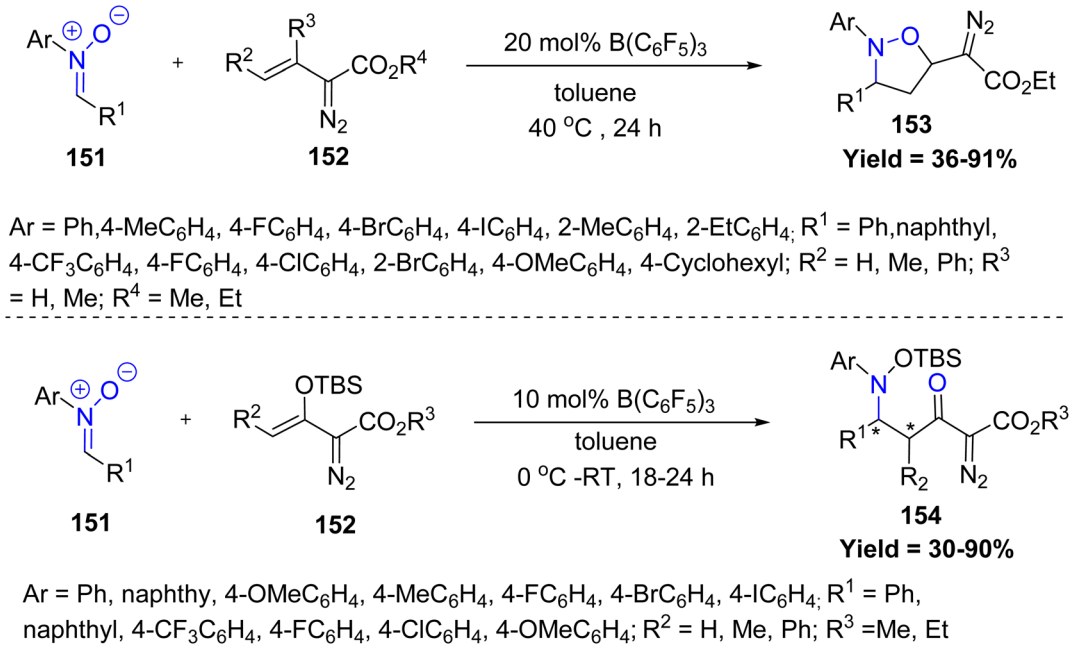

Scheme 38 $B(C_6F_5)_3$-Catalyzed diastereo selective and divergent reactions of vinyldiazo esters with nitrones.

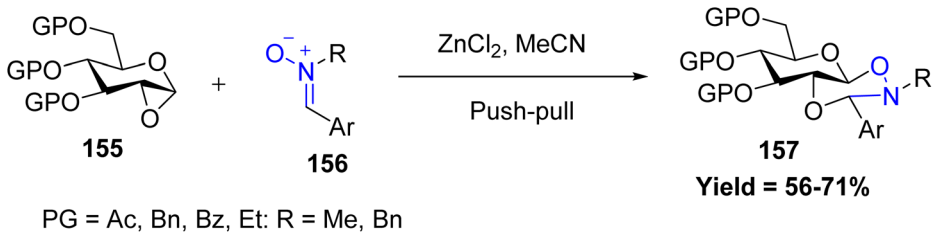

Scheme 39 Zinc chloride catalyzed reaction of 1,2-anhydro sugars and *N*-substituted aromatic nitrones.

Rongqiang Tian *et al.*, involving *in situ* generated 1-phosphafulvene **148** and nitrones **149** to give phospholene-fused β-phosphinolactam derivatives **150.** The reaction works best with nitrones that are not strongly electron-withdrawing or sterically bulky, because such groups slow down the redox step and decrease product formation. A key limitation of the method is that strongly hindered or highly electron-poor nitrones give much lower yields or do not react efficiently. Mechanistically, biphosphole **148** first undergoes dissociation to generate 1 phosphafulvene **A.** The redox reaction between **A** and nitrone **149** provides 1-phosphafulvene oxide **B** and imine. The oxidation of 1-phosphafulvene boosts its reactivity toward imine. The nucleophilic addition of imine to **B** affords intermediate **C.** The cyclization of **C** produces β-phosphinolactam, leading to the isolated product **150.** The negative ion of **C** shifts to exocyclic carbon atom results in intermediate **D.** The instability of phosphole oxide caused by slight antiaromaticity disfavours the negative ion migration from **C** to **D.** The intramolecular nucleophilic addition of carbanion to iminium ion produces **E.** The subsequent [3 + 2] cycloaddition reaction between phosphole oxide and nitrone phospholene **149** provided fused isoxazolidine **150′** (Scheme 37).[84]

2.2 Acid-catalysed pathways

Acid catalysis has emerged as a versatile strategy in nitrone-based heterocyclic synthesis, providing efficient, metal-free alternatives to transition-metal-catalyzed transformations. In 2023, Rebecca L. Melen and co-workers reported a transition-metal-free, Lewis acid-catalyzed reaction for the diastereoselective synthesis of highly functionalized isoxazolidine-derived diazo compounds **153** in excellent yields. Reactivity mainly depends on the strong Lewis acidity and steric features of $B(C_6F_5)_3$, along with the electronic nature of the nitrone. However, electron-rich or bulky nitrones, *N*-alkyl nitrones, internal vinyldiazo esters, and coordination-prone solvents reduce or prevent reactivity (Scheme 38).[85]

In this context, Debaraj Mukherjee *et al.* reported a zinc chloride-catalyzed, one-pot, diastereoselective approach for the synthesis of sugar-fused dioxazinane derivatives starting from 1,2-anhydro sugars **155** and *N*-substituted aromatic nitrones **156.** These 1,2-annulated pyranose frameworks, fused with six-membered heterocycles, represent a valuable class of carbohydrate scaffolds **157** with significant synthetic and biological relevance. The methodology exhibits broad substrate tolerance,

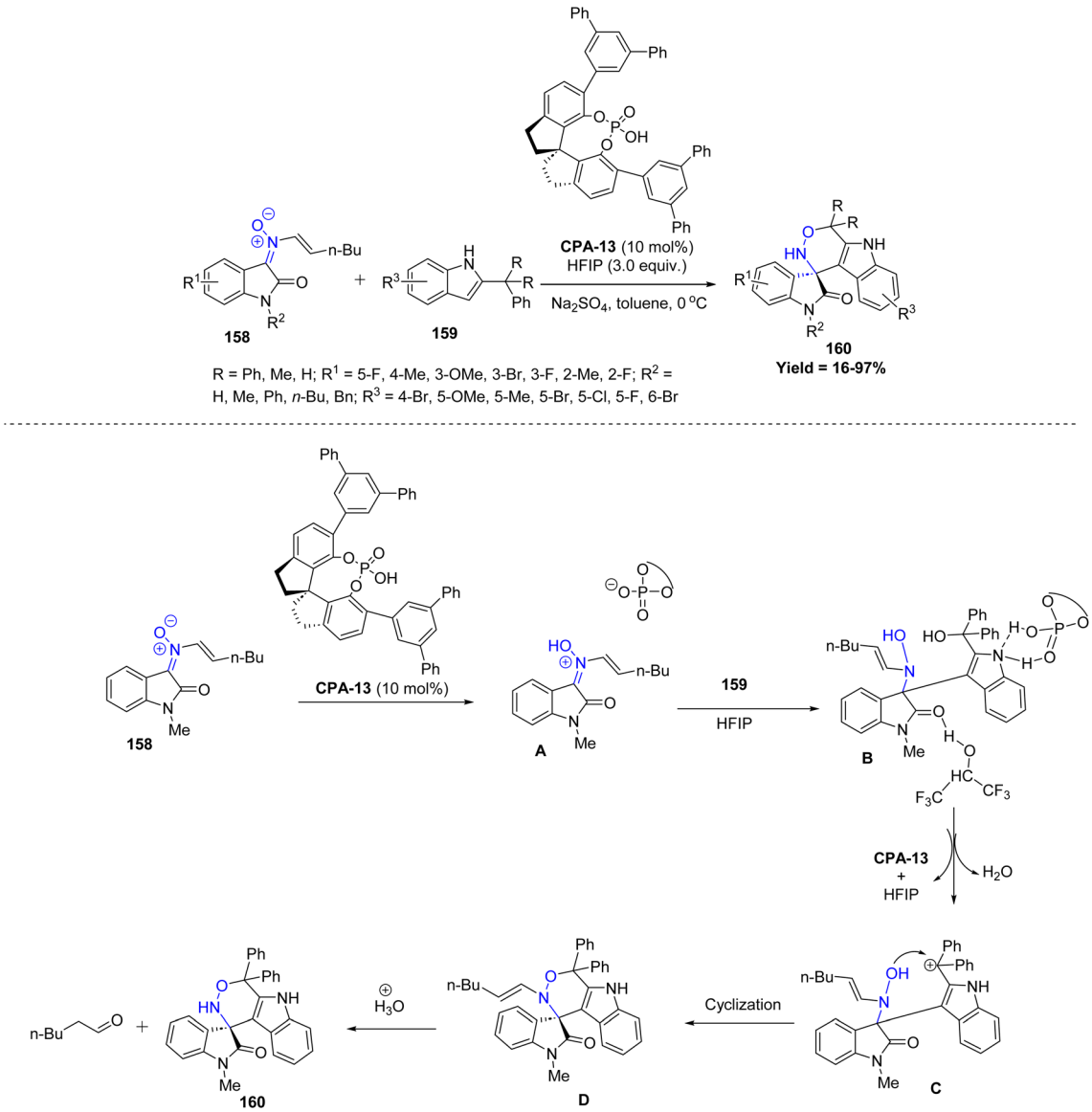

Scheme 40 Chiral phosphoric acid (CPA) catalyzed asymmetric [3 + 3] cycloaddition of *N*-viny oxindole nitrones with 2-indolylmethanols.

accommodating diverse aromatic nitrones with electron-donating and electron-withdrawing substituents, and is compatible with both ester- and ether-protected sugars. Mechanistically, $ZnCl_2$ activates the anhydrosugar **155**, promoting nucleophilic attack by the nitrone **156**, followed by an intramolecular cyclization to furnish the fused dioxazinane products **157** (Scheme 39).[86]

In 2024, Wen-Jun Zhou *et al.* introduced an enantioselective strategy for constructing spirooxindole[1,2]oxazine frameworks **160** *via* a chiral phosphoric acid (CPA)-catalyzed [3 + 3] cycloaddition between *N*-vinyl oxindole nitrones **158** and 2-indolylmethanols **159**. The substrate scope is reasonably broad, allowing a variety of aromatic, heteroaromatic, and moderately substituted starting materials to participate effectively. However, the method still shows certain limitations, such as reduced efficiency with highly bulky substrates, intolerance toward strongly electron-withdrawing groups, and occasional formation of side products under harsh conditions. The proposed mechanism suggests initial activation of nitrone **158** by CPA-13, leading to intermediate **A**. Subsequent reaction with **159** in HFIP facilitates formation of intermediate **B**, which undergoes dehydration to yield intermediate **C**, concurrently releasing the catalyst and solvent. An intramolecular cyclization of **C** furnishes intermediate **D**, which upon hydrolytic cleavage of the enamine moiety under acidic aqueous conditions, results in the formation of the spirooxindole[1,2]oxazine product **160** along with 1-hexanal (Scheme 40).[87]

2.3 Redox and photochemical approaches

Chao Feng and co-workers in 2023 reported a novel visible-light-driven, photoredox-catalyzed [3 + 3] dipolar cycloaddition of nitrones **162** with aryl cyclopropanes **161** for the synthesis of complex six-membered heterocycles **163**. Mechanistically, the

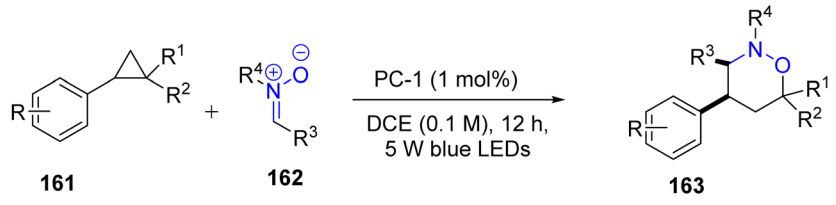

R = H, 3-CF_3, Ph, napthalene, 4-TMS, 3-F, 4-CF_3, 4-OMe, 3-F 4-OMe, 3-Cl 4-OMe, 3-Br 4-OMe, 3-CO_2Me 4-OMe, 4-Ph, 6-OMe, 4-Me, 4-TMS, 3-Me 4-OMe, 4-Cl; R^1 = H, Me; R^2 = Me,4-OMe C_6H_4, C_2H_3; R^3 = Ph, 4-FC_6H_4, 4-ClC_6H_4, 4-PhC_6H_4, 4-MeC_6H_4, napthalene, thiophene, py, 4-$NO_2C_6H_4$, 3-MeC_6H_4, 4-BrC_6H_4, 4-IC_6H_4, ^{t}Bu, ^{i}Pr, 4-CNC_6H_4, 4-$OMeC_6H_4$, 4-$CF_3C_6H_4$; R^4 = Me, Ph, Bn, 4-FC_6H_4, ^{t}Bu, CO_2Me

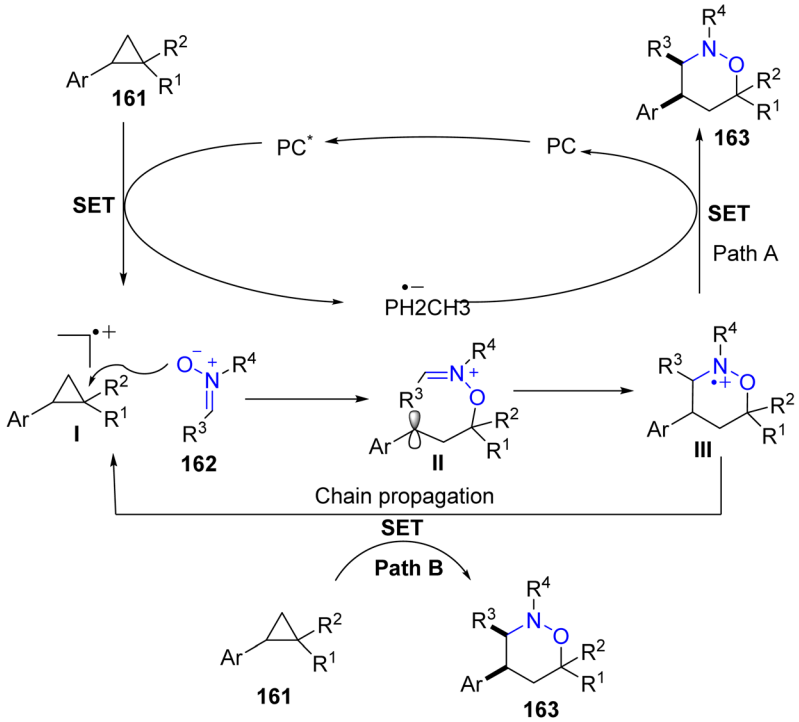

Scheme 41 Photoredox-catalyzed [3 + 3] dipolar cycloaddition of nitrones with aryl cyclopropanes.

reaction is initiated by the excitation of an acridinium photocatalyst under blue light (450 nm), which undergoes single-electron transfer (SET) with the aryl cyclopropane **161** to generate a radical cation **I**. The nitrone **162** then engages in a regio- and stereoselective nucleophilic attack on this radical cation, promoting ring opening and forming a benzylic radical intermediate **II**. This intermediate subsequently undergoes a 6-*endo*-trig radical cyclization to form a new C–C bond, delivering a second radical intermediate **III**. A final SET from the reduced photocatalyst regenerates the ground-state catalyst and completes the catalytic cycle, furnishing the cycloadduct **163** with high diastereoselectivity. Reactivity trends indicate that nitrone attack occurs at the more electron-rich cyclopropyl carbon, and substrates capable of easy SET oxidation react best. Limitations arise with sterically bulky or strongly electron-withdrawing substrates, and cyclopropanes that cannot undergo SET remain unreactive (Scheme 41).[88]

Baohua Chen *et al.* reported a highly efficient and environmentally friendly strategy for the synthesis of valuable benzoxazole derivatives *via* a self-oxidative cyclization pathway involving N–O bond cleavage. This metal-free protocol utilizes readily accessible nitrones **164** as starting materials and proceeds smoothly under simple, one-pot conditions. This metal-free oxidative cyclization shows broad functional-group tolerance, with most electron-rich and electron-poor *N*-aryl nitrones reacting smoothly. Reactivity is largely unaffected by electronics, but strong electron-withdrawing groups such as CF_3 and CN suppress radical formation and give no product. Aryl aldehydes work well, alkenyl and aliphatic aldehydes react poorly, marking the main limitations of this otherwise efficient

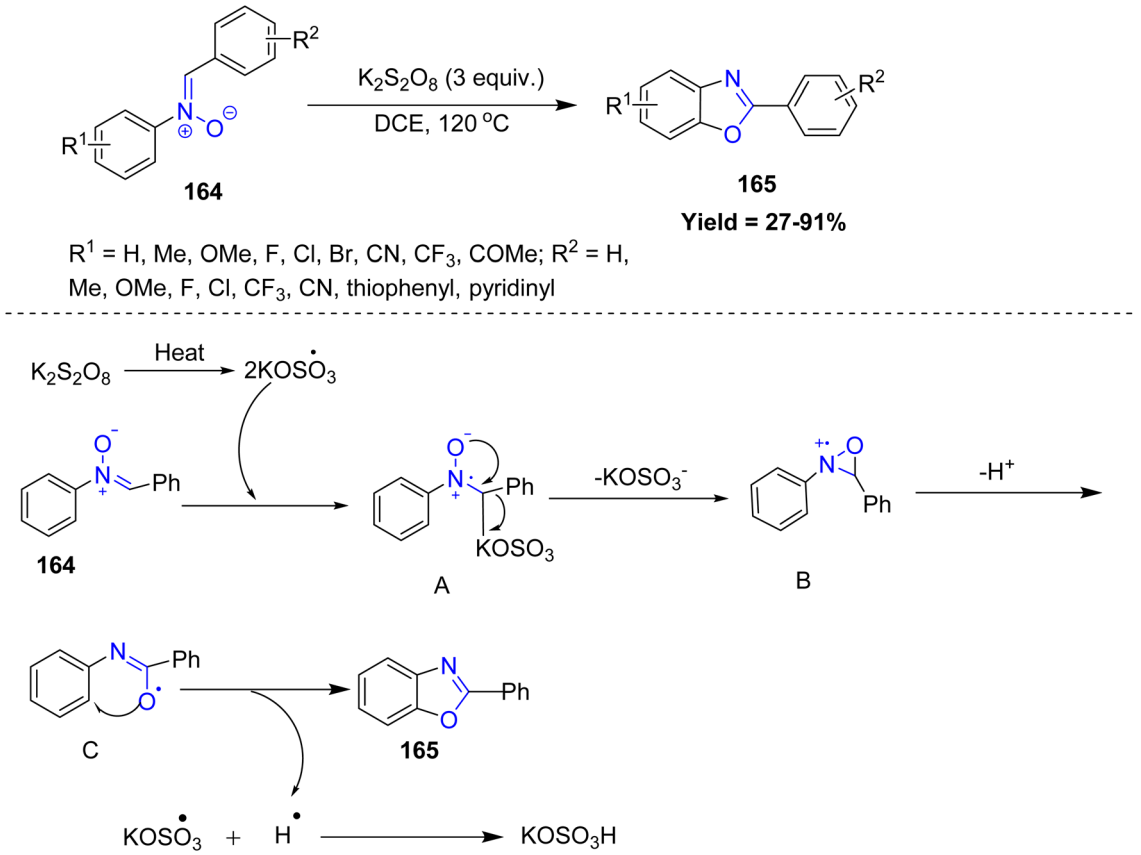

Scheme 42 Self-oxidative cyclization of nitrone compound.

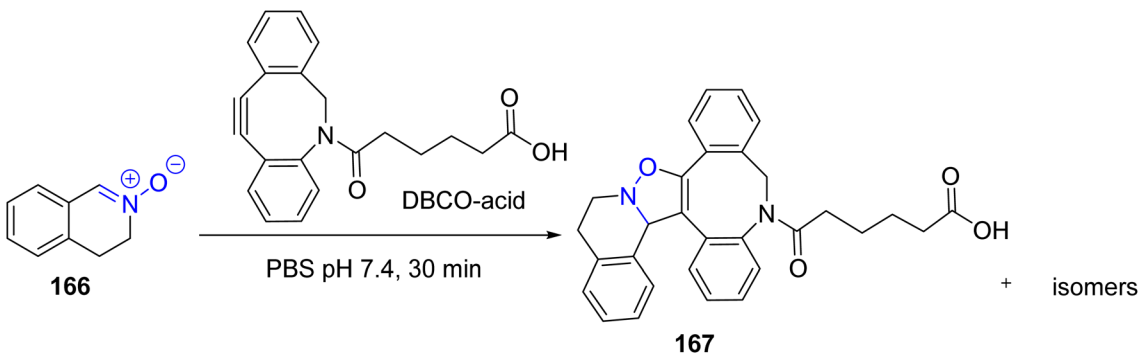

Scheme 43 Asymmetric click reaction using cyclic nitrone and strained alkynes.

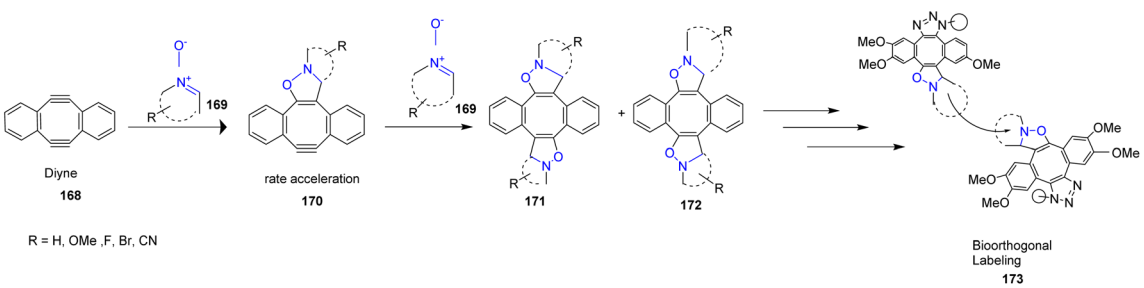

Scheme 44 Strain-promoted double-click reaction of nitrone with dibenzocyclooctadiyne.

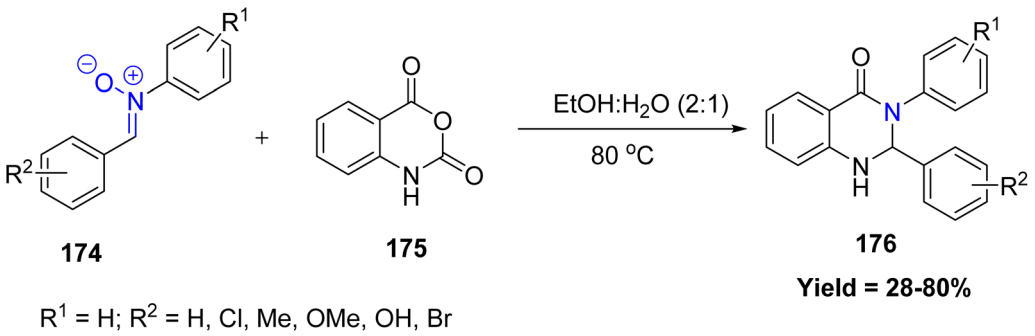

Scheme 45 Deoxygenative cycloaddition of nitrones with isatoic anhydride.

and green protocol. Mechanistically, the reaction is initiated by the formation of sulfate radical anions ($SO_4^{\bullet -}$) from thermolysis of potassium persulfate ($K_2S_2O_8$), which abstract a hydrogen atom from the substrate **164** to generate a benzyl radical intermediate **A.** This radical then undergoes intramolecular cyclization to form a strained tricyclic intermediate **B.** Subsequent concerted cleavage of the N–O bond, accompanied by proton release, drives the ring opening to yield intermediate **C.** Finally, **C** undergoes further oxidation by excess sulfate radicals, giving the final compound 2-aryl-substituted (benzo) oxazole products **165** (Scheme 42).[89]

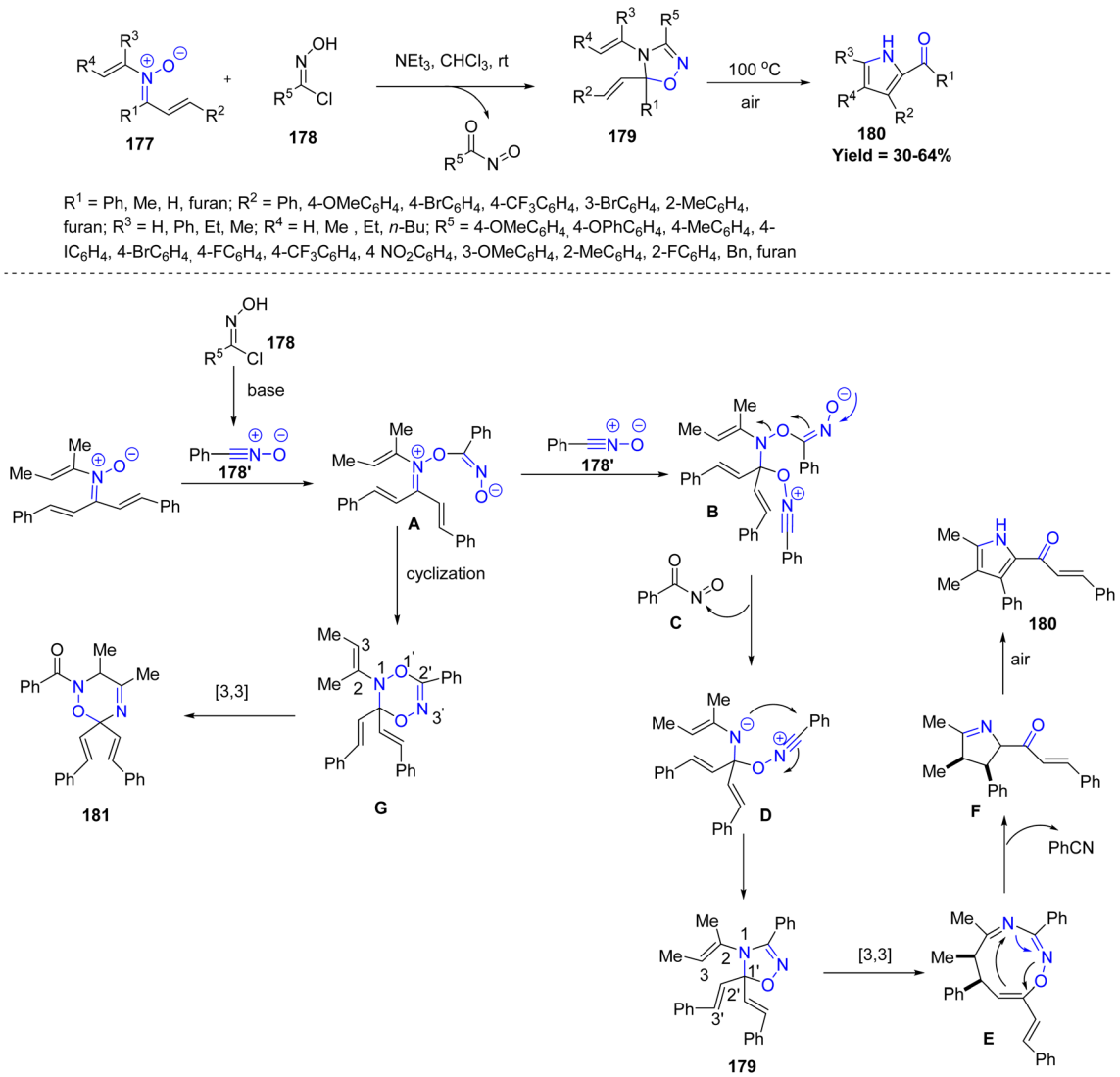

Scheme 46 Deoxygenative cyclization cascade reaction between *N*-vinyl-α,β-unsaturated nitrones and nitrile oxides.

2.4 Miscellaneous approaches

2.4.1 Asymmetric click reactions. Tsung-Shing Andrew Wang *et al.* in 2025 reported a strain-promoted alkyne-nitrone cycloaddition (SPANC) using cyclic nitrone **166** and strained alkynes as modular building blocks. This click strategy enabled a convenient 2- and 3-component assembly of multifunctional biomolecules, including PROTACs and biological probes. Their method allows rapid construction of bifunctional and trifunctional degraders, demonstrating efficient in-cell assembly, and the synthesis of caged or trifunctional PROTACs through sequential nitrone formation and SPANC (Scheme 43).[90]

John Paul Pezacki *et al.* in 2023 demonstrated strain-promoted double-click (SPDC) reaction of nitrone **169** to the strain-promoted dibenzo-cyclooctadiyne **168**, highlighting their potential for efficient bioorthogonal labeling. Detailed mechanistic investigations revealed that these transformations share a similar rate-limiting step with dual cycloaddition processes. Examination of the reaction scope and mechanism identified key limitations associated with nitrone cyclooctadiyne cycloadditions, while also providing insights into conditions under which the rate-limiting step can shift (Scheme 44).[91]

2.4.2 Deoxygenative cyclization. Rakesh Kumar *et al.* reported a novel deoxygenative cycloaddition of nitrones **174** with isatoic anhydride **175** for the synthesis of quinazolinones derivatives **176** under metal-free conditions without using any acid or base catalyst. The study shows that nitrones can undergo a deoxygenative cycloaddition in water, making this an efficient and environmentally friendly approach for building useful quinazolinone structures (Scheme 45).[92]

Dong-Liang Mo *et al.* in 2023, developed a metal-free deoxygenative cyclization cascade reaction between *N*-vinyl-α,β-unsaturated nitrones **177** and nitrile oxides **178′** for the synthesis of various functionalized 1,2,4-oxadiazolinesand 1,2,5-oxadiazolines **179**. Both linear and cyclic *N*-vinyl groups, as well as heteroaryl moieties, were tolerated. Hydroxamoyl chlorides with diverse electronic properties worked efficiently, though bulky groups often reduced yields. Formation of 1,2,5-oxadiazolines required specific solvents and bases, indicating sensitivity to reaction conditions. Mechanistically, the nitrile oxide **178′**, generated *in situ* from **178** under basic conditions, reacts with nitrone **177** to afford intermediate **A**. Subsequent nucleophilic addition of a second nitrile oxide **178′** furnishes intermediate **B**, which upon elimination yields **D**. An

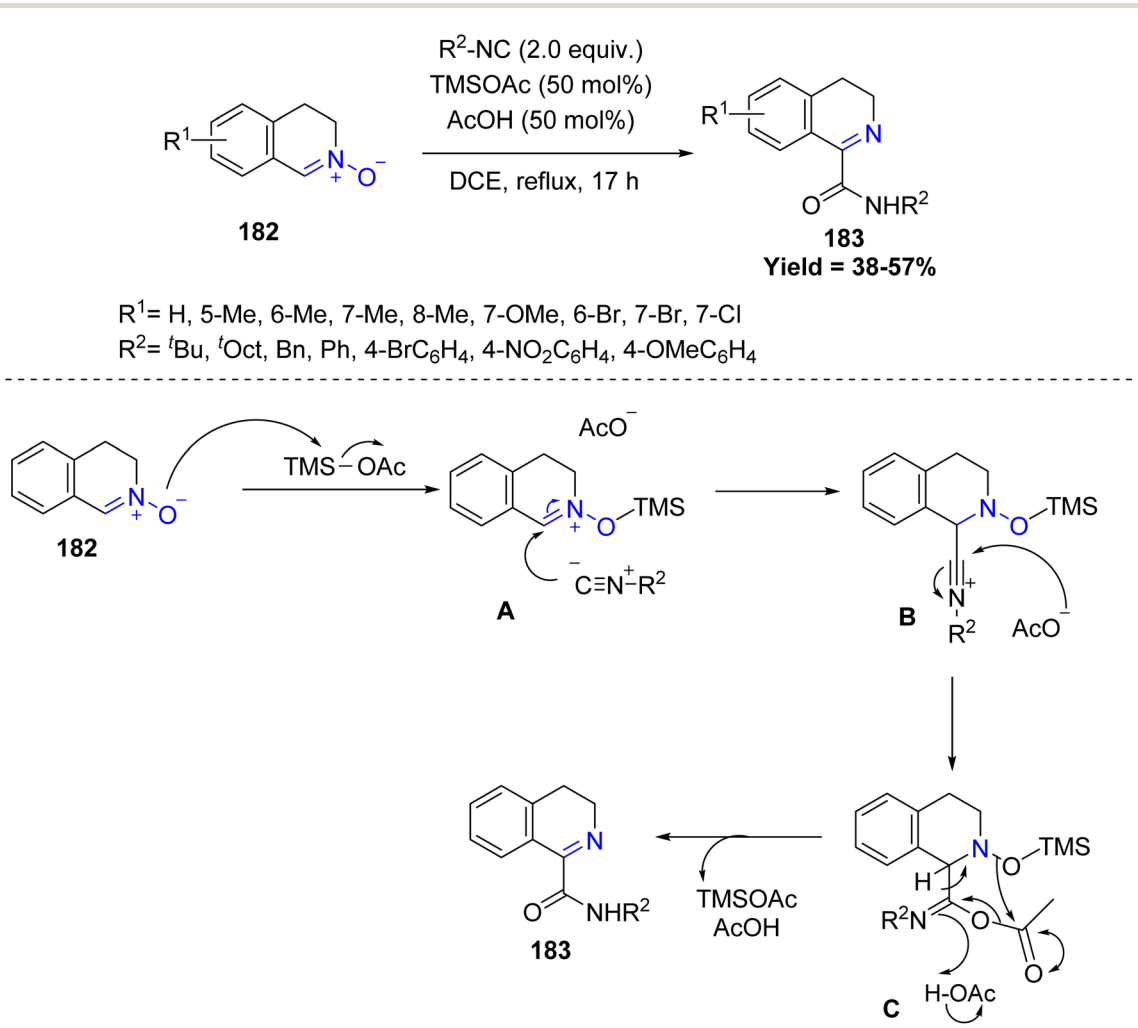

Scheme 47 Silylacetate-promoted addition reaction of isocyanides to nitrones.

intramolecular cyclization of **D** produces the stable 1,5-diene **179**, which undergoes a [3,3]-sigmatropic rearrangement to give the nine-membered ring **E**. Further N–O bond cleavage, elimination, and oxidation of the corresponding intermediate **F** provide pyrrole **180**. Alternatively, intermediate **A** can undergo intramolecular cyclization to generate **G**, which through a selective [3,3]-rearrangement affords compound **181** (Scheme 46).[93]

2.4.3 Silylacetate-promoted additions. Takahiro Soeta *et al.*, in 2024 reported the addition of isocyanides to 3,4-dihydroisoquinoline-*N*-oxides **182** *via* an innovative variation of the Ugi reaction to give the respective 3,4-dihydroisoquinoline-1-carboxylamide derivatives **183**. Mechanistically the reaction is initiated by coordination of the nitrone oxygen with TMSOAc, generating intermediate **A**. This step is followed by stabilization of the resulting nitrilium intermediate *via* acetate addition, affording the imidoyl acetate **C**. Finally, regeneration of TMSOAc occurs concurrently with acyl group transfer, leading to the formation of the final product **183**. Aliphatic isocyanides, particularly bulky tertiary and secondary alkyl groups, reacted efficiently, giving good to high yields, whereas aromatic isocyanides generally exhibited lower reactivity, with strongly electron-withdrawing substituents completely inhibiting the reaction. Limitations include reduced efficiency with electron-deficient or sterically hindered substrates, sensitivity to solvent choice, and lower reactivity for certain aromatic isocyanides, highlighting the need for optimized conditions for each substrate class (Scheme 47).[94]

3 Conclusion

Nitrones continue to represent a highly versatile class of intermediates in heterocyclic synthesis, enabling access to structurally diverse scaffolds with wide-ranging biological and material applications. Traditional transition-metal-catalyzed strategies have provided remarkable control over regio- and stereoselectivity, yet their high cost and limited substrate scope often restrict broader adoption. In parallel, the development of transition-metal-free methodologies has opened new opportunities for sustainable and scalable synthesis, particularly through [3 + 2], [2 + 2] and [4 + 2] cycloadditions, as well as emerging approaches such as asymmetric click chemistry, deoxygenative cyclization, Ugi reactions, photoredox catalysis, and self-oxidative cyclizations. Collectively, these methods showcase the adaptability of nitrone chemistry to diverse synthetic challenges while advancing the principles of green and economical synthesis. Despite these advances, significant challenges remain. The development of protocols that combine high selectivity, broad functional group tolerance, and operational simplicity under environmentally benign conditions is still a pressing need. In particular, catalyst-free strategies and photocatalytic approaches hold considerable promise for addressing issues of cost, scalability, and sustainability. Moreover, expanding the substrate scope to accommodate complex, multifunctional molecules will be vital for translating laboratory methodologies into practical applications. By addressing existing limitations and embracing interdisciplinary strategies, the field of nitrone-derived heterocycles is well-positioned to deliver transformative advances in both synthetic methodology and real-world applications. We believe this review will serve as a timely resource, offering insights that may inspire future innovations and guide researchers toward the development of more efficient, sustainable, and widely applicable nitrone-based transformations.

Author contributions

Suhasini Mohapatra: conceptualization, writing original draft; Kamalika Prusty: review and editing; Subhashree Bhol: review and editing; Gopinatha Panigrahi: review and editing; Sabita Nayak: conceptualization, validation, supervision, funding acquisition, editing original draft.

Conflicts of interest

There is no conflict of interest among the authors.

Data availability

No data was used for the research described in the article.

Acknowledgements

SN is thankful to MRIP, ODISHA (24EM/CH/36) for providing research grant and also thankful to the Centre of Excellence in Environment and Public Health by the Higher Education Department, Government of Odisha (Grant No. 26913/HED/HE-PTC-WB-02-17 OHEPEE). SM acknowledges the SERB-SURE New Delhi (Ref. SURI2022/0002527) for providing financial support in the form of project fellowship.

References

1 (*a*) H. Xu, K. M. Piekarz, J. L. Brown, S. Bhaskaran, N. Smith, R. A. Towner and H. Van Remmen, *GeroScience*, 2024, 1–11; (*b*) A. Escobar-Peso, E. Martínez-Alonso, D. Hadjipavlou-Litina, A. Alcázar and J. Marco-Contelles, *Eur. J. Med. Chem.*, 2024, **266**, 116133; (*c*) J. Marco-Contelles, *J. Med. Chem.*, 2020, **63**, 13413–13427; (*d*) M. Rosselin, B. Poeggeler and G. Durand, *Curr. Top. Med. Chem.*, 2017, **17**, 2006–2022.

2 (*a*) G. Barriga-González, C. Aliaga, E. Chamorro, C. Olea-Azar, E. Norambuena, W. Porcal, M. González and H. Cerecetto, *RSC Adv.*, 2020, **10**, 40127–40135; (*b*) R. Nikam and A. Chattopadhyay, *Int. J. Quantum Chem.*, 2024, **124**, e27369; (*c*) A. Deletraz, K. Zéamari, K. Hua, M. Combes, F. A. Villamena, B. Tuccio, N. Callizot and G. Durand, *J. Org. Chem.*, 2020, **85**, 6073–6085; (*d*) J. Marco-Contelles, *J. Antioxid. Act.*, 2024, **13**, 440.

3 (*a*) E. H. Wong, T. Junkers and C. Barner-Kowollik, *Polym. Chem.*, 2011, **2**, 1008–1017; (*b*) D. Z. Mutlaq, Q. M. Hassan, H. A. Sultan and C. A. Emshary, *Opt. Mater.*, 2021, **113**, 110815; (*c*) D. Kurandina, B. Huang, W. Xu, N. Hanikel, A. Darù, G. D. Stroscio, K. Wang, L. Gagliard, F. D. Toste

and O. M. Yaghi, *Angew. Chem., Int. Ed.*, 2023, **62**, e202307674.
4 (*a*) N. Noël, A. Martinez, F. Massicot, J. L. Vasse and J. B. Behr, *Org. Lett.*, 2024, **26**, 3917–3922; (*b*) K. Rück-Braun, T. H. Freysoldt and F. Wierschem, *Chem. Soc. Rev.*, 2005, **34**, 507–516; (*c*) L. L. Anderson, *Asian J. Org. Chem.*, 2016, **5**, 9–30; (*d*) Y. Wang, A. Hennig, T. Küttler, C. Hahn, A. Jäger and P. Metz, *Org. Lett.*, 2020, **22**, 3145–3148.
5 (*a*) Y. Xu, H. X. Gao, C. Pan, Y. Shi, C. Zhang and G. Huang, *Angew. Chem., Int. Ed.*, 2023, **135**, e202310671; (*b*) R. Hammami, P. Maldivi, C. Philouze, S. Carret, B. Darses, S. Touil and J. F. Poisson, *Adv. Synth. Catal.*, 2023, **365**, 1385–1390; (*c*) A. Hazra, A. Ghosh, N. Yadav and P. Banerjee, *Chem. Commun.*, 2023, **59**, 11133–11136; (*d*) S. Guo, Z. Zhang, Z. Wei, Y. Zhu and X. Fan, *J. Org. Chem.*, 2023, **88**, 3845–3858; (*e*) J. Zhang, J. Y. Su, H. Zheng, H. Li and W. P. Deng, *Angew. Chem., Int. Ed.*, 2024, **136**, e202318476.
6 (*a*) S. I. Murahashi and Y. Imada, *Chem. Rev.*, 2019, **119**, 4684–4716; (*b*) G. Soldaini, F. Cardona and A. Goti, *Org. Lett.*, 2007, **9**, 473–476; (*c*) F. Kang, X. Wang, C. Chen, C. S. Lee, Y. Han and Q. Zhang, *J. Am. Chem. Soc.*, 2023, **145**, 15465–15472; (*d*) G. Shukla, D. Yadav, S. Singh and M. S. Singh, *Adv. Synth. Catal.*, 2022, **364**, 1982–1988.
7 (*a*) Y. Hu, Y. Zhao, J. F. Peng, L. Dong and Y. J. Xu, *Org. Lett.*, 2024, **26**, 4616–4620; (*b*) J. Xing, H. Y. Tang, J. L. Chen, Z. Huang, J. J. Liang, Y. S. Quan and J. G. Mao, *J. Org. Chem.*, 2024, **89**, 9841–9852; (*c*) T. Sandmeier and E. M. Carreira, *Angew. Chem., Int. Ed.*, 2021, **60**, 9913–9918.
8 G. Durand, F. Choteau, B. Pucci and F. A. Villamena, *J. Phys. Chem. A*, 2008, **112**, 12498–12509.
9 G. P. Novelli, P. Angiolini, R. Tani, G. Consales and L. Bordi, *Free Radic. Res. Commun.*, 1986, **1**, 321.
10 X. Cao and J. W. Phillis, *Brain Res.*, 1994, **644**, 267.
11 H. Mori, T. Arai, H. Ishii, T. Adachi, N. Endo, K. Makino and K. Mori, *Neurosci. Lett.*, 1998, **241**, 99–102.
12 A. Jotti, L. Paracchini, G. Perletti and F. Piccinini, *Pharmacol. Res.*, 1992, **26**, 143–147.
13 T. Parman, M. J. Wiley and P. G. Wells, *Nat. Med.*, 1999, **5**, 582–585.
14 R. A. Floyd, K. Hensley, M. J. Forster, J. A. Kelleher-Andersson and P. L. Wood, *Mech. Ageing Dev.*, 2002, **123**, 1021–1031.
15 R. A. Floyd, *Aging Cell*, 2006, **5**, 51–57.
16 A. R. Green, *Crit. Rev. Neurobiol.*, 2004, **16**, 91–103.
17 (*a*) E. Maurelli, M. Culcasi, M.-C. Delmas-Beauvieux, M. Miollan, J.-L. Gallis, T. Tron and S. Pietri, *Free Radic. Biol. Med.*, 1999, **27**, 34–45; (*b*) S. Pietri, T. Liebgott, C. Frejaville, P. Tordo and M. Culcasi, *Eur. J. Biochem.*, 1998, **254**, 256–265; (*c*) A. Tosaki, I. E. Blasig, T. Pali and B. Ebert, *Free Radic. Biol. Med.*, 1990, **8**, 363–370.
18 C. Frejaville, H. Karoui, B. Tuccio, F. Le Moigne, M. Culcasi, S. Pietri, R. Lauricella and P. Tordo, *J. Med. Chem.*, 1995, **38**, 258–265.
19 A. Zeghdaoui, B. Tuccio, J.-P. Finet, V. Cerri and P. Tordo, *J. Chem. Soc., Perkin Trans. 2*, 1995, 2087–2093.
20 O. Tamura, *Chem. Pharm. Bull.*, 2024, **72**, 731–746.
21 (*a*) B. Loh, L. Vozzolo, B. J. Mok, C. C. Lee, R. J. Fitzmaurice, S. Caddick and A. Fassati, *Chem. Biol. Drug Des.*, 2010, **75**, 461–468; (*b*) C. L. Lynch, A. L. Gentry, J. J. Hale, S. G. Mills, M. MacCoss, L. Malkowitz, M. S. Springer, S. L. Gould, J. A. DeMartino, S. J. Siciliano, M. A. Cascieri, G. Doss, A. Carella, G. Carver, K. Holmes, W. A. Schleif, R. Danzeisen, D. Hazuda, J. Kessler, J. Lineberger, M. Miller and E. Emini, *Bioorg. Med. Chem. Lett.*, 2002, **12**, 677–682; (*c*) E. V. Sirotkina, M. M. Efremova, A. S. Novikov, V. V. Zarubaev, I. R. Orshanskaya, G. L. Starova, R. R. Kostikov and A. P. Molchanov, *Tetrahedron*, 2017, **73**, 3025–3032.
22 (*a*) R. V. Kumar, S. Mukherjee, A. K. P. Prasad, C. E. Olsen, S. J. C. Schäffer, S. K. Sharma, A. C. Watterson, W. Errington and V. S. Parmar, *Tetrahedron*, 2005, **61**, 5687–5694; (*b*) M. P. Sadashiva, H. Malleshha, N. A. Hitesh and K. S. Rangappa, *Bioorg. Med. Chem.*, 2004, **12**, 6389–6395.
23 (*a*) O. Bortolini, A. D. Nino, T. Eliseo, R. Gavioli, L. Maiuolo, B. Russo and F. Sforza, *Bioorg. Med. Chem.*, 2010, **18**, 6970–6977; (*b*) D. G. Piotrowska, M. Cieślak, K. Królewska and A. E. Wróblewski, *Arch. Pharm.*, 2011, **344**, 301–308.
24 F. Galietti, G. E. Giorgis, A. Oliaro, D. Boaro, A. Ardizzi, S. Barberis and G. M. Massaglia, *Minerva Med.*, 1991, **82**, 477–484.
25 H. Miyachi, *Expert Opin. Ther. Pat.*, 2005, **15**, 1521–1532.
26 M. G. Mulinos, *Antibiot. Annu.*, 1955, **3**, 131–140.
27 (*a*) F. Hu and M. Szostak, *Adv. Synth. Catal.*, 2015, **357**, 2583–2590; (*b*) K. Rück-Braun, T. H. E. Freysoldt and F. Wierschem, *Chem. Soc. Rev.*, 2005, **34**, 507–517; (*c*) K. V. Gothelf and K. A. Jørgensen, *Chem. Commun.*, 2000, 1449–1456; (*d*) P. N. Confalone and E. M. Huie, *Org. React.*, 1988, **36**, 1–320.
28 (*a*) K. R. R. Kumar, H. Mallesha and K. S. Rangappa, *Arch. Pharm.*, 2003, **336**, 159–167; (*b*) M. P. Sibi, N. Prabagaran, S. G. Ghorpade and C. P. Jasperse, *J. Am. Chem. Soc.*, 2003, **125**, 11796–11805; (*c*) T. Kano, T. Hashimoto and K. Maruoka, *J. Am. Chem. Soc.*, 2005, **127**, 11926–11934.
29 S. Yokoshima, *Nat. Prod. Rep.*, 2025, **42**, 1071–1090.
30 S. Rossiter and A. P. Dobbs, *Imines and Their N-Substituted Derivatives: Oximes and Their O-R Substituted Analogs*, Elsevier, 2005, vol. 3, pp. 451–467.
31 S. Thakur, A. Das and T. Das, *New J. Chem.*, 2021, **45**, 11420–11456.
32 A. Padwa and W. H. Pearson, *Synthetic Applications of 1,3-Dipolar Cycloaddition Chemistry toward Heterocycles and Natural Products*, Wiley, New York, 2002.
33 V. Nair and T. D. Suja, *Tetrahedron*, 2007, **63**, 12247–12275.
34 W.-M. Shi, X.-P. Ma, G.-F. Su and D.-L. Mo, *Org. Chem. Front.*, 2016, **3**, 116–130.
35 T. Hashimoto and K. Maruoka, *Chem. Rev.*, 2015, **115**, 5366–5412.
36 L. Xie, H. Bai, J. Li, X. Yu, Z. Zhang and B. Fu, *Tetrahedron*, 2017, **73**, 2923–2931.
37 X. Shen, A. Shatskiy, Y. Chen, M. D. Karkas, X.-S. Wang and J.-Q. Liu, *J. Org. Chem.*, 2020, **85**, 3560–3569.

38 X.-P. Ma, C.-M. Nong, J. Zhao, X. Lu, C. Liang and D.-L. Mo, *Adv. Synth. Catal.*, 2020, **362**, 478–486.
39 X. Yang, F. Cheng, Y.-D. Kou, S. Pang, Y.-C. Shen, Y.-Y. Huang and N. Shibata, *Angew. Chem., Int. Ed.*, 2017, **129**, 1532–1536.
40 H. Liu, Y. Zhao, Z. Li, H. Jia, C. Zhang, Y. Xiao and H. Guo, *RSC Adv.*, 2017, **7**, 29515–29522.
41 X. Cheng, W. Fei, Z. Luo, J. Lia, Z. Wang and W. Yao, *Synthesis*, 2020, **52**, 3632–3640.
42 K. B. Jensen, K. V. Gothelf, R. G. Hazell and K. A. Jørgensen, *J. Org. Chem.*, 1997, **62**, 2471–2477.
43 H. Zheng, I. Faghihi and M. P. Doyle, *Helv. Chim. Acta*, 2021, **104**, e2100081.
44 P.-P. Xu, S.-G. Xin, X. Li, C. Liang and D.-L. Mo, *Adv. Synth. Catal.*, 2023, **365**, 735–740.
45 A. Torelli, E. S. Choi, A. Dupeux, M. N. Perner and M. Lautens, *Org. Lett.*, 2023, **25**, 8520–8525.
46 T. A. Pothi and C. V. Ramana, *Org. Lett.*, 2024, **26**, 2233–2237.
47 L. Huang, Z. Yao, G. Huang, Y. Ao, B. Zhu, S. Li and X. Cui, *Adv. Synth. Catal.*, 2021, **363**, 5092–5098.
48 B. Xu, Z.-M. Zhang, J. Han, G. Gu and J. Zhang, *Chin. J. Chem.*, 2022, **40**, 1407–1412.
49 D. Barik and R.-S. Liu, *J. Org. Chem.*, 2022, **87**, 7097–7105.
50 S. D. Tanpure, M. D. Dhole and R.-S. Liu, *Adv. Synth. Catal.*, 2023, **365**, 2936–2942.
51 D. Barik, C. Maitra, C.-T. Hsieh, M.-J. Cheng and R.-S. Liu, *ACS Catal.*, 2024, **14**, 1525–1531.
52 A. V. Sasane, C.-T. Chiou, M.-Y. Chang and W.-T. Li, *Org. Lett.*, 2024, **26**, 6675–6680.
53 M. Li, Y. Dong, C. Zhou, J. Bai, J. Cheng, J. Sun and S. Sun, *Org. Lett.*, 2021, **23**, 8229–8234.
54 X.-T. Qin, N. Zou, X.-L. Cheng, C. Liang and D.-L. Mo, *Adv. Synth. Catal.*, 2022, **364**, 500–505.
55 S. Guo, Z. Zhang, Z. Wei, Y. Zhu and X. Fan, *J. Org. Chem.*, 2023, **88**, 3845–3858.
56 Y. Wang and L.-M. Zhao, *Adv. Synth. Catal.*, 2023, **365**, 3713–3717.
57 N. Aravindan and M. Jeganmohan, *Org. Lett.*, 2023, **25**, 3853–3858.
58 S. Min, T. Kim, T. Jeong, J. Yang, Y. Oh, K. Moon, A. Rakshit and I. S. Kim, *Org. Lett.*, 2023, **25**, 4298–4302.
59 X. Yu, X. Ji, D. Shang, L. Yu, P. W. H. Chan and W. Rao, *Org. Lett.*, 2024, **26**, 6631–6636.
60 M. Liu, L. Xie, L. Hou, L. Lin and X. Feng, *Chem. Commun.*, 2022, **58**, 5482.
61 J. Brześkiewicz and R. Loska, *Adv. Synth. Catal.*, 2023, **365**, 4241–4247.
62 Y.-Z. Wu, Y. Leng, Y.-X. Chen, S.-Q. Huang, N. Zou, C.-H. Chen and D.-L. Mo, *Chin. J. Chem.*, 2025, **43**, 417–422.
63 K. Punjajom, S. Chonradeenitchakul, J. Tummatorn, S. Ruchirawat and C. Thongsornkleeb, *Org. Lett.*, 2024, **26**, 10066–10071.
64 T.-T. Wang and L.-M. Zhao, *Chem. Commun.*, 2022, **58**, 11099.
65 S.-G. Xin, S. Chen, J.-H. Qin, H.-Y. Bi, C. Liang, C.-H. Chen and D.-L. Mo, *J. Org. Chem.*, 2025, **90**, 1922–1933.
66 Z.-N. Zhao, F.-K. He, Y.-H. Wang, Y.-C. Li, Z.-H. Li, X.-Y. Yang, U. Schneider and Y.-Y. Huang, *ACS Catal.*, 2024, **14**, 13291–13302.
67 Y. Hashimoto, H. Ishiwata, S. Tachikawa, S. Ban, N. Morita and O. Tamura, *Chem. Commun.*, 2017, **53**, 2685.
68 R. Chen, S. Sun, G. Wang and H. Guo, *Tetrahedron Lett.*, 2018, **59**, 1916.
69 R. Saruengkhanphasit, D. Collier and I. Coldham, *J. Org. Chem.*, 2017, **82**, 6489.
70 N. Zou, J.-W. Jiao, Y. Feng, C.-H. Chen, C. Liang, G.-F. Su and D.-L. Mo, *Adv. Synth. Catal.*, 2017, **359**, 3545.
71 V. A. Dmitriev, M. M. Efremova, A. S. Novikov, V. V. Zarubaev, A. V. Slita, A. V. Galochkina, G. L. Starova, A. V. Ivanov and A. P. Molchanov, *Tetrahedron Lett.*, 2018, **59**, 2327.
72 R. Hammami, P. Maldivi, C. Philouze, S. Carret, B. Darses, S. Touil and J.-F. Poisson, *Adv. Synth. Catal.*, 2023, **365**, 1385–1390.
73 N. Noël, A. Martinez, F. Massicot, J.-L. Vasse and J.-B. Behr, *Org. Lett.*, 2024, **26**, 3917–3922.
74 X. Xu, R.-P. Li, Z. Zhang, X. Gong, Y. Zheng and S. Tang, *Org. Lett.*, 2024, **26**, 6825–6829.
75 Y. Zhang, Q. Wang, Z. Long, Y. Zuo, L. Liu and L. Yan, *J. Org. Chem.*, 2024, **89**, 10327–10332.
76 N. Ishihara, S. Harada, M. Nakajima and S. Arai, *Org. Lett.*, 2024, **26**, 2908–2912.
77 K. Behera, S. Mohapatra, S. Nayak, S. Mohapatra, S. P. Parida, D. Bhattacharya, U. K. Rout and C. R. Sahoo, *ChemistrySelect*, 2024, **9**, e202404850.
78 C. Xu, Y. Wang, M. Xiao, R. Tian and Z. Duan, *Chin. J. Chem.*, 2025, **43**, 1161–1166.
79 A. Tabassum, J. Samanta, D. Kumari, H. B. Bhore, A. K. Katare, K. Singh, T. Palmo, I. Venkatesan and Y. P. Bharitkar, *Bioorg. Chem.*, 2025, **154**, 108087.
80 H. Yuan, D.-L. Lu, C. Liang and D.-L. Mo, *Adv. Synth. Catal.*, 2022, **364**, 1409–1414.
81 S. Mohapatra, S. P. Parida, S. Nayak, K. Behera and S. Mohapatra, *Asian J. Org. Chem.*, 2025, **14**, e202500029.
82 H. Sagara, Y. Suzuki, N. Morita, S. Ban, K. Tanaka, A. Yamamoto, Y. Hashimoto and O. Tamura, *Adv. Synth. Catal.*, 2023, **365**, 3927–3934.
83 J. Zhang, J.-Y. Su, H. Zheng, H. Li and W.-P. Deng, *Angew. Chem., Int. Ed.*, 2024, **63**, e202318476.
84 Y. Liu, Y. Ji, J. Li, X. Liu, C. Wang, H. Zhang and R. Tian, *Org. Lett.*, 2024, **26**, 8747–8751.
85 K. Stefkova, M. G. Guerzoni, Y. van Ingen, E. Richards and R. L. Melen, *Org. Lett.*, 2023, **25**, 500–505.
86 A. Ahmed, N. Sakander, F. Rasool, N. Hussain and D. Mukherjee, *Org. Biomol. Chem.*, 2022, **20**, 1436.
87 N. Zou, Y.-Z. Wu, X.-Y. Zhong, C. Wei, L.-M. Liao, D.-L. Mo and W.-J. Zhou, *Adv. Synth. Catal.*, 2024, **366**, 4960–4965.
88 Y. Xu, H.-X. Gao, C. Pan, Y. Shi, C. Zhang, G. Huang and C. Feng, *Angew. Chem., Int. Ed.*, 2023, **62**, e202310671.
89 X. Yang, X. Guo, X. Yuan and B. Chen, *Org. Chem. Front.*, 2022, **9**, 4034.
90 S.-T. Lin, C.-H. Wang, A.-L. Chen and T.-S. A. Wang, *Chem.–Eur. J.*, 2025, **31**, e202403184.

91 D. A. Bilodeau, K. D. Margison, S. S. Masoud, M. Nakajima and J. P. Pezacki, *ACS Chem. Biol.*, 2023, **18**, 2430–2438.
92 D. Bharti, M. Kaur, K. K. Gurjar, A. Rani, V. Kumar, J. N. Babu, S. C. Sahoo, P. K. Verma and R. Kumar, *J. Mol. Struct.*, 2025, **1336**, 141947.
93 C.-M. Nong, S.-N. Lv, W.-M. Shi, C. Liang, G.-F. Su and D.-L. Mo, *Org. Lett.*, 2023, **25**, 267–271.
94 T. Soeta, S. Yao, H. Sugiyama and Y. Ukaji, *Org. Biomol. Chem.*, 2024, **22**, 1619.